University of Strathclyde

Department of Pure and Applied Chemistry

The Solid-State Structure of Tricyclic Antidepressants

Kiara Lobato

MPhil Chemistry 2020

This thesis is the result of the author's original research. It has been composed by the author and has not been previously submitted for examination which has led to the award of a degree.

Signed: Date:

Abstract

The active pharmaceutical ingredient (API) is the biologically active molecule present in medication. These are most commonly formulated in the crystalline solid state due to the stability and advantageous material properties generally demonstrated. The pharmaceutical industry is interested in the stability of their APIs, because it is important that it does not change during production, while on the shelf or while in the recipient's home. Solubility is another chemical property to control for maximum efficacy of a drug, as it aids bioavailability and distribution of the API to the desired site of action. Other important properties include melting point, mechanical hardness, and particle size. These properties have a large effect on the manufacturability of APIs as they affect processes such as grinding, mixing, and tabletting of solid products. Aqueous solubility, hygroscopicity, melting point, mechanical hardness and particle size are all examples of material properties of the bulk solid of solid form APIs. They strongly depend on the number, type and strength of intermolecular interactions in the solid and are therefore properties that can be controlled and altered by changing the solid-state structure without having to alter the API molecule.

There are four main ways to alter the solid-state structure and change material properties without altering the API molecule. Altering the solid-state structure affects the number, type and strength of intermolecular interactions. The options to alter these interactions include the choice between amorphous and crystalline material, investigating the polymorphic landscape of the API, and co-crystal or salt formation. Salt formation was the route that was focussed on in this work.

A salt screen was carried out on four closely related tricyclic antidepressants (TCAs): amitriptyline, nortriptyline, imipramine, and doxepin. All salt formation experiments were carried out exclusively in water in order to reduce the number of variables when comparing the resulting salt forms. A dataset of 29 newly elucidated crystal structures of TCA salt forms was generated.

From this dataset a selection of nortriptyline salt forms was made for an apparent aqueous solubility study. The salt forms were selected due to the counterions being ‘Generally Regarded as Safe’ (GRAS) for use in pharmaceutical industry. The salt forms used were bromide, iodide, salicylate, tosylate, besylate and oxalate. A clear trend was observed, where the salt forms with halogen counterions showed a higher solubility than organic counterions. The most soluble salt form of nortriptyline was the chloride salt which was over 200 times more soluble than the salicylate salt, which was determined to be the least soluble.

Structural analysis was carried out on the dataset which found that it would appear that all four TCA bases were much more likely to form Z’ > 1 structures than is normal. Only 8.8% of structures in the Cambridge Structural Database (CSD) were found to have a Z’ value larger than 1, compared to 52% of newly elucidated TCA crystal structures from this work. Three conformational motifs were investigated as possible causes for this increased likelihood of anomalous Z’ values. Three ring/chain conformations were identified, as well as three torsion angle α, and two torsion angle β options. Indeed, in structures with higher Z’ values, API molecules with mixtures of these conformations were observed. In addition, five of the Z’ = 1 TCA salt structures contained a cation site where all atoms of the cation were disordered. There is a chance that larger super cells or modulated structures have not been identified here and that these structures could be ordered with higher Z’ values.

The structures were further analysed as part of a larger data set of tricyclic antidepressants obtained from the CSD by the crystal packing similarity tool in Mercury. Four isostructural groups were identified. It appeared that the four cation packing isostructural groups could be divided into two types. Groups 1 and 2 contained different API molecules and/or very diverse counterions, and different hydration states. This illustrated that cation packing can be isostructural even where the structures that make up the groups involve different cations, different anions, and different solvation states. Group 1 seems to be a group where identical cation packing is caused by the

presence of the picrate anion. In contrast groups 3 and 4 contain pairs of closely related structures which differ only in the detail of the halide anion. Here isostructural packing of the cation is simply a subset of a larger structural similarity.

The crystal packing similarity analysis was repeated with a dataset of 85 carbamazepine and dihydrocarbamazepine structures found in the CSD. Here, 12 isostructural groups were identified, that could be split into three types. Type 1, groups 1 and 2, consisted of polymorphic forms. In group 1, it may be possible that the structures were not isostructural, but indeed the same form, but solved in different crystals systems. For type 2, it appeared the groups were made up of structures where the co-formers were geometrically and functionally similar to each other. Here, isostructural packing of the cation is simply a subset of a larger structural similarity, as in the second type of TCA isostructural groups. Type 3 had less in common, the structures in each group contained either dissimilar co-formers or different solvation states. The driving force of isostructural packing here seemed to be the hydrogen bonding motif and the link between this and the structures in the type 3 groups being channel solvates. Overall, in most cases in groups 3 through 12, the unit cell dimensions were very similar. This could be further studied as a tool to predict isostructural forms.

Acknowledgements

I would like to thank my supervisor, Dr. Alan Kennedy for all his help, guidance and support throughout both my BSc and my MPhil projects. Without his support, this work would not have been possible.

I would also like to thank Lygia de Silva-Moraes for her advice throughout the year and for teaching me all about structural analysis.

Thanks also go out to the other academics in our section; Dr. Michael Rogers, Dr. Chris Dodds, and Dr. Donna Ramsay and also the final year students; Alex, Elliot, Sky and Rowan.

Additionally, I would like to thank Dr. Jonathan Loughrey, my manager at my current position, for his advice and insights from the solid-state industry perspective.

Finally, thank you to my family and friends for always being there for me.

Table of contents

Table of tables

Table of figures

1 Introduction

An Active Pharmaceutical Ingredient, also known as an API, is the biologically active molecule present in medication. APIs are designed and synthesised based on the desired interaction within the human body, be it treating symptoms or curing a specific disease.

The pharmaceutical industry is one of the largest industries in the world. According to the Business Research Company, it was worth $934.8 billion in 2017 and growing by 5.8% per year.[1] Constant innovation is key to pharmacy companies, because their competitors are able to bring out generic versions of their API once a patent runs out. Use of generic APIs is especially prevalent in developing economies such as India and China. [1] The driving forces of the industry are therefore discovery and marketing of new APIs. It is in the pharmaceutical companies' best interest to develop novel medicines that are cheaper, are more efficacious, have fewer side effects, and have a more accessible dosage and method of application than their competitors.

1.1 Patient medication adherence

One of the most important determining factors of successful treatment is patient medication adherence. This means that patients comply with the dosage and medication schedule that was set out by their doctor. There are several types of medication nonadherence, these are known as primary nonadherence, non-persistence, and nonconforming. Primary nonadherence, sometimes known as non-fulfilment, means the patient either never takes the medication or does not even fulfil the prescription. Non persistence means the patient ceases to take the medication earlier than they should. Finally, non-conforming means the patient takes the medication wrongly with regards to dose or time.[2] As well as having a negative impact on the patient's health, medication non adherence can have a negative influence on the pharmaceutical industry, because non adherence can make a successful API seem unsuccessful due to a reduced efficacy.[2] Therefore, it is in the pharmaceutical companies' best interest to make it as easy as possible for patients to adhere to the prescribed APIs.

There are several methods of administration of APIs. These include solution injection, oral ingestion of tablets, particle inhalation, and topical application of creams. Some studies show that patient medication adherence is improved by oral administration of the API in the form of tablets.[3]

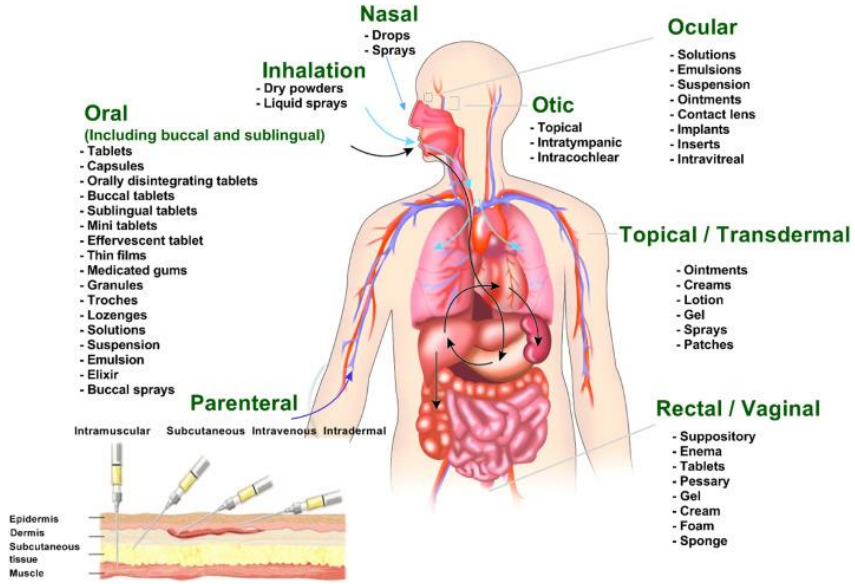

Figure 1: Diagram of methods of administration of medicine[4]

Thus, the pharmaceutical companies prefer to formulate APIs in their solid form whenever possible. Of course, this brings with it its own challenges in formulation, due to the way medicine travels through the digestive system. Most drugs should be absorbed in the small intestine so that they reach the bloodstream through the liver where they are metabolised. In order to pass through the intestinal wall, the API must have a high enough aqueous solubility. However, if solubility is too high, the API will begin to absorb before it reaches the small intestine and lose its potency.[5] On the other hand, if the aqueous solubility is too low, the API will dissolve slowly and will not be concentrated enough.

1.2 Material properties

For solid state APIs to be bioavailable in the human body, it is important that they have the appropriate aqueous solubility. Solubility is one of the main chemical properties to control for maximum efficacy of a drug, as it aids distribution of the API to the desired site of action. As the aqueous solubility goes up, so does the dissolution rate. This in turn increases bioavailability as bioavailability is dependent on localised high concentrations to move APIs across body membranes.[6]

Besides aqueous solubility, the pharmaceutical industry is interested in the stability of their APIs, because it is important that their product doesn't change during production, while on the shelf or while in the recipient's home. As an example, one main measure of stability is hygroscopicity, which is described as the capacity of a product to react with moisture in the air. Moisture absorption is undesirable because it changes the advertised form of an API and its activity by creating hydrated forms of the API molecule.[7]

Other important properties include melting point, mechanical hardness, and particle size. These properties have a large effect on the manufacturability of APIs as they affect processes such as grinding, mixing, and tabletting of solid products. The melting point needs to be high enough that the solid API

doesn’t melt during grinding and undergo phase changes. A mechanical hardness that is too high or too low can cause problems in grinding and tabletting. When the particle size is too large, the distribution of the API will be negatively impacted throughout batches of medicine, resulting in tablets having different dosages.[7]

Finally, pharmaceutical companies are interested in toxicity and the price of APIs. An API that treats a disease while simultaneously being poisonous or causing bad side effects is undesirable. Similarly, an API that is very expensive to make may not be accessible to all and of course won’t be as profitable.[7]

Aqueous solubility, hygroscopicity, melting point, mechanical hardness and particle size are all examples of material properties of the bulk solid of solid form APIs. They strongly depend on the number, type and strength of intermolecular interactions in the solid and are therefore properties that can be controlled and altered by changing the solid-state structure without having to alter the API molecule.[7]

1.3 Altering the solid-state structure

There are four main ways to alter the solid-state structure and change material properties without altering the API molecule. Altering the solid-state structure affects the number, type and strength of intermolecular interactions.

1.3.1 Amorphous vs crystalline product

The first option is to consider the amorphous versus the crystalline product, see Figure 2. The amorphous product is the kinetic product which means it forms quicker, is more reactive, and more soluble, but therefore also less stable than the equivalent crystalline product which is the thermodynamic product.[7]

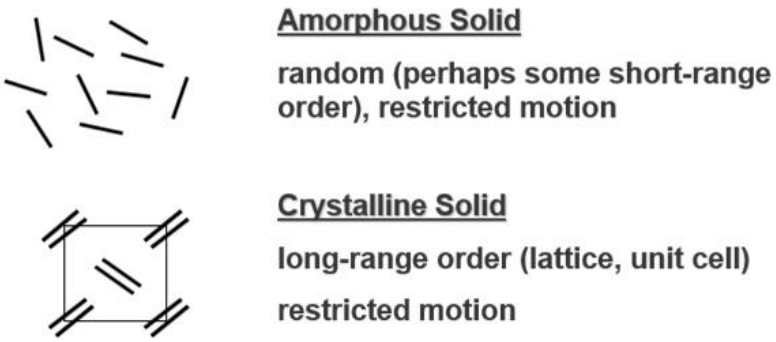

Figure 2: Diagram of amorphous vs crystalline solid structure[8]

Insulin is an exception to the stability rule, where, in the dried solid form, amorphous insulin is more stable than crystalline insulin. Pikal and Rigsbee found that the rate of degradation increased as the water content increased for the solid form crystalline insulin, but the rate of degradation of solid form amorphous insulin remained the same despite an increase in water content.[9]

Generally, although pharmaceutical companies may use amorphous materials in order to access say a higher solubility, they prefer to use crystalline products, because their inherent stability safeguards them from spontaneous phase changes from the kinetic to the thermodynamic product.[7]

1.3.2 Crystalline polymorphism

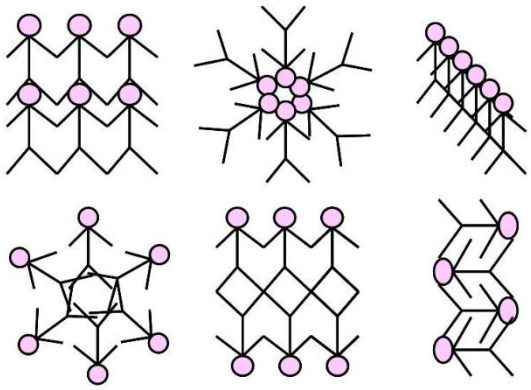

Figure 3: Polymorphism diagram[11]

Polymorphism in pharmaceuticals is when an API can adopt more than one 3 dimensional packed structure in the crystal. The forms must be chemically identical in order to be considered polymorphs. This means the same drug molecule packs in different ways with different intermolecular interactions, see Figure 3. Polymorphs can develop over time or they can be achieved by using different solvents, conditions, or crystallisation techniques. The Ostwald step rule states that the least thermodynamically favoured polymorph observed for a system will be that which forms first.[10]

Paracetamol is a prime example of an API that has multiple polymorphs with different material properties. See Figure 4 for structural illustrations of two of the three known polymorphs, forms I and II. Sudha and Srinivasan found that the three polymorphs could be produced under specific conditions using variable supersaturation and rapid cooling. At lower supersaturation, they found the stable monoclinic form I was formed. At intermediate supersaturation, metastable orthorhombic form II was found. The unstable polymorph III was produced in the higher supersaturation region but couldn't be isolated due to instability.[12] The different crystallisation regions correspond to an increase in solubility as supersaturation went up. Di Martino et al found that form III transforms into form II when exposed to the atmosphere, this phase change occurs in between 10 minutes and one hour. Although form I is the one available on the market, there are some issues with tableting this form due to its mechanical hardness. Di Martino et al found that form II displayed much better compression and hence tableting.[13]

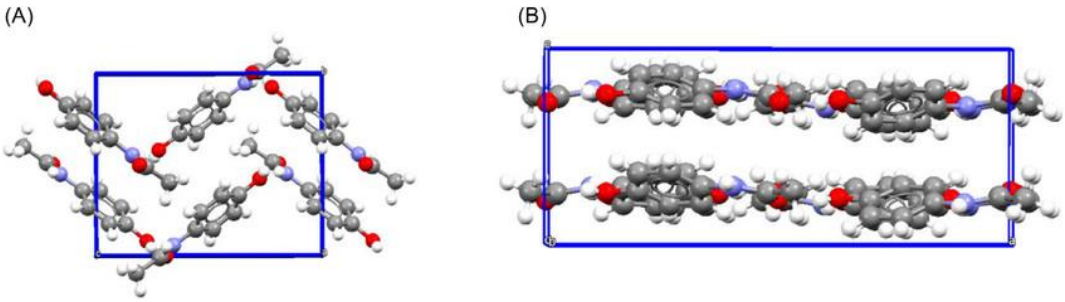

Figure 4: Crystal packing of paracetamol polymorph I (A) and polymorph II (B)[43]

Polymorphism can be a huge challenge in the pharmaceutical industry. This is partly due to practical considerations and partly due to patents and licensing being phase specific.

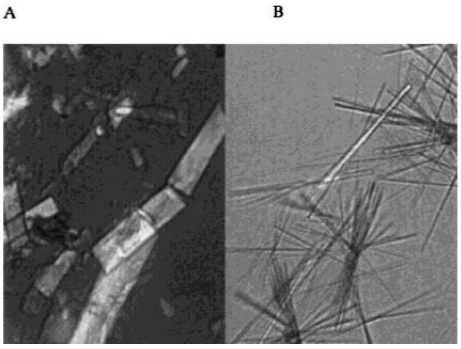

Figure 5: Photomicrographs for ritonavir polymorphs. Form I (A), form II (B)[15]

Ritonavir is an antiviral medication for AIDS. It is possibly one of the most severe cases of polymorphism having a negative effect on production of an API. Due to a lack of bioavailability in the solid-state, ritonavir was formulated in a solution of ethanol and water and marketed as a semi-solid capsule. After 240 successful batches of these capsules, the newer batches failed quality control checks for dissolution. Further inspection showed the newer batches contained a new polymorph, see Figure 5. Form II has a much lower solubility which was detrimental to the bioavailability. Soon after form II was discovered, the newly discovered and more thermodynamically favourable polymorph became prevalent in all production areas and made it impossible to manufacture form I. Ritonavir had to be reformulated at great expense to the manufacturer. In addition to the cost, Ritonavir was the number 1 antiviral drug on the market, meaning that many very ill patients had to go without essential medicine during reformulation.[15]

1.3.3 Co-crystals and solvates

Another way of altering the solid-state structure of a drug molecule is formation of co-crystals or solvates. Co-crystals of APIs contain the neutral API molecule and one or more other neutral molecules within the unit cell of the crystal structure. A major advantage of co-crystallisation is that it is potentially possible with all APIs whether they are basic, acidic or neutral molecules. This means that the neutral molecules can be formulated from a wide variety of potential Generally Regarded as Safe (GRAS) counter molecules including other APIs, as well as solvent molecules such as ethanol or water. Co-crystals containing solvent molecules are known as solvates. More specifically, they are known as hydrates when they contain water molecules.[16]

Co-crystallisation adds another set of functional groups to the solid-state structure. These additional functional groups will have big effects on the intermolecular interactions and thus on the material properties. For example, McNamara et al found that the 1:1 co-crystal of a sodium channel blocker and glutaric acid dissolved 18 times faster than the API by itself.[17]

Unfortunately, there are drawbacks as well. Co-crystallisation is hard to control, because it is hard to predict reaction outcome. Two neutral molecules may not react at all and crystallise separately instead, or two ionisable molecules may form a salt instead of a co-crystal. Another disadvantage is that while co-crystallisation has a big effect on properties it is difficult to predict how the properties will change by addition of the neutral counter molecule. Finally, solvates are quite unstable, because a change in conditions, such as an increase in temperature, can cause the solvent to evaporate. This drastically changes the crystal structure and thus solvates are not used often in drug formulations. Additionally, solvates are generally less soluble in their corresponding solvents than the pure API.[18]

Notably, the cons appear to outweigh the pros as a recent review showed that there are currently no commercially available API co-crystals on the market.[16]

1.3.4 Salt formation

The most common option used by pharmaceutical companies to change ionisable APIs is salt formation. Salts consist of two charged ions and must therefore be formed from either an acidic or basic API and a basic or acidic counterion respectively. This slightly limits the possible GRAS counter molecules compared to co-crystallisation but there are still many acceptable options available.

An advantage of salt formation is that it generally leads to big property changes due to big changes in intermolecular interactions. The main property that is easily and positively changed, is to increase aqueous solubility due to the inherent polarity of salt forms. Salt formation also affects hardness, stability and melting point due to the additional intermolecular interactions.

Salt formation is predictable and controllable, because reaction success is largely determined by the pKa difference between the API free base or acid and the pKa of the chosen counterion formers. A difference of at least 2 units is preferable for the reaction to yield a stable salt, but there are of course exceptions to this rule.[19] Another aspect of salt formation predictability is the formal charge of the chosen counterion which will directly influence the stoichiometry of the salt.

The majority of basic APIs use chloride from hydrochloric acid as a counterion for salt formation, and the vast majority of acidic APIs use sodium from sodium hydroxide, see Figure 6. This is because both chloride and sodium are non-toxic GRAS counterions, have low molecular weight and are very affordable.

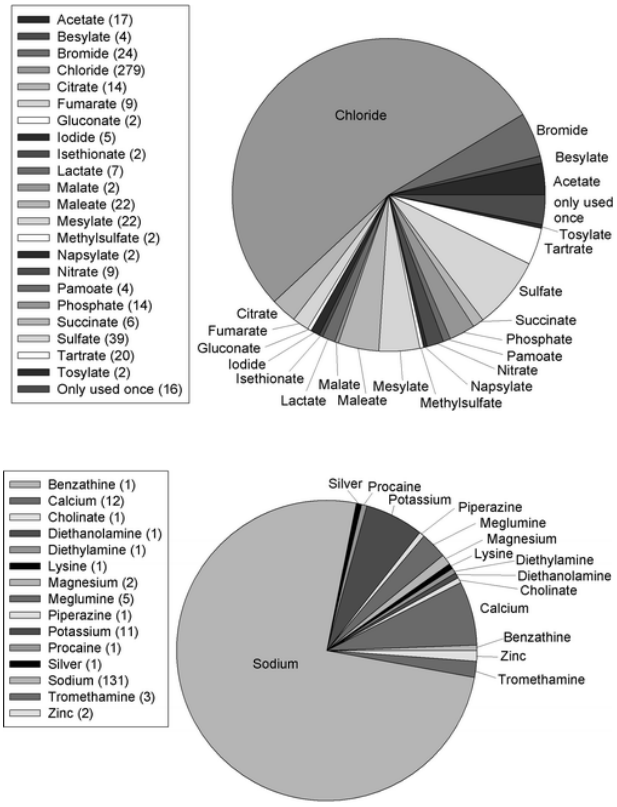

Figure 6: The overall distribution of anions and cations used in APIs of category II in the Orange Book[21]

However, these popular counterions do have disadvantages. For example, sodium cations are very hygroscopic which in turn affects the hygroscopicity of sodium salts.[20] Chloride salt aqueous solubility can be negatively affected by stomach acid, which is part of the oral administration route, this phenomenon is known as the common ion effect. The dissolution reaction of solid-state API chloride salts is pushed towards the solid form due to an excess of chloride ions from the HCl stomach acid on the right-hand side of the equilibrium equation, see Figure 7.[20]

$$[API(H)][Cl]\ (s) \underset{}{\overset{HCl\ (aq)}{\rightleftharpoons}} [API(H)]^{+}\ (aq) + [Cl]^{-}\ (aq)$$

Figure 7: Dissolution reaction of chloride salts in stomach acid

Normally the benefits of using sodium and chloride counterions far outweigh these disadvantages, as evidenced by their prevalence in pharmaceutical salt formulations. The major advantages being that these are stable and non-toxic counterions. Research conducted by Paulekuhn et al in 2007 found that although chloride and sodium were still the most popular counterions, the distribution of anions and cations used in APIs was diversifying. While chloride was the chosen anion for 53.4% of basic API salts overall, its share

drastically dropped to 38.9% when they exclusively reviewed the 2002-2006 period. A similar trend was observed for the use of sodium for acidic API salts, with a change from a 75.3% overall to 62.5% in 2002-2006.[21]

1.4 Tricyclic antidepressants

Tricyclic antidepressants (TCAs) are a class of antidepressants that get their name from their distinct chemical structure that includes three rings. There are five classes of tricyclic antidepressants; two major classes: Dibenzocycloheptadienes, and dibenzazepines, and three minor ones: dibenzoxepins, dibenzothiephines and dibenzoxazepines. These are distinguished by variations in the central ring. Individual TCAs usually also feature a chain motif that originates from the central ring. Thus dibenzazepines have a nitrogen atom in the 7-membered ring where the chain originates, see Figure 8b. Dibenzoxepins and dibenzothiepines are similar to dibenzocycloheptadienes but respectively have an oxygen or sulphur atom in the cycloheptane ring, see Figure 8c and Figure 8d. Dibenzoxazepines have an oxygen and a nitrogen in the cycloheptane ring, see Figure 8e.

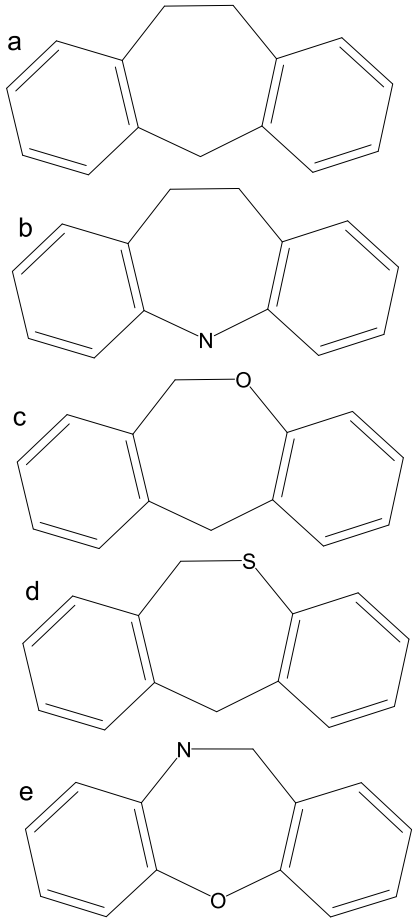

Figure 8: TCA classes. Dibenzocycloheptadienes (a), dibenzazepines (b), dibenzoxepins (c), dibenzothiepines (d), and dibenzoxazepines (e)

The majority of the TCAs act primarily as serotonin and norepinephrine reuptake inhibitors by blocking the serotonin and norepinephrine transporters.[22]

In this work, crystal structures will be elucidated for amitriptyline and nortriptyline (dibenzocycloheptadienes), imipramine (dibenzazepine), and doxepin (dibenzoxepin).

1.4.1 History

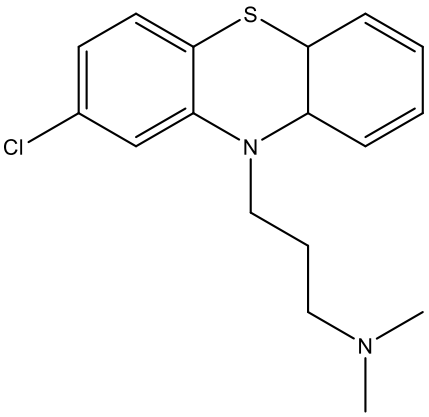

Figure 10: Structure of chlorpromazine

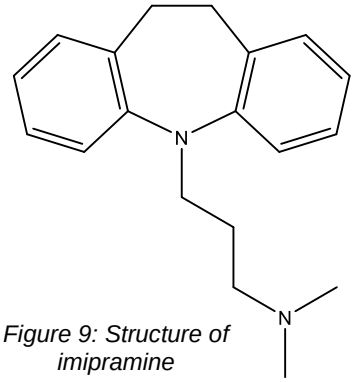

Figure 9: Structure of imipramine

The first tricyclic antidepressant precursor was discovered in 1951 by Paul Charpentier and was named chlorpromazine, see Figure 10. Chlorpromazine became the first widely used psychiatric drug.[23] Imipramine was also synthesised in 1951 to be used as an antihistamine, see Figure 9. However, due to structural similarities of chlorpromazine and imipramine, possible antipsychotic effects of imipramine were studied in the following year. Imipramine proved unsuccessful in treating psychotic symptoms, but its manic effect on psychiatric patients was found to be beneficial for treating depression. Several years later and after further clinical research spearheaded by Kuhn, imipramine was marketed to treat depression in 1958, and thus the first antidepressant was born.[24]

1.4.2 Previous work

Thirteen single crystal structures of tricyclic antidepressants have previously been elucidated and are available from the Cambridge Structural Database (CSD).[25] From the dibenzocycloheptadiene class of TCAs, structures have been elucidated for amitriptyline chloride[26], amitriptyline picrate[27], and nortriptyline chloride[28]. From the dibenzazepine class, structures have been elucidated for imipramine chloride[29], imipramine bromide[30], and imipramine picrate[31], desipramine picrate[32], desipramine picrate hydrate[33], and desipramine chloride[34], clomipramine chloride[35] and clomipramine picrate[36], trimipramine maleate[37] and finally lofepramine chloride.[38] See Figure 11 for the free base structures of the TCAs. These structures were used in the structural analysis section of this work. See sections 3.8 and 4.5.

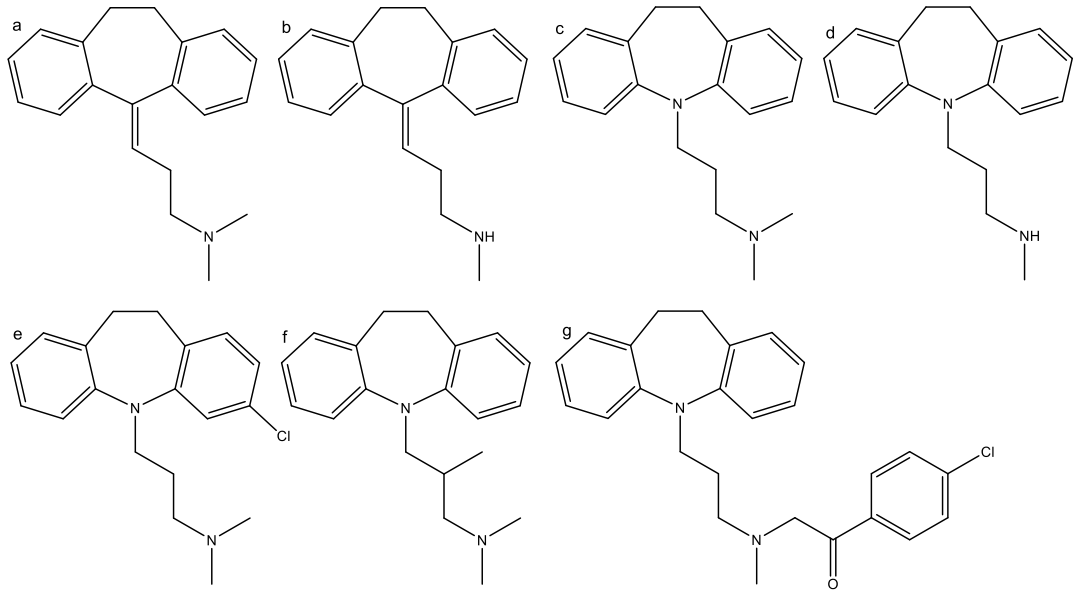

Figure 11: Structures of amitriptyline (a), nortriptyline (b), imipramine (c), desipramine (d), clomipramine (e), trimipramine (f), and lofepramine (g)

In this work, amitriptyline, nortriptyline, imipramine, and doxepin were investigated further due to ease of commercial availability of these APIs and their fit with the previous work.

1.5 References

1) Market Research. https://blog.marketresearch.com/the-growing-pharmaceuticals-market-expert-forecasts-and-analysis (accessed 06/06/2019).

2) Jimmy, B.; Jose, J. *Oman Med J.*, **2011**, *26*, 155-159.

3) Stewart, K.D.; Johnston, J.A.; Matza, L.S.; Curtis, S.E.; Havel, H.A.; Sweetana, S.A.; Gelhorn, H.L. *Patient Prefer. Adherence*, **2016**, *10*, 1385-1399.

4) Khan, M.S.; Roberts, M.S. *Adv. Drug Deliv. Rev.*, **2018**, *135*, 3–38

5) Le, J. Drug Administration. MSD Manual Consumer Version. https://www.msdmanuals.com/en-gb/home/drugs/administration-and-kinetics-of-drugs/drug-administration (accessed 18/06/2019).

6) Schanker, L.S. *Pharmacol Rev*, **1962**, *14, 501-530.*

7) Ladd, M.F.C.; *Bonding, structure and solid-state chemistry*, Oxford University Press: Oxford, **2016**.

8) Kennedy, A.R. CH513: Solid-state Chemistry. Presented at the University of Strathclyde, Glasgow, UK, September 2018.

9) Pikal, M.J.; Rigsbee, D.R. *Pharm Res.*, **1997**, *14*, 1379-1387.

10) Van Santen, R.A. *J. Phys. Chem.*, **1984**, *88*, 5768-5769.

11) Particle Analytical. What is a polymorph? https://particle.dk/what-is-a-polymorph/ (accessed 16/06/2019).

12) Sudha, C.; Srinivasan, K. *J Cryst Growth*. **2014**, *401*, 248–251.

13) Di Martino, P.; Conflant, P.; Drache, M.; Huvenne, J.-P.; Guyot-Hermann, A.-M. *J. Thermal Anal*., **1997**, *48*, 447-458.

14) Thakuria, R.; Thakur, T. S. Crystal Polymorphism in Pharmaceutical Science. In *Comprehensive Supramolecular Chemistry II*; Atwood, J. L., Ed.; Elsevier: Oxford, **2017**; *5*, 283-309.

15) Bauer, J.; Spanton, S.; Henry, R.; Quick, J.; Dziki, W.; Porter, W.; Morris, J. *Pharm Res*, **2004**, *18*, 859–866.

16) Steed, J. W. *Trends Pharmacol Sci.*, **2013**, *34*, 185-193.

17) McNamara, D. P.; Childs, S. L.; Giordano, J.; Iarriccio, A.; Cassidy, J.; Shet, M. S.; Mannion, R.; O'Donnell, E.; Park, A. *Pharm. Res.*, **2006**, *23*, 1888-1897.

18) Griesser, U. The Importance of Solvates. in Polymorphism. In *The Pharmaceutical Industry*; Hilfiker, R., ed.; Wiley-VCH: Weinheim, **2006**; 225.

19) Gokhale, M.Y.; Mantri, R.V.; API Solid-Form Screening and Selection. In *Developing Solid Oral Dosage Forms*, 2; Qiu, Y., Chen, Y., Zhang, G.G.Z., Yu, L., Mantri, R.V., Eds.; Elsevier: Oxford, **2017**; 85-112.

20) P. Stahl and C. Wermuth, ed., Pharmaceutical Salts; Properties, Selection and Use. John Wiley & Sons, **2002**.

21) Paulekuhn, G.S.; Dressman, J.B.; Saal, C. *J. Med. Chem*., **2007**, *50* 6665-6672.

22) Gillman, P.K. *Br J Pharmacol.*, **2007**, *151*, 737-748.

23) Ban, T.A. *Neuropsychiatr Dis Treat.* **2007**, *3*, 495-500.

24) Brown, W.A.; Rosdolsky, M. *Am J Psychiatry*, **2015**, *172*, 426-429.

25) Groom, C. R.; Allen, F. H. *Angew. Chem. Int. Ed.*, **2014**. *53*, 662-671.

26) Klein, C.L.; Lear, J.; O'Rourke, S.; Williams, S.; Liang, L. *J. Pharm. Sci.*, **1994**, *83*, 1253-1256.

27) Bindya, S.; Wong, W-T.; Ashok, M.A.; Yathirajan, H.S.; Rathore, R.S. *Acta Cryst. C*, **2007**, *63*, 546-548.

28) Klein, C.L.; Banks, T.A.; Rouselle, D. *Acta Cryst. C*, **1991**, *47*, 1478-1480.

29) Post, M.L.; Kennard, O.; Horn, A.S. *Acta Cryst. B*, **1975**, *31*, 1008-1013.

30) Paulus, E.F. *Acta Cryst. B*, **1978**, *34*, 1942-1947.

31) Harrison, W.T.A.; Bindya, S., Ashok, M.A.; Yathirajan, H.S.; Narayana, B. *Acta Cryst. E*, **2007**, *63*, 3143.

32) Swamy, M.T.; Ashok, M.A.; Yathirajan, H.S.; Narayana, B.; Bolte, M. *Acta Cryst. E*, **2007**, *63*, 4919.

33) Harrison, W.T.A.; Swamy, M.T.; Nagaraja, P.; Yathirajan, H.S.; Narayana, *Acta Cryst. E*, **2007**, *63*, 3892.

34) Jasinski, J.P.; Butcher, R.J.; Hakim Al-Arique, Q.N.M.; Yathirajan, H.S.; Ramesha, A.R. *Acta Cryst. E*, **2010**, *66*, 674-675.

35) Reck, G. *CSD Communication*, **2006**.

36) Jasinski, J.P.; Butcher, R.J.; Hakim Al-Arique, Q.N.M.; Yathirajan, H.S.; Narayana, B. *Acta Cryst. E*, **2010**, *66*, 347-348.

37) Jasinski, J.P.; Butcher, R.J.; Hakim Al-Arique, Q.N.M.; Yathirajan, H.S.; Narayana, B. *Acta Cryst. E*, **2010**, *66*, 366-367.

38) Bandoli, G.; Nicolini, M.; Casellato, U. *J. Chem. Crystallogr.*, **1987**, *17*, 281-293.

2 Aims

This work was carried out in order to study possible links between counterion functionality and structural features of resulting salt forms such a hydration state, conformation and packing of the API molecule, and hydrogen bonding in order to determine if this data could be used to predict these factors in the future. Particularly, tricyclic antidepressants were chosen as the class of API to expand on the small number of structures available in the CSD database and due to the many conformational possibilities of the molecules which would allow a range of different packing motifs to be studied. Additionally, TCAs are structurally closely related to carbamazepine which has been studied extensively. Single crystal X-ray diffraction was used to study these structural features as this allowed the salt forms to be accurately modelled. In addition to structural analysis, a solubility assessment was carried out on a selection of salt forms because increasing API solubility is a major factor in favour of salt formation for pharmaceutical companies and studying the link between counterion selection and solubility would be beneficial. The aims of this work were therefore summarised in five points:

1. To generate a number of salt forms of four different but structurally related tricyclic antidepressants, namely amitriptyline, nortriptyline, imipramine, and doxepin.

2. To crystallise these salts in such a way as to produce the relatively large high quality single crystals needed to elucidate crystal structures using single crystal x-ray crystallography.

3. To analyse multiple salt forms of the four chosen APIs by single crystal x-ray diffraction.

4. To conduct aqueous solubility measurements on selected salt forms.

5. To analyse the TCA structures generated, together with those available in the CSD, for common structural features (e.g. hydration state, molecular conformation, hydrogen bonding, cation packing) to enhance understanding

of the structural chemistry of these important compounds. Their structural chemistry will also be compared with the well-known structural chemistry of carbamazepine.

3 Experimental

3.1 Materials

Amitriptyline, nortriptyline, imipramine and doxepin containing starting materials were purchased from Sigma Aldrich. The acid and salt reagents used were from commercial sources and used as found in the laboratory.

3.2 Analysis

3.2.1 Single crystal x-ray diffraction

Most single crystal diffraction experiments were carried out with an Oxford Diffraction Gemini instrument. All measurements were made with graphite monochromated CuKα (λ = 1.54184) radiation and at low temperature. Raw data was processed using CrysalisPro[1]. Structures were solved using the programs SHELXS or SIR92.[2,3] All structures were refined to convergence using all unique reflections and against F^2. The refinement program was SHELX-2014 and all programs were implemented within the WINGX interface.[2,4]

Measurements on samples amitriptyline (ami) BF_4, and ami metanilate, nortriptyline (nor) malonate, nor edisylate, nor glutarate, nor 4-hydroxyphenylacetate, nor salicylate, and nor mucate, imipramine (imi) citrate, and imi salicylate were carried out by the UK National Crystallography Service (NCS) at the University of Southampton.[5] Of these, ami metanilate, nor 4-hydroxyphenylacetate, nor salicylate, and imi citrate were further analysed at the Diamond Light Source on beamline i19.[6]

Selected crystallographic and refinement details for each structure are given in tables in sections 3.3.4, 3.4.4, 3.5.4, and 3.6.4 with a note as to which instrument was used to carry out single crystal X-ray diffraction. Full descriptions of all single crystal structures are available in the electronic appendix as a cif (crystallographic information file) format.

3.2.2 Powder diffraction

Powder diffraction measurements were made by Dr Kenneth Shankland at the University of Reading. The following parameters were used.

- Bruker D8 Advance operating in transmission capillary mode, monochromatic $K\alpha_1$ radiation, with a LynxEye detector.
- The samples were added into borosilicate glass capillaries as slurries in unbuffered water. The capillaries were 0.7 mm for all samples, except for the salicylate where a 1.0 mm capillary was used.
- Data collection parameters were as follows:
    - Data collected at room temperature.
    - Range 3-30 degrees 2θ.
    - Step size 0.017 degrees.
    - Count time 0.8 sec/step for all samples, except for the besylate, where a longer count time of 1.6 sec/step was used due to weak scattering.
- Visual comparison of observed data with data calculated from the supplied cifs was used in the initial evaluation. Pawley fitting (using cell and space group information from the cifs, but not structure information) was then used as a more definitive method of confirming the physical form.

3.2.3 Spectroscopic analysis

IR analysis was carried out using the A2 Attenuated Total Reflectance (ATR FT-IR) instrument. Solution phase UV/VIS analysis was carried out using a Photonics CCD Array UV/VIS Spectrophotometer.

3.2.4 Melting point

Melting points were determined from a single measurement due to small material availability using the Gallenkamp melting point apparatus.

3.3 Amitriptyline salt formation

3.3.1 The reaction of amitriptyline HCl with sodium salts

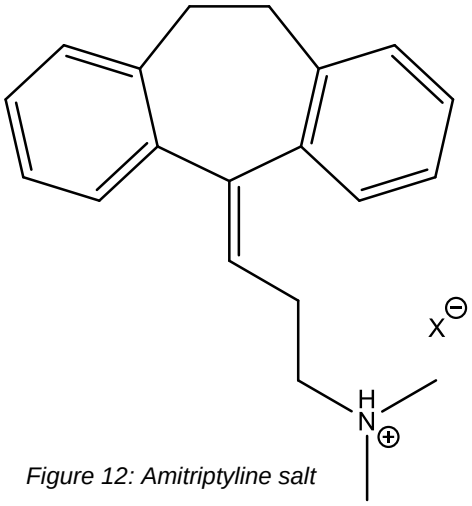

Figure 12: Amitriptyline salt

The formation of a variety of amitriptyline salt forms was carried out by reacting amitriptyline hydrochloride with a variety of s-block metal salts (MX). Thereby producing MCl and the X salt of the API. An example procedure was as follows. 0.20 g (0.64 mmol) of amitriptyline HCl was dissolved in roughly 2.5 mL of water before 0.15 g (1.50 mmol) of sodium bromide was added, giving an excess of the sodium salt. Additional deionised water was added to dissolve the reactants and the solution was stirred at 50 °C for 30 minutes. After 30 minutes, the vessel containing the solution was wrapped in cotton wool and aluminium foil to encourage slow cooling. Note, this procedure was designed to maximise chances of growing single crystals and not to maximise yield of bulk material.

This procedure was repeated for 0.25 g (1.5 mmol) potassium iodide. The procedure was also repeated on a smaller scale with 0.05 g (0.16 mmol) of amitriptyline HCl and 0.40 mmol of the additional sodium salts listed in Table 1.

Table 1: List of sodium and potassium salts used for amitriptyline and nortriptyline salt formation

Name	Formula	MW (g/mol)	Moles	Mass (g)
Sodium bromide	NaBr (a)	102.89	1.5E-03	0.15
Potassium iodide	KI (b)	166.00	1.5E-03	0.25
Sodium salicylate	$C_7H_5NaO_3$ (c)	160.11	4.0E-04	0.06
Sodium carbonate	Na_2CO_3 (d)	105.99	4.0E-04	0.04
Sodium nitrite	$NaNO_2$ (e)	69.00	4.0E-04	0.03
Sodium hydrogen orthophosphate	Na_2HPO_4 (f)	141.96	4.0E-04	0.06
Sodium thiosulfate pentahydrate	$Na_2S_2O_3.5H_2O$ (g)	248.18	4.0E-04	0.10
Sodium hexafluorosilicate	$Na_2Si\ F_6$ (h)	188.06	4.0E-04	0.08
Sodium citrate	$C_6H_5Na_3O_7.2H_2O$ (i)	294.10	4.0E-04	0.12

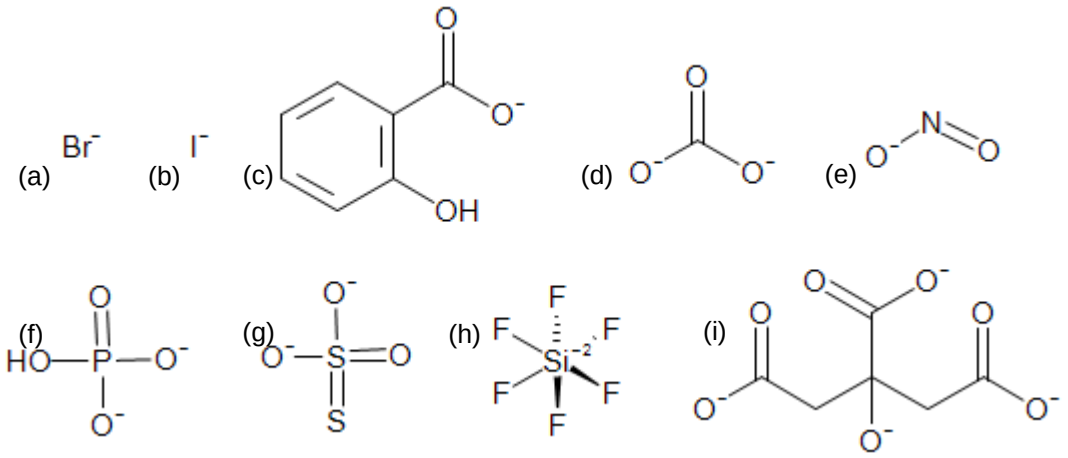

Figure 13: Anion structures of salts used for salt formation

Crystals suitable for single crystal x-ray crystallography were only obtained from the reaction between amitriptyline hydrochloride and sodium salicylate. Alternative crystallisation techniques were not attempted in this work, although this may be expanded as further work. FT-IR spectroscopic screening was carried out on the crystals and the starting materials to determine whether or not crystals formed were the desired product. If the spectra were found to be different, single crystal x-ray diffraction (SXD) was carried out to elucidate the crystal structure. The bulk sample was then dried and weighed, and the melting point was determined, these are listed in Table 2 below.

Table 2: Amitriptyline salicylate chemical properties

Compound	Yield (g)	% Yield	Melting point (°C)	Major IR peaks (cm^{-1})
Amitriptyline salicylate	0.01 g	3.8	119.2 – 120.1	3229, 1651, 161

3.3.2 Generating the amitriptyline free base

The amitriptyline free base was generated by reacting the amitriptyline HCl salt with a 1:3 amount of 2 molar ammonia solution. This reaction formed the API free base and ammonium chloride according to Figure 14.

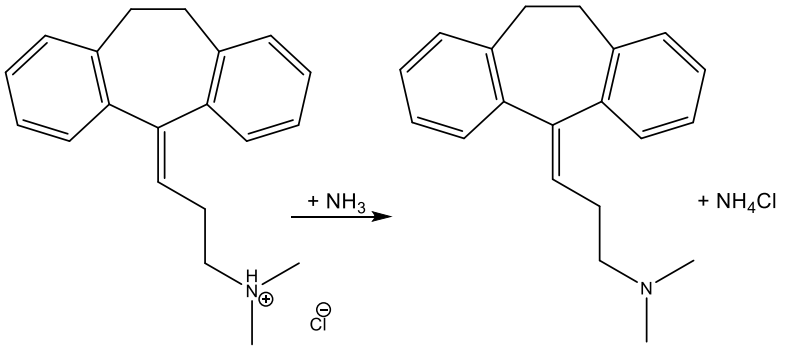

Figure 14: Reaction of amitriptyline with ammonia solution

5.0 g (16 mmol) of amitriptyline hydrochloride was weighed out and dissolved in approximately 20 mL deionised water. 25 mL (50 mmol) of 2 M ammonia solution was added to the amitriptyline hydrochloride solution while heating at 50 °C and stirring for half an hour.

The reaction yielded an oily precipitate which was washed and purified using a separating funnel. Diethyl ether was used as the organic solvent and deionised water was used as the aqueous solvent. The organic layer dissolved the API free base precipitate while the aqueous layer dissolved the ammonium chloride salt and any remaining starting materials. The aqueous layer was washed three times with roughly 150 mL of diethyl ether each time. The solvent was removed from the aqueous layer using a rotary evaporator. FT-IR analysis of the solid residue from this layer showed it to contain no organic compounds and confirmed the presence of NH_4^+. The organic layer was left to evaporate to yield the desired product. Unfortunately, the product

oiled out of solution so no yield could be calculated. Several attempts to crystallise the oily product were made. First, a small amount of petroleum ether was added to encourage mobility. Second, a glass rod was used to scratch the beaker to provide sites for nucleation. Third, the product was heated to attempt to evaporate trapped solvent. Finally, the product was placed in a fridge for three days to reduce solubility. Unfortunately, none of these methods were successful. For further reactions, the oily product was dissolved in ethanol and a yield of 75% was assumed, so 1 mL of solution would correspond to 0.5 mmol of amitriptyline free base.

3.3.3 Salt formation from reaction of amitriptyline free base with acidic compounds

The amitriptyline free base was reacted with the acids listed in Table 3.

Table 3: List of the amount and type of acid used for salt formation with 1 mmol of the amitriptyline and nortriptyline free base

Acid compound	Molecular weight (g/mol)	Moles	Mass (g)
adipic acid	146.14	2.0E-03	0.29
benzoic acid	122.12	2.0E-03	0.24
3-aminobenzoic acid	137.14	2.0E-03	0.27
4-aminobenzoid acid	137.14	2.0E-03	0.27
2-chlorobenzoic acid	156.57	2.0E-03	0.31
3-chlorobenzoic acid	156.57	2.0E-03	0.31
4-chlorobenzoic acid	156.57	2.0E-03	0.31
2-fluorobenzoic acid	140.11	2.0E-03	0.28
3-fluorobenzoic acid	140.11	2.0E-03	0.28
4-fluorobenzoic acid	140.11	2.0E-03	0.28
3-hydroxybenzoic acid	138.12	2.0E-03	0.28
4-hydroxybenzoic acid	138.12	2.0E-03	0.28
2-nitrobenzoic acid	167.12	2.0E-03	0.33
3-nitrobenzoic acid	167.12	2.0E-03	0.33
4-nitrobenzoic acid	167.12	2.0E-03	0.33
o-toluic acid	136.20	2.0E-03	0.27
m-toluic acid	136.20	2.0E-03	0.27
p-toluic acid	136.20	2.0E-03	0.27
citric acid	192.12	2.0E-03	0.38
maleic acid	116.10	2.0E-03	0.23

Acid compound	Molecular weight (g/mol)	Moles	Mass (g)
malic acid	134.09	2.0E-03	0.27
malonic acid	104.06	2.0E-03	0.21
mandelic acid	152.15	2.0E-03	0.30
oxalic acid	90.03	2.0E-03	0.18
salicylic acid	138.12	2.0E-03	0.28
succinic acid	118.09	2.0E-03	0.24
methane sulfonic acid	96.10	2.0E-03	0.19
ethane disulfonic acid	190.20	2.0E-03	0.38
benzene sulfonic acid	158.18	2.0E-03	0.32
4-hydroxybenzene sulfonic acid	174.17	2.0E-03	0.35
tartaric acid	150.09	2.0E-03	0.30
p-acetamidobenzoic acid	179.18	1.1E-03	0.20
acetyl salicylic acid	180.16	1.1E-03	0.20
4-aminophenyl acetic acid	151.16	1.1E-03	0.17
p-aminosalicylic acid	153.14	1.1E-03	0.17
5-aminosalicylic acid	153.14	1.1E-03	0.17
n-caproic acid	116.16	1.1E-03	0.13
r-(-)-3-chloromandelic acid	186.59	1.1E-03	0.21
chlorosulfonic acid	116.52	1.1E-03	0.13
p-coumaric acid	164.05	1.1E-03	0.18
d-glucuronic acid	194.14	1.1E-03	0.21
l-glutamic acid	147.13	1.1E-03	0.16
glutaric acid	132.12	1.1E-03	0.15
hippuric acid	179.17	1.1E-03	0.20
1-hydroxy-2-naphthoic acid	188.18	1.1E-03	0.21
2-hydroxyphenylacetic acid	152.15	1.1E-03	0.17
4-hydroxyphenylacetic acid	152.15	1.1E-03	0.17
2-hydroxy-pyridine-3-carboxylic acid	139.11	1.1E-03	0.15
isonicotinic acid	123.11	1.1E-03	0.14
metanilic acid	173.19	1.1E-03	0.19
mucic acid	210.14	1.1E-03	0.23
1-naphthoic acid	172.18	1.1E-03	0.19
phenylacetic acid	136.15	1.1E-03	0.15
pimelic acid	160.17	1.1E-03	0.18
sulphamic acid	97.10	1.1E-03	0.11
thiomalic acid	150.15	1.1E-03	0.17
p-toluenesulfonic acid	190.22	1.1E-03	0.21
trans-cinnamic acid	148.16	1.1E-03	0.16
uric acid	168.11	1.1E-03	0.18

A typical procedure was as follows. 0.18 g (2.0 mmol) of salicylic acid was weighed out and dissolved in deionised water. 2 mL (1.0 mmol) of the amitriptyline free base solution in ethanol, prepared as described in section 3.3.2, was added to the reaction vessel for an approximate 2:1 excess of acid to API. The solution was heated and stirred at 50 °C for half an hour to form amitriptyline salicylate as shown in Figure 15. After 30 minutes, any undissolved solid was removed by filtration and checked by IR to ensure it was unreacted starting material and not the desired product. The clear solution was left to slowly cool to room temperature. Again, the aim was to produce high quality single crystals and not to maximise bulk yield.

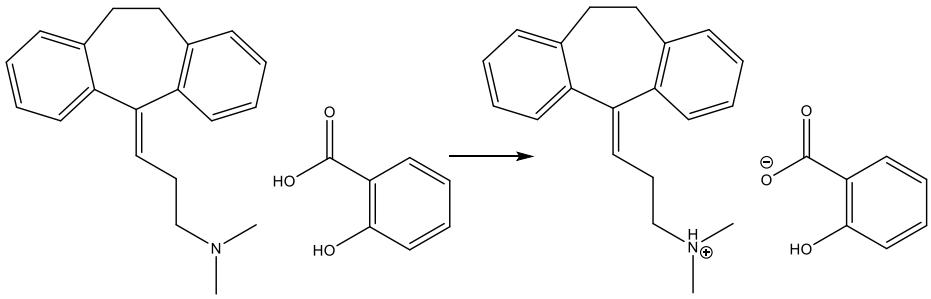

Figure 15: Reaction scheme for amitriptyline free base with salicylic acid to form amitriptyline salicylate

This procedure was repeated for the other acidic compounds listed in Table 3. However, the experiments often yielded crystals of the acid starting material instead of the desired API salt. To combat this, the molar ratio was reduced to 1.1:1 acid to API free base for the second large set of experiments. The mass of acid used for each experiment was listed in Table 3 with the lesser excess experiments in the bottom half. Whenever the experiments yielded crystals of the acid starting material as determined by FT-IR spectroscopy or by single crystal diffraction, the crystals were removed from solution using gravity filtration and the remaining clear solutions were left to recrystallise by slow evaporation.

Additionally, reactions of the API with the acids listed in Table 4 were attempted using *ca.* 1 mL of the acid e.g. with a large excess. The procedure outlined above was followed.

Table 4: List of commercially available acid starting materials used in salt formation that were supplied as solutions

Acid compound	Molecular weight (g/mol)	Concentration
nitric acid	63.01	68%
tetrafluoroboric acid	87.81	48%
sulfuric acid	98.08	98%
phosphoric acid	98.00	85%

Crystals of the desired amitriptyline salt forms that were suitable for single crystal x-ray crystallography were grown for amitriptyline tetrafluoroborate, amitriptyline oxalate, amitriptyline 4-nitrobenzoate, amitriptyline mucate, and amitriptyline metanilate. These crystals were checked by FT-IR spectroscopy and then their crystal structures were elucidated using single crystal X-ray crystallography. Finally, the bulk samples were dried, weighed, and their melting points determined. Note that amitriptyline tetrafluoroborate appeared to have degraded before the bulk material could be isolated and analysed. The properties are listed in Table 5.

Table 5: Chemical properties of amitriptyline salt forms

Compound	Yield (g)	% Yield *	Melting point (°C)	Major IR peaks (cm^{-1})
Amitriptyline tetrafluoroborate	N/A		N/A	N/A
Amitriptyline oxalate	0.02 g	2.7	175.1 – 177.0	3038, 3010, ~1640, 1487
Amitriptyline 4-nitrobenzoate	< 0.01 g	< 0.8	129.1 – 129.7	2922, 1706, 1522
Amitriptyline mucate	0.01 g	1.1	153.4 – 155.1	broad OH stretch at *ca.* 3450, 1600, 1392
Amitriptyline metanilate	0.08 g	4.9	60.8 – 61.3	3421, 1595, 1481

* Note that the concentration of the amitriptyline stock solution was based on an assumed yield due to the oily nature of the free base and the %yield are based on this assumption.

3.3.4 Crystal data for amitriptyline salt forms

Table 6: Crystal data for amitriptyline salt forms (1)

Structure ID	ami_4nitrobenz	ami_hbf4
Salt form	Amitriptyline 4-nitrobenzoate	Amitriptyline tetrafluoroborate
Formula	$O_8N_3C_{34}H_{33}$	$F_4O_{1.25}NC_{20}BH_{26.5}$
Formula weight	611.64	387.73
Crystal system	monoclinic	Triclinic
Space group	$P2_1/n$	P-1
Temperature/K	123(2)	123(2)
a/Å	14.4704(7)	10.5107(11)
b/Å	13.7781(4)	10.8809(9)
c/Å	15.9719(11)	36.7424(18)
α/°	90	83.371(5)
β/°	108.622(7)	83.143(6)
γ/°	90	75.973(8)
Volume/Å^3	3017.7(3)	4031.3(6)
Z	4	8
ρ_{calc}g/cm^3	1.346	1.278
μ/mm^{-1}	0.097	0.874
F(000)	1288	1636
Radiation	CuKα (λ = 1.54184)	CuKα (λ = 1.54184)
2Θ range for data collection/°	7.184 to 146.802	10.534 to 131.996
Index ranges	-17 ≤ h ≤ 17, -16 ≤ k ≤ 12, -19 ≤ l ≤ 17	-12 ≤ h ≤ 8, -12 ≤ k ≤ 12, -42 ≤ l ≤ 43
Reflections collected	11894	28463
Independent reflections	5931 [R_{int} = 0.0538, R_{sigma} = 0.0845]	14031 [R_{int} = 0.0778, R_{sigma} = 0.1195]
Data/restraints/parameters	5931/1/412	14031/137/1030
Goodness-of-fit on F^2	1.01	1.095
Final R indexes [I>=2σ (I)]	R_1 = 0.0624, wR_2 = 0.1515	R_1 = 0.1299, wR_2 = 0.3339
Final R indexes [all data]	R_1 = 0.1024, wR_2 = 0.1756	R_1 = 0.2131, wR_2 = 0.4086
Largest diff. peak/hole / e Å^{-3}	0.30/-0.30	0.92/-0.47

Table 7: Crystal data for amitriptyline salt forms (2)

Structure ID	ami_meta	ami_mucic
Salt form	Amitriptyline metanilate	Amitriptyline mucate
Formula	$ClO_6N_3C_{46}H_{60}S$	$O_7N_1C_{23}H_{34}$
Formula weight	818.48	436.51
Crystal system	triclinic	monoclinic
Space group	P-1	I2/a
Temperature/K	100(2)	123(2)
a/Å	10.4824(7)	10.4981(4)
b/Å	10.9330(7)	10.3829(4)
c/Å	20.1504(14)	43.147(2)
α/°	90.306(6)	90
β/°	104.225(6)	96.300(4)
γ/°	103.646(6)	90
Volume/Å^3	2170.4(3)	4674.7(3)
Z	2	8
ρ_{calc}g/cm^3	1.252	1.24
μ/mm^{-1}	0.187	0.751
F(000)	876	1880
Radiation	synchrotron (λ = 0.6889)	CuKα (λ = 1.54184)
2Θ range for data collection/°	2.026 to 48	8.246 to 146.376
Index ranges	-12 ≤ h ≤ 12, -12 ≤ k ≤ 12, -23 ≤ l ≤ 23	-9 ≤ h ≤ 12, -10 ≤ k ≤ 12, -53 ≤ l ≤ 52
Reflections collected	25623	9201
Independent reflections	7396 [R_{int} = 0.3192, R_{sigma} = 0.2412]	4581 [R_{int} = 0.0633, R_{sigma} = 0.0953]
Data/restraints/parameters	7396/52/596	4581/0/431
Goodness-of-fit on F^2	1.04	1.011
Final R indexes [I>=2σ (I)]	R_1 = 0.1192, wR_2 = 0.2924	R_1 = 0.0632, wR_2 = 0.1212
Final R indexes [all data]	R_1 = 0.1386, wR_2 = 0.3267	R_1 = 0.1206, wR_2 = 0.1520
Largest diff. peak/hole / e Å^{-3}	0.56/-0.50	0.19/-0.22

Table 8: Crystal data for amitriptyline salt forms (3)

Structure ID	ami_oxalic	ami_salicylate
Salt form	Amitriptyline oxalate	Amitriptyline salicylate
Formula	$O_4NC_{22}H_{25}$	$O_3NC_{27}H_{29}$
Formula weight	367.43	415.51
Crystal system	triclinic	monoclinic
Space group	P-1	$P2_1/n$
Temperature/K	123(2)	123(2)
a/Å	8.4118(6)	9.5730(5)
b/Å	11.1755(9)	15.3376(8)
c/Å	21.3188(13)	15.8590(10)
α/°	89.737(6)	90
β/°	87.457(5)	99.370(5)
γ/°	73.787(6)	90
Volume/Å^3	1922.4(2)	2297.5(2)
Z	4	4
ρ_{calc}g/cm^3	1.269	1.201
μ/mm^{-1}	0.704	0.615
F(000)	784	888
Radiation	CuKα (λ = 1.54184)	CuKα (λ = 1.54184)
2Θ range for data collection/°	8.24 to 146.628	8.072 to 139.606
Index ranges	-10 ≤ h ≤ 10, -13 ≤ k ≤ 13, -20 ≤ l ≤ 26	-11 ≤ h ≤ 11, -10 ≤ k ≤ 18, -19 ≤ l ≤ 17
Reflections collected	10848	12014
Independent reflections	10848 [R_{sigma} = 0.0605]	4250 [R_{int} = 0.0754, R_{sigma} = 0.0729]
Data/restraints/parameters	10848/4/500	4250/0/286
Goodness-of-fit on F^2	0.926	1.05
Final R indexes [I>=2σ (I)]	R_1 = 0.0639, wR_2 = 0.1625	R_1 = 0.0813, wR_2 = 0.2098
Final R indexes [all data]	R_1 = 0.0900, wR_2 = 0.1744	R_1 = 0.1209, wR_2 = 0.2526
Largest diff. peak/hole / e Å^{-3}	0.39/-0.26	0.34/-0.37

3.4 Nortriptyline salt formation

3.4.1 The reaction of nortriptyline HCl with sodium salts

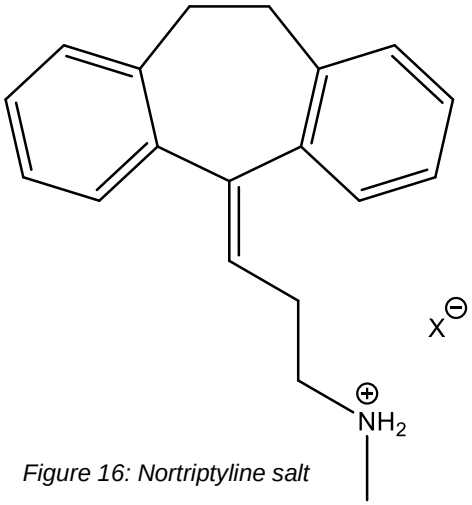

Figure 16: Nortriptyline salt

The formation of a variety of nortriptyline salt forms was carried out by reacting nortriptyline hydrochloride with a variety of s-block metal salts (MX). Thereby producing MCl and the X salt of the API. HBr was also used as a reagent in place of MX. An example procedure was as follows. 0.20 g (0.67 mmol) of nortriptyline HCl was dissolved in roughly 17 mL of water before 0.15 g (1.50 mmol) of sodium bromide was added to give an excess of metal salt over the API. Deionised water was added to dissolve the reactants and the solution was stirred at 50 °C for 30 minutes. After 30 minutes, the vessel containing the solution was wrapped in cotton wool and aluminium foil to encourage slow cooling and crystal growth.

This procedure was repeated for 0.25 g (1.5 mmol) potassium iodide. The procedure was also repeated on a smaller scale with 0.05 g (0.17 mmol) of nortriptyline HCl and the salts listed above in Table 1. Additionally, nortriptyline hydrochloride was reacted with bromic acid.

Crystals suitable for single crystal x-ray crystallography were obtained for both nortriptyline bromide reactions, nortriptyline iodide and nortriptyline hexafluorosilicate. FT-IR spectroscopy was carried out on these crystals and the acid starting materials to determine whether they were the product or rather free acid. After the spectra were found to be different, single crystal X-ray crystallography was carried out to elucidate the crystal structure. Then, the crystals were dried, weighed, and the melting points determined. These chemical properties were listed below in Table 9.

Table 9: Chemical properties of nortriptyline salt forms

Compound	Yield (g)	% Yield	Melting point (°C)	Major IR peaks (cm^{-1})
Nortriptyline bromide (NaBr)	N/A		N/A	2950, 2785, 1485
Nortriptyline bromide (HBr)	0.06 g	26.0	195.5 – 197.0	2952, 2789, 1485
Nortriptyline iodide	0.02 g	30.1	184.4 – 185.5	2948, 2785, 1485
Nortriptyline hexafluorosilicate	0.03 g	12.2	104.3 – 105.0	3084, 2911, 1599, 1472

3.4.2 Generating the nortriptyline free base

The nortriptyline free base was generated by reacting the nortriptyline HCl salt with a 1:3 amount of 2 molar ammonia solution. Similarly, to the amitriptyline reaction outlined above in figure 3.2.1, this reaction formed the API free base and ammonium chloride.

5.0 g (17 mmol) of nortriptyline hydrochloride was weighed out and dissolved in approximately 100 mL deionised water. 25 mL (50 mmol) of 2 M ammonia solution was added to the amitriptyline solution while heating at 50 °C and stirring for half an hour.

The reaction yielded an oily precipitate which was washed and purified using a separating funnel. The organic and aqueous solvents were diethyl ether and deionised water respectively. The organic layer dissolved the API free base while the aqueous layer dissolved the ammonium chloride salt and any remaining starting materials. The aqueous layer was washed three times with roughly 150 mL of diethyl ether each time. The organic layer was then left to evaporate to yield the desired product. Unlike the amitriptyline free base, the nortriptyline free base yielded a crystalline powder as the product. FT-IR analysis determined the spectrum closely matched the nortriptyline HCl salt. The yield for the first batch was 97%. The product was dissolved in 25 mL ethanol. The molarity of the nortriptyline free base ethanol solution was 0.65 mol/L.

3.4.3 Salt formation reactions of the nortriptyline free base with acidic compounds

Nortriptyline salt formation was attempted with the same acidic compounds as listed above in Table 3.

A typical procedure was as follows. 0.18 g (2.0 mmol) of salicylic acid was weighed out and dissolved in deionised water. 2 mL (1.3 mmol) of the nortriptyline free base solution in ethanol, prepared as described in section 3.4.2, was added to the reaction vessel for a 2:1 excess of acid to API. The solution was heated and stirred at 50 °C for half an hour to form nortriptyline salicylate. After 30 minutes, any undissolved solid was filtered off and checked by IR to ensure it was unreacted starting material and not the desired product. The clear solution was left to slowly cool to room temperature. This procedure was repeated for the other acidic compounds listed in Table 3. Unfortunately, many of the experiments yielded crystals of the acid starting material as determined by FT-IR spectroscopy or by single crystal diffraction. In these cases, the crystals were removed from solution using gravity filtration and the clear solutions were left to recrystallise by slow evaporation. To minimise the chances of acid starting materials crystallising, later experiments were conducted with a lower molar ratio of 1.1:1 acid to API free base.

Additionally, where commercial acids were supplied as concentrated solutions, reactions of the API were carried out with a large excess of the acids (Table 4), *ca.* 1 mL of the acid. The procedure outlined above was followed.

Crystals of the desired nortriptyline salt forms that were suitable for single crystal x-ray crystallography were obtained for nortriptyline tetrafluoroborate, nortriptyline besylate, nortriptyline tosylate, nortriptyline edisylate, nortriptyline malonate, nortriptyline glutarate, nortriptyline 4-hydroxyphenylacetate, nortriptyline mucate, and nortriptyline salicylate. These crystals were examined by FT-IR spectroscopy and then their crystal structures were elucidated using single crystal x-ray crystallography. Material

amounts dependent, the bulk crystals were dried, weighed, and the melting points determined. These chemical properties are listed in Table 10.

Table 10: Chemical properties of nortriptyline salt forms

Compound	Yield (g)	% Yield	Melting point (°C)	Major IR peaks (cm^{-1})
Nortriptyline tetrafluoroborate	0.32 g	45.6	136.7 – 139.4	3233, 1599
Nortriptyline besylate	0.09 g	10.7	183.1 – 185.0	3062, 3015, 1422
Nortriptyline tosylate	0.01 g	1.1	N/A	N/A
Nortriptyline edisylate	0.01 g	0.7	137.9 – 139.2	N/A
Nortriptyline malonate	N/A		131.2 – 133.7	3017, 2931, 1721, 1426
Nortriptyline glutarate	N/A		N/A	3376, 2939, 1537
Nortriptyline 4-hydroxyphenylacetate	0.01 g	0.6	149.7 – 150.8	1548, 1509
Nortriptyline mucate	0.01 g	0.7	175.6 – 177.1	N/A
Nortriptyline salicylate	N/A		N/A	3229, 1656, 1608, 1442

3.4.4 Crystal data for nortriptyline salt forms

Table 11: Crystal data for nortriptyline salt forms (1)

Structure	nor_4hydphenace	nor_benzsulf
Salt form	Nortriptyline 4-hydroxyphenyl acetate	Nortriptyline benzenesulfonate
Formula	$C_{54}H_{56}N_2O_6$	$C_{25}H_{27}NO_3S$
Formula weight	829.03	421.53
Crystal system	triclinic	monoclinic
Space group	P-1	$P2_1$
Temperature/K	173(2)	123(2)
a/Å	9.42280(10)	12.4849(5)
b/Å	15.3246(2)	7.3912(3)
c/Å	15.6402(2)	12.5187(5)
α/°	82.9490(10)	90
β/°	87.2140(10)	110.949(5)
γ/°	87.7440(10)	90
Volume/Å^3	2237.46(5)	1078.84(8)
Z	2	2
ρ_{calc}g/cm^3	1.231	1.298
μ/mm^{-1}	0.08	1.542
F(000)	884	448
Radiation	synchrotron (λ = 0.6889)	CuKα (λ = 1.54184)
2Θ range for data collection/°	2.596 to 71.904	7.562 to 146.67
Index ranges	-15 ≤ h ≤ 15, -25 ≤ k ≤ 25, -26 ≤ l ≤ 25	-15 ≤ h ≤ 15, -9 ≤ k ≤ 8, -15 ≤ l ≤ 14
Reflections collected	47157	8852
Independent reflections	20054 [R_{int} = 0.0834, R_{sigma} = 0.1026]	4048 [R_{int} = 0.0420, R_{sigma} = 0.0523]
Data/restraints/parameters	20054/2/579	4048/5/278
Goodness-of-fit on F^2	1.038	1.057
Final R indexes [I>=2σ (I)]	R_1 = 0.0849, wR_2 = 0.2391	R_1 = 0.0421, wR_2 = 0.1058
Final R indexes [all data]	R_1 = 0.1161, wR_2 = 0.2686	R_1 = 0.0451, wR_2 = 0.1084
Largest diff. peak/hole / e Å^{-3}	1.04/-0.38	0.35/-0.28

Table 12: Crystal data for nortriptyline salt forms (2)

Structure	nor_edisulf	nor_glutaric
Salt form	Nortriptyline edisylate	Nortriptyline glutarate
Formula	$C_{40}H_{48}N_2O_6S_2$	$C_{43}H_{52}N_2O_5$
Formula weight	716.92	676.86
Crystal system	triclinic	triclinic
Space group	P-1	P-1
Temperature/K	123(2)	123(2)
a/Å	7.7532(5)	8.5745(2)
b/Å	9.2216(6)	9.0307(2)
c/Å	28.337(2)	23.6642(5)
α/°	86.772(5)	81.189(2)
β/°	88.388(6)	85.931(2)
γ/°	67.300(6)	83.444(2)
Volume/Å^3	1866.0(2)	1796.27(7)
Z	2	2
ρ_{calc}g/cm^3	1.276	1.251
μ/mm^{-1}	0.192	0.642
F(000)	764	728
Radiation	MoKα (λ = 0.71073)	CuKα (λ = 1.54184)
2Θ range for data collection/°	4.32 to 50.154	7.572 to 136.5
Index ranges	-9 ≤ h ≤ 9, -10 ≤ k ≤ 10, -33 ≤ l ≤ 33	-10 ≤ h ≤ 10, -10 ≤ k ≤ 10, -28 ≤ l ≤ 28
Reflections collected	7130	32519
Independent reflections	7130 [R_{sigma} = 0.0527]	6537 [R_{int} = 0.0599, R_{sigma} = 0.0406]
Data/restraints/parameters	7130/87/452	6537/20/579
Goodness-of-fit on F^2	1.119	1.042
Final R indexes [I>=2σ (I)]	R_1 = 0.0896, wR_2 = 0.2101	R_1 = 0.0466, wR_2 = 0.1202
Final R indexes [all data]	R_1 = 0.0993, wR_2 = 0.2152	R_1 = 0.0563, wR_2 = 0.1258
Largest diff. peak/hole / e Å^{-3}	0.86/-0.92	0.37/-0.28

Table 13: Crystal data for nortriptyline salt forms (3)

Structure	nor_hbf4	nor_hbr
Salt form	Nortriptyline tetrafluoroborate	Nortriptyline bromide form 1
Formula	$C_{19}H_{22}BF_4N$	$C_{19}H_{22}BrN$
Formula weight	351.18	344.28
Crystal system	triclinic	triclinic
Space group	P-1	P-1
Temperature/K	123(2)	123(2)
a/Å	11.0161(4)	10.5487(8)
b/Å	11.0388(4)	10.9693(8)
c/Å	15.9635(5)	15.2603(15)
α/°	72.531(3)	75.269(7)
β/°	82.988(3)	83.718(7)
γ/°	81.388(3)	80.706(6)
Volume/Å^3	1824.69(11)	1681.0(3)
Z	4	4
ρ_{calc}g/cm^3	1.278	1.36
μ/mm^{-1}	0.861	3.259
F(000)	736	712
Radiation	CuKα (λ = 1.54184)	CuKα (λ = 1.54184)
2Θ range for data collection/°	8.144 to 145.972	8.416 to 147.162
Index ranges	-13 ≤ h ≤ 13, -9 ≤ k ≤ 13, -18 ≤ l ≤ 19	-12 ≤ h ≤ 12, -13 ≤ k ≤ 13, -18 ≤ l ≤ 18
Reflections collected	17230	15966
Independent reflections	7201 [R_{int} = 0.0198, R_{sigma} = 0.0208]	15966 [R_{int} = ?, R_{sigma} = 0.0669]
Data/restraints/parameters	7201/90/519	15966/0/380
Goodness-of-fit on F^2	1.042	1.04
Final R indexes [I>=2σ (I)]	R_1 = 0.0572, wR_2 = 0.1519	R_1 = 0.0978, wR_2 = 0.2593
Final R indexes [all data]	R_1 = 0.0628, wR_2 = 0.1571	R_1 = 0.1156, wR_2 = 0.2819
Largest diff. peak/hole / e Å^{-3}	0.54/-0.45	2.33/-1.86

Table 14: Crystal data for nortriptyline salt forms (4)

Structure	nor_ki	nor_malonic
Salt form	Nortriptyline iodide	Nortriptyline malonate
Formula	$C_{19}H_{22}IN$	C22H24NO4
Formula weight	391.27	366.42
Crystal system	triclinic	monoclinic
Space group	P-1	$P2_1/c$
Temperature/K	123(2)	123(2)
a/Å	10.7791(5)	24.8546(5)
b/Å	11.1443(5)	8.76702(18)
c/Å	15.4690(8)	8.7354(2)
α/°	73.801(4)	90
β/°	82.551(4)	97.250(2)
γ/°	80.722(4)	90
Volume/Å^3	1754.06(15)	1888.23(7)
Z	4	4
ρ_{calc}g/cm^3	1.482	1.289
μ/mm^{-1}	14.274	0.717
F(000)	784	780
Radiation	CuKα (λ = 1.54184)	CuKα (λ = 1.54184)
2Θ range for data collection/°	8.334 to 139.97	10.71 to 136.52
Index ranges	-13 ≤ h ≤ 8, -13 ≤ k ≤ 13, -18 ≤ l ≤ 18	-29 ≤ h ≤ 29, -10 ≤ k ≤ 10, -10 ≤ l ≤ 9
Reflections collected	14642	17484
Independent reflections	6649 [R_{int} = 0.1351, R_{sigma} = 0.1373]	3459 [R_{int} = 0.0316, R_{sigma} = 0.0233]
Data/restraints/parameters	6649/0/381	3459/0/253
Goodness-of-fit on F^2	1.409	1.045
Final R indexes [I>=2σ (I)]	R_1 = 0.1466, wR_2 = 0.3890	R_1 = 0.0531, wR_2 = 0.1262
Final R indexes [all data]	R_1 = 0.1858, wR_2 = 0.4494	R_1 = 0.0548, wR_2 = 0.1273
Largest diff. peak/hole / e Å^{-3}	2.36/-5.98	0.76/-0.29

Table 15: Crystal data for nortriptyline salt forms (5)

Structure	nor_mucic	nor_nabr
Salt form	Nortriptyline mucate	Nortriptyline bromide form 2
Formula	$C_{44}H_{52}N_2O_8$	$C_{19}H_{22}BrN$
Formula weight	736.87	344.28
Crystal system	monoclinic	monoclinic
Space group	$P2_1/c$	$P2_1/n$
Temperature/K	123(2)	123(2)
a/Å	21.4667(9)	17.440(5)
b/Å	8.8602(3)	10.134(5)
c/Å	10.1106(4)	20.811(5)
α/°	90	90
β/°	98.251(4)	112.105(5)
γ/°	90	90
Volume/Å^3	1903.12(13)	3408(2)
Z	2	8
ρ_{calc}g/cm^3	1.286	1.342
μ/mm^{-1}	0.711	3.215
F(000)	788	1424
Radiation	CuKα (λ = 1.54184)	CuKα (λ = 1.54184)
2Θ range for data collection/°	8.324 to 134.142	8.358 to 147.496
Index ranges	-25 ≤ h ≤ 25, -10 ≤ k ≤ 10, -11 ≤ l ≤ 11	-21 ≤ h ≤ 20, -12 ≤ k ≤ 9, -25 ≤ l ≤ 22
Reflections collected	16479	19414
Independent reflections	3380 [R_{int} = 0.1240, R_{sigma} = 0.0701]	6713 [R_{int} = 0.1061, R_{sigma} = 0.1552]
Data/restraints/parameters	3380/0/257	6713/0/379
Goodness-of-fit on F^2	1.13	1.047
Final R indexes [I>=2σ (I)]	R_1 = 0.0993, wR_2 = 0.2672	R_1 = 0.1369, wR_2 = 0.3371
Final R indexes [all data]	R_1 = 0.1105, wR_2 = 0.2770	R_1 = 0.2265, wR_2 = 0.4149
Largest diff. peak/hole / e Å^{-3}	0.66/-0.45	3.31/-0.96

Table 16: Crystal data for nortriptyline salt forms (6)

Structure	nor_ptolsulf	nor_sal
Salt form	Nortriptyline tosylate	Nortriptyline salicylate
Formula	$C_{26}H_{29}NO_3S$	$C_{26}H_{27}NO_3$
Formula weight	435.56	401.48
Crystal system	triclinic	monoclinic
Space group	P-1	$P2_1/n$
Temperature/K	123(2)	100(2)
a/Å	7.6655(3)	9.2889(6)
b/Å	9.3406(4)	15.8865(11)
c/Å	16.2705(6)	15.5186(11)
α/°	80.402(3)	90
β/°	81.506(3)	106.972(6)
γ/°	79.952(3)	90
Volume/Å^3	1122.58(8)	2190.3(3)
Z	2	4
ρ_{calc}g/cm^3	1.289	1.218
μ/mm^{-1}	1.499	0.079
F(000)	464	856
Radiation	CuKα (λ = 1.54184)	synchrotron (λ = 0.6889)
2Θ range for data collection/°	9.718 to 146.256	4.464 to 47.998
Index ranges	-7 ≤ h ≤ 9, -11 ≤ k ≤ 11, -20 ≤ l ≤ 20	-10 ≤ h ≤ 10, -18 ≤ k ≤ 18, -18 ≤ l ≤ 18
Reflections collected	12847	25989
Independent reflections	4437 [R_{int} = 0.0233, R_{sigma} = 0.0221]	3778 [R_{int} = 0.1187, R_{sigma} = 0.1118]
Data/restraints/parameters	4437/0/286	3778/103/295
Goodness-of-fit on F^2	1.061	1.749
Final R indexes [I>=2σ (I)]	R_1 = 0.0446, wR_2 = 0.1221	R_1 = 0.1459, wR_2 = 0.4456
Final R indexes [all data]	R_1 = 0.0478, wR_2 = 0.1260	R_1 = 0.1677, wR_2 = 0.4735
Largest diff. peak/hole / e Å^{-3}	0.64/-0.42	1.16/-0.52

Table 17: Crystal data for nortriptyline salt forms (7)

Structure	nor_sif6
Salt form	Nortriptyline hexafluorosilicate
Formula	$C_{76}H_{100}F_{12}N_4O_6Si_2$
Formula weight	1449.77
Crystal system	triclinic
Space group	P-1
Temperature/K	123(2)
a/Å	13.8200(6)
b/Å	14.1174(5)
c/Å	18.8850(8)
α/°	94.708(3)
β/°	90.340(3)
γ/°	94.931(3)
Volume/Å^3	3658.2(3)
Z	2
ρ_{calc}g/cm^3	1.316
μ/mm^{-1}	1.166
F(000)	1536
Radiation	CuKα (λ = 1.54184)
2Θ range for data collection/°	12.858 to 146.348
Index ranges	-17 ≤ h ≤ 12, -13 ≤ k ≤ 17, -23 ≤ l ≤ 21
Reflections collected	26214
Independent reflections	14339 [R_{int} = 0.0314, R_{sigma} = 0.0417]
Data/restraints/parameters	14339/55/1083
Goodness-of-fit on F^2	1.014
Final R indexes [I>=2σ (I)]	R_1 = 0.0573, wR_2 = 0.1461
Final R indexes [all data]	R_1 = 0.0729, wR_2 = 0.1608
Largest diff. peak/hole / e Å^{-3}	0.43/-0.49

3.5 Imipramine salt formation

3.5.1 The reaction of imipramine HCl with sodium salts

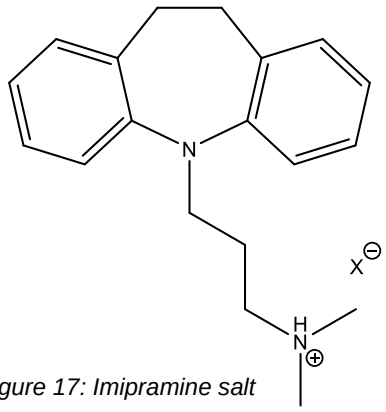

Figure 17: Imipramine salt

The formation of a variety of imipramine salt forms was carried out by reacting imipramine hydrochloride with a variety of s-block metal salts (MX), thereby producing MCl and the X salt of the API. An example procedure was as follows. 0.10 g (0.32 mmol) of imipramine HCl was dissolved in roughly 25 mL of water before 0.03 g (0.32 mmol) of sodium bromide was added. Deionised water was added to dissolve the reactants and the solution was stirred at 50 °C for 30 minutes. After 30 minutes, the vessel containing the solution was wrapped in cotton wool and aluminium foil to encourage slow cooling. As elsewhere the goal of these experiments is to grow x-ray quality crystals, rather than maximising overall yield.

This procedure was followed for 0.10 g (0.32 mmol) of imipramine hydrochloride and the sodium salts listed in Table 18 below.

Table 18: Sodium salts used for salt formation of imipramine and doxepin

Name	Formula	MW (g/mol)	Moles	Mass (g)
Sodium salicylate	$C_7H_5NaO_3$	160.11	3.2E-04	0.05
Sodium carbonate	Na_2CO_3	105.99	3.2E-04	0.03
Sodium nitrite	$NaNO_2$	69.00	3.2E-04	0.02
Sodium hydrogen orthophosphate	Na_2HPO_4	141.96	3.2E-04	0.05
Sodium thiosulfate pentahydrate	$Na_2S_2O_3.5H_2O$	248.18	3.2E-04	0.08
Sodium hexafluorosilicate	Na_2SiF_6	188.06	3.2E-04	0.06
Sodium citrate	$C_6H_5Na_3O_7.2H_2O$	294.10	3.2E-04	0.09
Sodium sulfite	Na_2SO_3	126.04	3.2E-04	0.04
Sodium sulfate	Na_2SO_4	142.04	3.2E-04	0.05
Sodium bromide	NaBr	102.91	3.2E-04	0.03
Sodium Iodide	NaI	149.89	3.2E-04	0.05

Crystals suitable for single crystal x-ray crystallography were obtained for imipramine sulfate, imipramine salicylate, and imipramine hexafluorosilicate. After FT-IR spectroscopy confirmed the crystals were not a starting material, single crystal x-ray crystallography was carried out to elucidate the crystal structure. Then, the bulk crystals were dried, weighed, and the melting points determined. These chemical properties are listed below in Table 19.

Table 19: Chemical properties of imipramine salts

Compound	Yield (g)	% Yield	Melting point (°C)	Major IR peaks (cm^{-1})
Imipramine sulfate	0.03 g	23.8	92.8 – 93.8	Broad OH stretch at *ca.* 3400, 2852, 1649, 1485
Imipramine salicylate	0.01	7.5	N/A	1656, 1483
Imipramine hexafluorosilicate	0.04 g	15.6	164.1 – 166.4	1640, 1485

3.5.2 Generating the imipramine free base

The imipramine free base was generated by reacting the imipramine HCl salt with a 1:3 amount of 2 molar ammonia solution. This reaction formed the API free base and ammonium chloride, similarly to the amitriptyline reaction outlined above in Figure 14.

5.0 g (16 mmol) of imipramine hydrochloride was weighed out and dissolved in approximately 100 mL deionised water. 25 mL (50 mmol) of ammonia solution was added to the imipramine solution while heating at 50 °C and stirring for half an hour.

The reaction yielded an oily precipitate which was washed and purified using a separating funnel. The organic and aqueous solvents were diethyl ether and deionised water respectively. The organic layer dissolved the API free base precipitate while the aqueous layer dissolved the ammonium chloride salt and any remaining starting materials. The aqueous layer was washed three times with roughly 150 mL of diethyl ether each time. The organic layer was then left to evaporate to yield the desired product. The imipramine free base yielded 2.8 g of crystalline powder product which was subsequently dissolved in 25 mL ethanol to give a 0.4 mmol/mL solution.

3.5.3 Salt formation reactions of the imipramine free base with acidic compounds

Imipramine salt formation was carried out with the acid starting materials listed below in Additionally, reaction of the API with the commercial acids of Table 4 was attempted using *ca.* 1 mL of the acid, i.e. a large excess. The procedure outlined above was followed.

Crystals of the desired nortriptyline salt forms that were suitable for single crystal x-ray diffraction were obtained for imipramine oxalate, imipramine 3-hydroxybenzoate, imipramine 4-hydroxybenzoate, imipramine tosylate, and imipramine tetrafluoroborate. These crystals were checked by FT-IR spectroscopy and then their crystal structures were elucidated using single crystal x-ray crystallography. Then, the bulk crystals were dried, weighed, and the melting points determined, where sufficient material amounts were available. These chemical properties are listed below in Table 21.

Table 20.

A typical procedure was as follows. 0.06 g (0.4 mmol) of salicylic acid was weighed out and dissolved in deionised water. 1 mL (0.4 mmol) of the imipramine free base solution in ethanol, prepared as described in section 3.4.2, was added to the reaction vessel for a 1:1 molar ratio acid to API. The solution was heated and stirred at 50 °C for half an hour to form imipramine salicylate. After 30 minutes, any undissolved solid was filtered off and checked by IR to ensure it was unreacted starting material and not the desired product. The clear solution was left to slowly cool to room temperature. This procedure was repeated for the other acidic compounds listed in Additionally, reaction of the API with the commercial acids of Table 4 was attempted using *ca.* 1 mL of the acid, i.e. a large excess. The procedure outlined above was followed.

Crystals of the desired nortriptyline salt forms that were suitable for single crystal x-ray diffraction were obtained for imipramine oxalate, imipramine 3-hydroxybenzoate, imipramine 4-hydroxybenzoate, imipramine tosylate, and imipramine tetrafluoroborate. These crystals were checked by FT-IR spectroscopy and then their crystal structures were elucidated using single crystal x-ray crystallography. Then, the bulk crystals were dried, weighed, and the melting points determined, where sufficient material amounts were available. These chemical properties are listed below in Table 21.

Table 20.

Additionally, reaction of the API with the commercial acids of Table 4 was attempted using *ca.* 1 mL of the acid, i.e. a large excess. The procedure outlined above was followed.

Crystals of the desired nortriptyline salt forms that were suitable for single crystal x-ray diffraction were obtained for imipramine oxalate, imipramine 3-hydroxybenzoate, imipramine 4-hydroxybenzoate, imipramine tosylate, and imipramine tetrafluoroborate. These crystals were checked by FT-IR spectroscopy and then their crystal structures were elucidated using single crystal x-ray crystallography. Then, the bulk crystals were dried, weighed, and the melting points determined, where sufficient material amounts were available. These chemical properties are listed below in Table 21.

Table 20: List of acid starting materials used in salt formation with imipramine and doxepin

Acid	Molecular weight (g/mol)	Moles	Mass (g)
benzoic acid	122.12	4.00E-04	0.05
2-chlorobenzoic acid	156.57	4.00E-04	0.06
3-chlorobenzoic acid	156.57	4.00E-04	0.06
4-chlorobenzoic acid	156.57	4.00E-04	0.06
2-fluorobenzoic acid	140.11	4.00E-04	0.06
3-fluorobenzoic acid	140.11	4.00E-04	0.06
4-fluorobenzoic acid	140.11	4.00E-04	0.06
3-hydroxybenzoic acid	138.12	4.00E-04	0.06
4-hydroxybenzoic acid	138.12	4.00E-04	0.06
2-nitrobenzoic acid	167.12	4.00E-04	0.07
3-nitrobenzoic acid	167.12	4.00E-04	0.07
4-nitrobenzoic acid	167.12	4.00E-04	0.07
malonic acid	104.06	4.00E-04	0.04
oxalic acid	90.03	4.00E-04	0.04
salicylic acid	138.12	4.00E-04	0.06
methane sulfonic acid	96.10	4.00E-04	0.04
4-hydroxybenzene sulfonic acid	174.17	4.00E-04	0.07
acetyl salicylic acid	180.16	4.00E-04	0.07
2-hydroxyphenylacetic acid	152.15	4.00E-04	0.06
4-hydroxyphenylacetic acid	152.15	4.00E-04	0.06
metanilic acid	173.19	4.00E-04	0.07
phenylacetic acid	136.15	4.00E-04	0.05
sulphamic acid	97.10	4.00E-04	0.04

Table 21: Chemical properties of imipramine salt forms

Compound	Yield (g)	% Yield	Melting point (°C)	Major IR peaks (cm^{-1})
Imipramine oxalate	0.06 g	37.7	67.7 – 71.0	1712,1595, 1487
Imipramine 3-hydroxybenzoate	0.03 g	9.0	186.9 – 188.4	1679, 1597, 1459
Imipramine 4-hydroxybenzoate	0.08 g	23.9	190.5 – 195. 4	1651, 1587, 1426
Imipramine tosylate	0.32 g	15.9	100.7 – 102.0	N/A
Imipramine tetrafluoroborate	0.20 g	13.6	59.9 – 61.6	N/A

3.5.4 Crystal data for imipramine salt forms

Table 22: Crystal data for imipramine salt forms (1)

Structure	imi_3hyd	imi_4hyd
Salt form	Imipramine 3-hydroxybenzoate	Imipramine 4-hydroxybenzoate
Formula	$C_{26}H_{30}N_2O_3$	$C_{26}H_{30}N_2O_3$
Formula weight	837.04	837.04
Crystal system	monoclinic	monoclinic
Space group	Cc	Cc
Temperature/K	123(2)	173(2)
a/Å	10.3343(2)	30.6014(15)
b/Å	15.1257(2)	28.2005(10)
c/Å	14.20390(10)	20.7824(13)
α/°	90	90
β/°	90.5190(10)	92.185(6)
γ/°	90	90
Volume/Å^3	2220.17(5)	17921.6(16)
Z	4	32
ρ_{calc}g/cm^3	1.252	1.239
μ/mm^{-1}	0.651	0.645
F(000)	896	7148
Radiation	CuKα (λ = 1.54184)	CuKα (λ = 1.54184)
2Θ range for data collection/°	10.368 to 136.462	5.78 to 134.246
Index ranges	-12 ≤ h ≤ 12, -18 ≤ k ≤ 17, -16 ≤ l ≤ 17	-36 ≤ h ≤ 36, -33 ≤ k ≤ 33, -24 ≤ l ≤ 24
Reflections collected	9356	75176
Independent reflections	3514 [R_{int} = 0.0247, R_{sigma} = 0.0189]	75176 [R_{sigma} = 0.1043]
Data/restraints/parameters	3514/2/288	75176/184/2286
Goodness-of-fit on F^2	1.072	1.316
Final R indexes [I>=2σ (I)]	R_1 = 0.0333, wR_2 = 0.0885	R_1 = 0.1253, wR_2 = 0.3436
Final R indexes [all data]	R_1 = 0.0334, wR_2 = 0.0885	R_1 = 0.1448, wR_2 = 0.3619
Largest diff. peak/hole / e Å^{-3}	0.14/-0.19	1.12/-0.67

Table 23: Crystal data for imipramine salt forms (2)

Structure	imi_hbf4	imi_oxa
Salt form	Imipramine tetrafluoroborate	Imipramine oxalate
Formula	$C_{19}H_{25}BF_4N_2$	$C_{21}H_{29}N_2O_{5.5}$
Formula weight	368.22	397.46
Crystal system	monoclinic	triclinic
Space group	Ia	P-1
Temperature/K	123(2)	123(2)
a/Å	14.2988(2)	10.7480(3)
b/Å	24.9694(3)	11.0316(3)
c/Å	21.3150(3)	18.9226(5)
α/°	90	100.156(2)
β/°	102.6520(10)	93.118(2)
γ/°	90	113.544(3)
Volume/Å^3	7425.36(17)	2005.14(10)
Z	16	4
ρ_{calc}g/cm^3	1.318	1.317
μ/mm^{-1}	0.105	0.783
F(000)	3104	852
Radiation	MoKα (λ = 0.71073)	CuKα (λ = 1.54184)
2Θ range for data collection/°	3.916 to 54.97	8.956 to 146.354
Index ranges	-18 ≤ h ≤ 18, -32 ≤ k ≤ 32, -27 ≤ l ≤ 27	-12 ≤ h ≤ 13, -13 ≤ k ≤ 13, -23 ≤ l ≤ 23
Reflections collected	96686	37863
Independent reflections	16923 [R_{int} = 0.0167, R_{sigma} = 0.0112]	7960 [R_{int} = 0.0954, R_{sigma} = 0.0516]
Data/restraints/parameters	16923/2/994	7960/0/544
Goodness-of-fit on F^2	1.029	1.025
Final R indexes [I>=2σ (I)]	R_1 = 0.0306, wR_2 = 0.0821	R_1 = 0.0546, wR_2 = 0.1537
Final R indexes [all data]	R_1 = 0.0312, wR_2 = 0.0828	R_1 = 0.0598, wR_2 = 0.1622
Largest diff. peak/hole / e Å^{-3}	0.36/-0.22	0.54/-0.29

Table 24: Crystal data for imipramine salt forms (3)

Structure	imi_ptolsulf	imi_sif6
Salt form	Imipramine tosylate	Imipramine hexafluorosilicate
Formula	$C_{26}H_{34}N_2O_4S$	$C_{38}H_{56.67}F_6N_4O_{5.5}Si$
Formula weight	470.61	799.63
Crystal system	monoclinic	triclinic
Space group	Pc	P-1
Temperature/K	123(2)	123(2)
a/Å	14.3203(6)	10.9886(4)
b/Å	17.2688(5)	21.0732(12)
c/Å	10.2820(4)	26.8087(16)
α/°	90	76.630(5)
β/°	105.417(4)	82.121(4)
γ/°	90	83.205(4)
Volume/Å^3	2451.19(16)	5958.5(6)
Z	4	6
ρ_{calc}g/cm^3	1.275	1.337
μ/mm^{-1}	1.451	1.186
F(000)	1008	2548
Radiation	CuKα (λ = 1.54184)	CuKα (λ = 1.54184)
2Θ range for data collection/°	6.402 to 146.228	9.982 to 129.992
Index ranges	-17 ≤ h ≤ 17, -21 ≤ k ≤ 13, -12 ≤ l ≤ 11	-11 ≤ h ≤ 12, -24 ≤ k ≤ 24, -31 ≤ l ≤ 31
Reflections collected	9542	41542
Independent reflections	6226 [R_{int} = 0.0349, R_{sigma} = 0.0612]	20243 [R_{int} = 0.0570, R_{sigma} = 0.0852]
Data/restraints/parameters	6226/2/619	20243/296/1662
Goodness-of-fit on F^2	1.034	1.028
Final R indexes [I>=2σ (I)]	R_1 = 0.0505, wR_2 = 0.1221	R_1 = 0.0989, wR_2 = 0.2538
Final R indexes [all data]	R_1 = 0.0607, wR_2 = 0.1327	R_1 = 0.1628, wR_2 = 0.3201
Largest diff. peak/hole / e Å^{-3}	0.38/-0.33	1.74/-0.71

Table 25: Crystal data for imipramine salt forms (4)

Structure	imi_sal	imi_sulfate
Salt form	Imipramine salicylate	Imipramine sulfate
Formula	$C_{26}H_{30}N_2O_3$	$C_{19}H_{30.89}N_2O_{5.61}S_{0.5}$
Formula weight	418.52	393.19
Crystal system	monoclinic	triclinic
Space group	$P2_1/c$	P-1
Temperature/K	123(2)	123(2)
a/Å	9.9046(2)	10.6937(7)
b/Å	15.2497(3)	11.1637(10)
c/Å	14.7491(3)	18.9822(11)
α/°	90	85.816(6)
β/°	94.682(2)	76.994(6)
γ/°	90	70.205(7)
Volume/Å^3	2220.30(8)	2077.5(3)
Z	4	4
ρ_{calc}g/cm^3	1.252	1.257
μ/mm^{-1}	0.651	1.206
F(000)	896	847
Radiation	CuKα (λ = 1.5414)	CuKα (λ = 1.54184)
2Θ range for data collection/°	8.352 to 136.382	8.418 to 145.878
Index ranges	-11 ≤ h ≤ 11, -17 ≤ k ≤ 18, -17 ≤ l ≤ 17	-12 ≤ h ≤ 13, -13 ≤ k ≤ 13, -12 ≤ l ≤ 23
Reflections collected	22143	15849
Independent reflections	4038 [R_{int} = 0.0273, R_{sigma} = 0.0173]	8102 [R_{int} = 0.0775, R_{sigma} = 0.1101]
Data/restraints/parameters	4038/0/288	8102/36/584
Goodness-of-fit on F^2	1.202	1.017
Final R indexes [I>=2σ (I)]	R_1 = 0.0584, wR_2 = 0.1918	R_1 = 0.0852, wR_2 = 0.1946
Final R indexes [all data]	R_1 = 0.0597, wR_2 = 0.1924	R_1 = 0.1384, wR_2 = 0.2372
Largest diff. peak/hole / e Å^{-3}	0.39/-0.27	0.46/-0.35

3.6 Doxepin salt formation

3.6.1 The reaction of doxepin HCl with sodium salts

The formation of a variety of doxepin salt forms was carried out by reacting doxepin hydrochloride with a variety of s-block metal salts (MX). Thereby producing MCl and the X salt of the API. An example procedure was as follows. 0.10 g (0.32 mmol) of doxepin HCl was dissolved in roughly 25 mL of water before 0.03 g (0.32 mmol) of sodium bromide was added. Deionised water was added to dissolve the reactants and the solution was stirred at 50 °C for 30 minutes. After 30 minutes, the vessel containing the solution was wrapped in cotton wool and aluminium foil to encourage slow cooling.

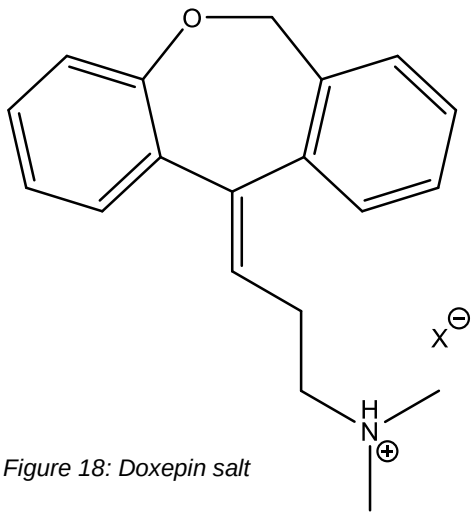

Figure 18: Doxepin salt

This procedure was followed for 0.10 g (0.32) of doxepin hydrochloride and the sodium salts listed in table 3.4.1 above.

No suitable crystals were obtained from any of these experiments.

3.6.2 Generating the doxepin free base

The doxepin free base was generated by reacting the doxepin HCl salt with a 1:3 amount of 2 molar ammonia solution. This reaction formed the API free base and ammonium chloride, as per the amitriptyline reaction outlined above in Figure 14.

5.0 g (16 mmol) of doxepin hydrochloride was weighed out and dissolved in approximately 100 mL deionised water. 25 mL (50 mmol) of ammonia solution was added to the doxepin solution while heating at 50 °C and stirring for half an hour.

The reaction yielded an oily precipitate which was washed and purified using a separating funnel. The organic and aqueous solvents were diethyl ether and deionised water respectively. The organic layer dissolved the API free base precipitate while the aqueous layer dissolved the ammonium chloride salt and any remaining starting materials. The aqueous layer was washed three times with roughly 150 mL of diethyl ether each time. The organic layer was then left to evaporate to yield the desired product. The doxepin free base yielded 2.8 g of a crystalline powder as the product. The recovered solid was subsequently dissolved in 25 mL ethanol giving a solution of 0.4 mmol/mL.

3.6.3 Salt formation reactions of the doxepin free base with acidic compounds

Doxepin salt formation was carried out with the acid starting materials listed above in Additionally, reaction of the API with the commercial acids of Table 4 was attempted using *ca.* 1 mL of the acid, i.e. a large excess. The procedure outlined above was followed.

Crystals of the desired nortriptyline salt forms that were suitable for single crystal x-ray diffraction were obtained for imipramine oxalate, imipramine 3-hydroxybenzoate, imipramine 4-hydroxybenzoate, imipramine tosylate, and imipramine tetrafluoroborate. These crystals were checked by FT-IR spectroscopy and then their crystal structures were elucidated using single crystal x-ray crystallography. Then, the bulk crystals were dried, weighed, and the melting points determined, where sufficient material amounts were available. These chemical properties are listed below in Table 21.

Table 20.

A typical procedure was as follows. 0.06 g (~ 0.4 mmol) of salicylic acid was weighed out and dissolved in deionised water. 1 mL (~ 0.4 mmol) of the doxepin free base solution in ethanol, prepared as described in section 3.6.2, was added to the reaction vessel for a 1:1 molar ratio acid to API. The solution was heated and stirred at 50 °C for half an hour to form imipramine salicylate. After 30 minutes, any undissolved solid was filtered off and checked by IR to ensure it was unreacted starting material and not the desired product. The clear solution was left to slowly cool to room temperature. This procedure was repeated for the other acidic compounds listed in Additionally, reaction of the API with the commercial acids of Table 4 was attempted using *ca.* 1 mL of the acid, i.e. a large excess. The procedure outlined above was followed.

Crystals of the desired nortriptyline salt forms that were suitable for single crystal x-ray diffraction were obtained for imipramine oxalate, imipramine 3-hydroxybenzoate, imipramine 4-hydroxybenzoate, imipramine tosylate, and imipramine tetrafluoroborate. These crystals were checked by FT-IR spectroscopy and then their crystal structures were elucidated using single crystal x-ray crystallography. Then, the bulk crystals were dried, weighed, and the melting points determined, where sufficient material amounts were available. These chemical properties are listed below in Table 21.

Table 20.

Additionally, reaction of the API with the commercial acid solutions of Table 4 was attempted using *ca.* 1 mL of the acid, i.e. a large excess. The procedure outlined above was followed.

Crystals of the desired doxepin salt forms that were suitable for single crystal x-ray crystallography were obtained for doxepin 4-nitrobenzoate and doxepin 4-hydroxybenzoate. The crystals were checked by FT-IR spectroscopy and then their crystal structures were elucidated using single crystal x-ray crystallography. Then, the bulk crystals were dried, weighed, and the melting points determined. These chemical properties were listed below in Table 26.

Table 26: Chemical properties of doxepin salt forms

Compound	Yield (g)	% Yield	Melting point (°C)	Major IR peaks (cm^{-1})
Doxepin 4-nitrobenzoate	0.02 g	8.1	128.1 – 130.1	1705, 1519,1387
Doxepin 4-hydroxybenzoate	0.07 g	35.5	118.9 – 120.1	1656, 1589, 1372

3.6.4 Crystal data for doxepin salt forms

Table 27: Crystal data for doxepin salt forms

Structure	dox_4hyd	dox_4nitro
Salt form	Doxepin 4-hydroxybenzoate	Doxepin 4-nitrobenzoate
Formula	$C_{29.5}H_{29}NO_6$	$C_{33}H_{31}N_3O_9$
Formula weight	493.54	613.61
Crystal system	orthorhombic	monoclinic
Space group	$Pca2_1$	$P2_1/n$
Temperature/K	123(2)	123(2)
a/Å	12.2294(3)	13.8379(6)
b/Å	8.54840(10)	13.7858(4)
c/Å	48.4673(9)	15.4762(5)
α/°	90	90
β/°	90	95.309(3)
γ/°	90	90
Volume/$Å^3$	5066.86(17)	2939.68(18)
Z	8	4
$\rho_{calc}g/cm^3$	1.294	1.261
μ/mm^{-1}	0.737	0.718
F(000)	2088	1180
Radiation	CuKα (λ = 1.54184)	CuKα (λ = 1.54184)
2Θ range for data collection/°	7.296 to 146.554	8.202 to 146.586

Index ranges	-11 ≤ h ≤ 14, -9 ≤ k ≤ 10, -60 ≤ l ≤ 59	-10 ≤ h ≤ 17, -16 ≤ k ≤ 16, -19 ≤ l ≤ 19
Reflections collected	19634	13904
Independent reflections	8203 [R_{int} = 0.0481, R_{sigma} = 0.0423]	5789 [R_{int} = 0.0630, R_{sigma} = 0.0593]
Data/restraints/parameters	8203/6/678	5789/104/483
Goodness-of-fit on F^2	1.085	1.038
Final R indexes [I>=2σ (I)]	R_1 = 0.0887, wR_2 = 0.2369	R_1 = 0.0965, wR_2 = 0.2604
Final R indexes [all data]	R_1 = 0.0908, wR_2 = 0.2386	R_1 = 0.1235, wR_2 = 0.2895
Largest diff. peak/hole / e $Å^{-3}$	0.54/-0.46	0.59/-0.53

3.7 Apparent solubility measurements for nortriptyline salt forms

3.7.1 Creating a calibration curve for nortriptyline hydrochloride

Known concentration solutions of nortriptyline hydrochloride were made up to generate a calibration curve. 0.0116 g (0.039 mmol) of the salt was added to a 1 L volumetric flask and the solution was made up to the mark with deionised water to create a solution with a concentration of $3.87*10^{-5}$ mol/L. 25 mL of this solution was pipetted into a 50 mL volumetric flask and this was made up to the mark with deionised water for a solution with concentration $1.93*10^{-5}$ mol/L. This procedure was repeated twice more to generate solutions with concentrations of $9.67*10^{-6}$ mol/L and $4.85*10^{-6}$ mol/L. Additionally, 2 mL of the initial solution was pipetted into a 50 mL volumetric flask. Deionised water was added to the mark on this flask to generate a $1.55*10^{-6}$ mol/L solution. All four of the further diluted solutions was analysed in triplicate using UV/VIS. The average absorbances of their peaks were plotted on a graph of absorbance vs concentration. The trendline was generated with an R^2 of 0.9998, see Figure 19.

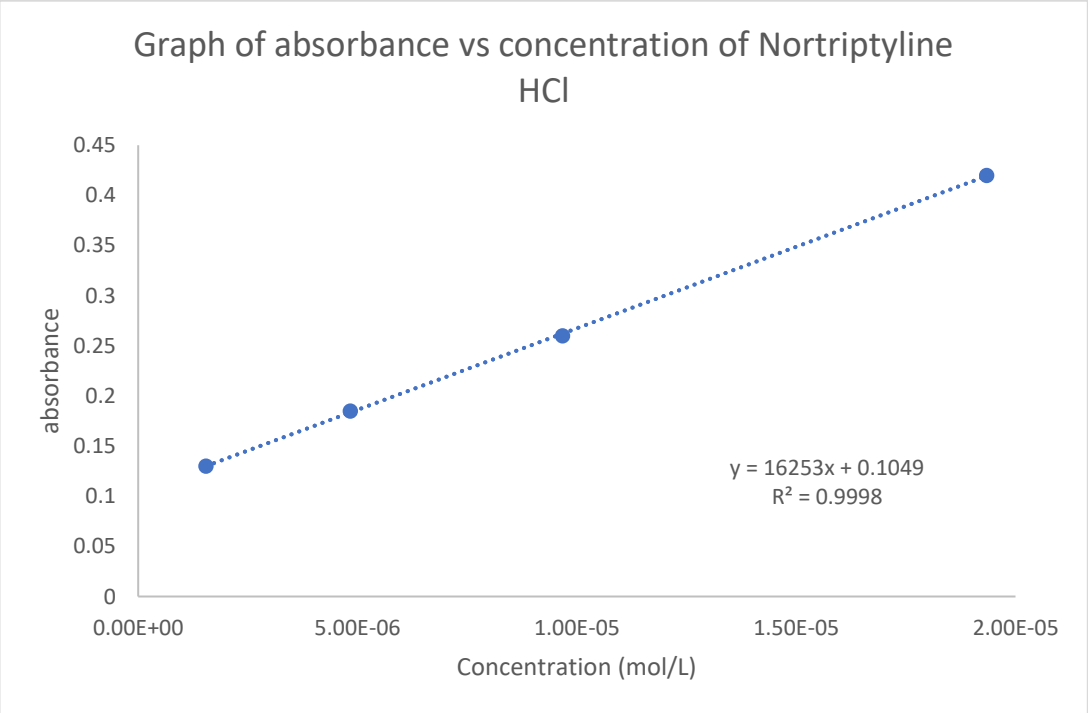

Figure 19: Graph of absorbance vs concentration of nortriptyline HCl.

3.7.2 Generating nortriptyline salt forms for solubility experiments

Nine counterions were selected to make nortriptyline salt forms on a roughly 1 gram scale for the solubility experiments. These were 'Generally Regarded as Safe' (GRAS) for use in pharmaceutical compounds and counterions for which single crystal structures were elucidated previously. The counterions used were bromide, iodide, salicylate, the anion of mucic acid, methane sulfonate, *p*-toluene sulfonate, benzene sulfonate and oxalate.

Sodium salts of selected anions were reacted with 1.0 g (3.34 mmol) of nortriptyline hydrochloride in a 1.1:1 molar ratio of sodium salt to API salt using the same procedure as outlined in section 3.4.1. The exact mass used for each salt as well as the yield is listed in Table 28 below.

The acid starting materials were reacted with 1.0 g (3.80 mmol) of nortriptyline free base which was produced according to the procedure outlined in section 3.4.2. The molar ratio was 1.1:1 of acid to base. The exact mass used for each acid as well as the yield was listed in Table 28 below.

Table 28: List of counterions used to produce nortriptyline salts for solubility tests

Name	Formula	Salt/acid input (g)	Product MW (g/mol)	Yield (g)	Crude Yield (%)
Nortriptyline hydrochloride	$C_{19}H_{21}NHCl$	1.0	299.84	0.75	75
Potassium bromide	KBr	0.44	343.29	1.23	107
Sodium iodide	NaI	0.55	391.29	0.31	24
Sodium salicylate	$C_7H_5NaO_3$	0.59	400.50	0.27	20
Mucic acid	$C_6H_{10}O_8$	0.88	473.52	N/A	0
Methanesulfonic acid	CH_4O_3S	0.40	359.48	N/A	0
p-Toluenesulfonic acid	$C_7H_8O_3S$	0.79	453.60	2.21	128
Benzenesulfonic acid	$C_6H_6O_3S$	0.66	421.56	1.02	64
Oxalic acid	$C_2H_2O_4$	0.38	353.41	N/A	0

The reactions between the nortriptyline free base and mucic acid and methane sulfonic acid were unsuccessful. The cases where a yield greater than 100% was obtained were likely due to residual surface solvent content.

3.7.3 Solubility slurry experiments

In order to do the experiments in duplicate, each nortriptyline salt form obtained was divided equally between two small beakers. As well as the salt form experiments, the same experiment was also conducted using 0.21 g of nortriptyline free base in two separate beakers.10 mL of deionised water was added to each small beaker so that there was a large excess of solid product present. Then a magnetic stirrer bar was added to each beaker, and they were covered in parafilm.

These beakers were placed on a hotplate stirrer with the heat turned off in an incubator set to 25°C. The experiments were left to stir and to reach an equilibrium over a period of 7 days.

0.1 mL of each saturated solution was accurately measured using a syringe equipped with a filter and added to clean 100 mL volumetric flasks. The flasks were then made up to the mark using deionised water. These solutions were analysed in triplicate using UV/VIS spectroscopy. The nortriptyline hydrochloride measurement was repeated with only 0.05 mL of each solution and the nortriptyline salicylate measurements were repeated using 0.2 mL in 100 mL volumetric flasks. These were repeated because the initial absorption was too high for nortriptyline hydrochloride and too low for nortriptyline salicylate for accurate readings.

The trendline equation obtained in section 3.7.1 was used to calculate the apparent solubility for each sample.

The undissolved solids recovered from the slurries by filtration were checked for phase and purity by powder x-ray diffraction.

3.8 Structural analysis

3.8.1 ConQuest database search

Structural comparison analysis was carried out using the Mercury software version 4.0.0[7] from the Cambridge Crystallography Data Centre (CCDC)[8]. First, the CCDC database was accessed using the ConQuest software[9]. A search was carried out for several tricyclic antidepressants (TCAs), namely amitriptyline, nortriptyline, protriptyline, butriptyline, imipramine, desipramine, clomipramine, trimipramine, lofepramine. No structures were found for protriptyline or butriptyline. See Figure 20 for the structures of the TCAs that returned results.

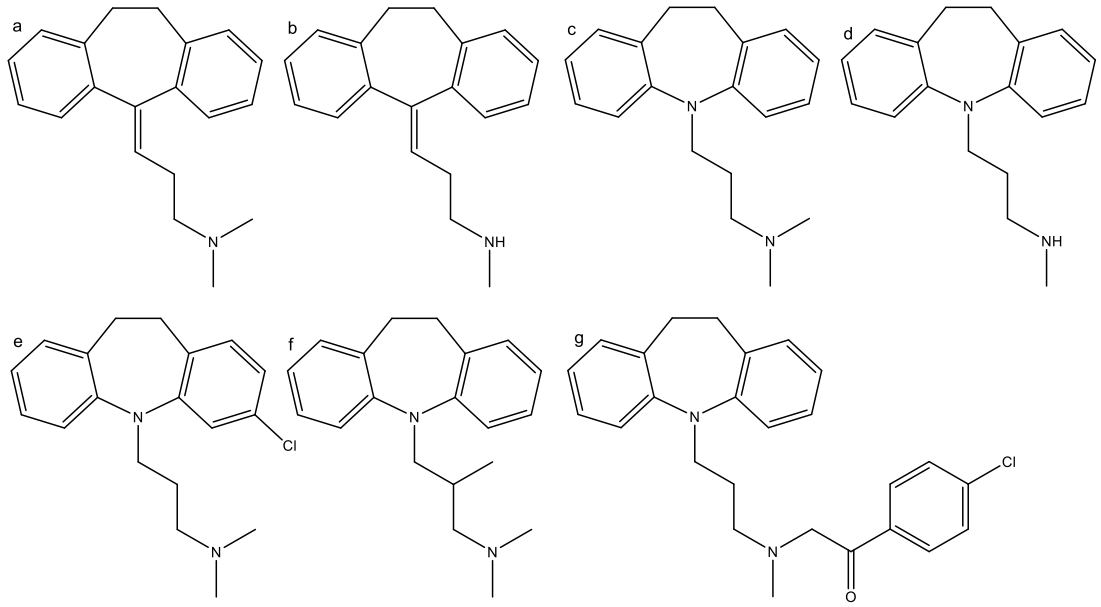

Figure 20: Structures of amitriptyline (a), nortriptyline (b), imipramine (c), desipramine (d), clomipramine (e), trimipramine (f), and lofepramine (g)

Several parameters were set to limit the results to those that would be most useful. The requirements used were single crystal structures only, including only organics and no polymers, an R factor less than 10%, and a determined 3D structure. Any duplicate structures were removed from the list.

The database search was repeated with the same restrictions for carbamazepine and dihydrocarbamazepine. These structures are illustrated in Figure 21.

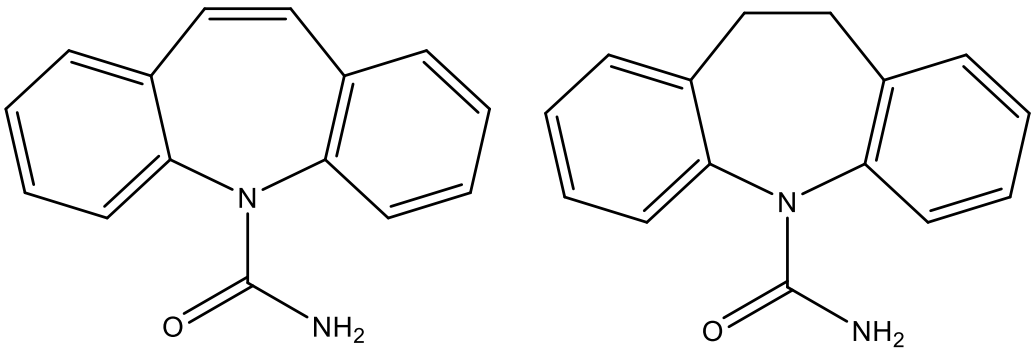

Figure 21: Structure of carbamazepine and dihydrocarbamazepine (aka carbamazepine dihydrogen)

3.8.2 Crystal packing similarity of tricyclic antidepressant salt forms

Crystal packing similarity is a tool in the Mercury software[7] which calculates the level of packing similarity between structures containing similar molecular fragments and can therefore be used to quantify packing similarity. This method is outlined by Childs et al.[10] and their practice was followed for this work.

The .cif files for the tricyclic antidepressants data set were used as input to Mercury[7]. Under the CSD-materials tab, 'search' was selected followed by 'crystal packing similarity'. In the pop-up, all the structures were selected on both the 'reference structures' and 'comparison structures' sides. For the first search, the cluster size was set to 15 molecules, the standard distance tolerance and angle tolerance were used, 20% and 20° respectively. 'Filter comparisons that do not have all 15 molecules in common' was selected as well as 'allow molecular differences', 'ignore hydrogen positions', ignore bond types', 'allow structure inversion', 'ignore each atom's hydrogen count', 'ignore each atom's bond count', and 'ignore smallest molecular components'. These settings were selected because the data set contained molecules with very similar but not identical structures. The search was repeated for 12, 8, 6, 4, 3, and 2 molecules as per the method outlined by Childs et al.[10] The results were grouped by similarity and were used to plot a crystal packing similarity tree diagram, see results in Section 4.5.2.

3.8.3 Crystal packing similarity of carbamazepine and dihydrocarbamazepine salt forms

The crystal packing similarity analysis was repeated using the carbamazepine and dihydrocarbamazepine structures found in the ConQuest database. The search was slightly more restricted than the one above due to the two cations forming a much more tightly knit structural group than the wider group with more molecular differences found in the tricyclic antidepressant data set. For the first search, the cluster size was set to 15 molecules, the standard distance tolerance and angle tolerance were used, 20% and 20° respectively. 'Filter comparisons that do not have all 15 molecules in common' was selected as well as, 'ignore hydrogen positions', ignore bond types', 'allow structure inversion', and 'ignore smallest molecular components'. 'Allow molecular differences', 'ignore each atom's hydrogen count', and 'ignore each atom's bond count' were deselected for this dataset. The search was repeated for 12, 8, 6, 4, 3, 2, and 1 molecules as per the method outlined by Childs et al.[10] The results were grouped by similarity and were used to plot a crystal packing similarity tree diagram as before, see results in Section 4.5.3.

3.9 References

1) CrysAlisPRO, Oxford Diffraction /Agilent Technologies UK Ltd, Yarnton, England.

2) Sheldrick, G., *Acta Cryst. A*, 2007, **64**, 112-122.

3) Altomare, A.; Cascarano, G.; Giacovazzo, C.; Guagliardi, A.; Burla, M. C.; Polidori, G.; Camalli, M., *J. Appl. Cryst*., 1994, **27**, 435.

4) Farrugia, L. J., *J. Appl. Cryst.*, 2012, **45**, 849-854.

5) Coles, S.; Gale, P., *Chem. Sci.*, 2012, **3**, 683-689.

6) Nowell, H.; Barnett, S. A.; Christensen, K. E.; Teat, S. J.; Allan, D. R., *J. Synch. Rad.*, **2012**, 19, 435-441.

7) Macrae, C.F.; Sovago, I.; Cottrell, S.J.; Galek, P. T. A.; McCabe, P.; Pidcock, E.; Platings, M.; Shields, G. P.; Stevens, J. S.; Towler, M.; Wood, P. A., *J. Appl. Cryst.*, **2020**, *53*, 226-235.

8) Groom, C.R.; Bruno, I. J.; Lightfoot, M. P.; Ward, S. C., *Acta Cryst.*, **2016,** *72*, 171-179.

9) Bruno, I. J.; Cole, J. C.; Edgington, P. R.; Kessler, M.; Macrae, C. F.; McCabe, P.; Pearson, J.; Taylor, R., *Acta Cryst.*, **2002**, *B58*, 389-397.

10) Childs, S.L.; Wood, A.P.; Rodríguez-Hornedo, N.; Sreenivas Reddy, L.; and Hardcastle, K.I., *Crystal Growth & Design*, **2009**, *9*, 1869–1888.

4 Results & discussion

29 new single crystal structures of tricyclic antidepressant compounds were elucidated in this work. Six of these were salt forms of amitriptyline, 13 were salt forms of nortriptyline, eight were imipramine salt forms and two were doxepin salt forms. Furthermore, out of 29 structures, 17 were simple salts containing only cations and anions, eight were hydrated salt forms, two were co-crystals of salts (i.e. they contained a neutral free acid molecule as well as the equivalent anion), one was a hydrated co-crystal of a salt, and finally, one was a hydrated double salt with two different anions. These divisions are illustrated in Figure 22 and listed in Table 29.

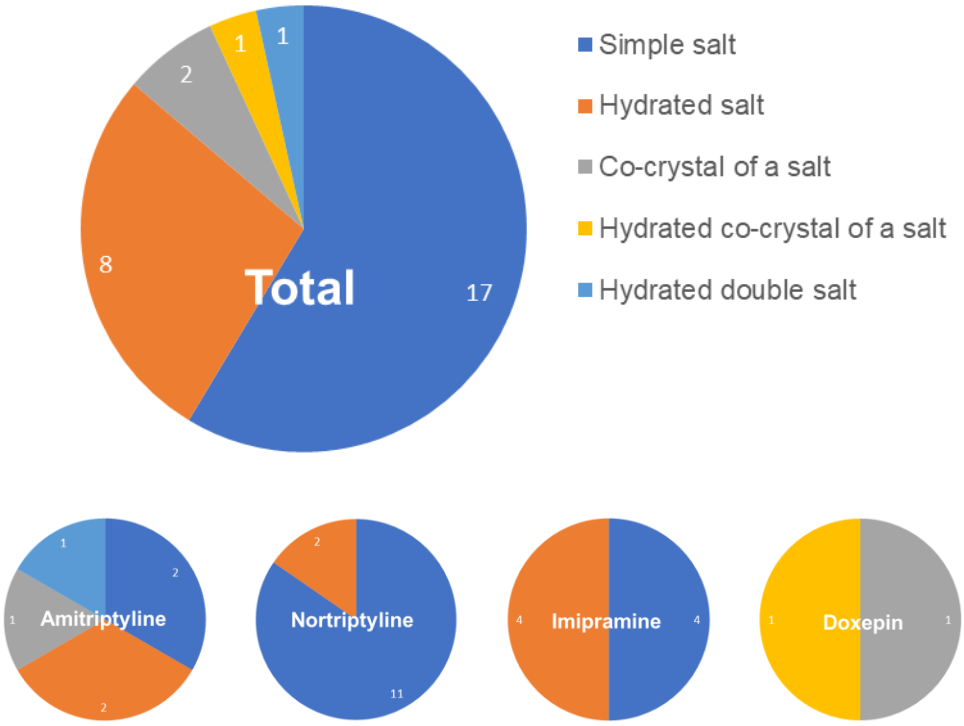

Figure 22: Break up of salt classification for all structures and per API.

Table 29: Break up of salt classification for all structures

Structure	Type
ami oxalate	S
ami mucate	HS
ami metanilate	HDS
ami salicylate	S
ami 4-nitrobenzoate	CCS
ami HBF_4	HS
nor HBr	S
nor NaBr	S
nor KI	S
nor malonate	S
nor glutarate	HS
nor mucate	S
nor salicylate	S
nor 4-hydroxyphenylacetate	S
nor edisylate	S
nor besylate	S
nor tosylate	S
nor HBF_4	S
nor SiF_6	HS
imi oxalate	HS
imi salicylate	S
imi 3-hydroxybenzoate	S
imi 4-hydroxybenzoate	S
imi sulfate	HS
imi tosylate	HS
imi HBF_4	S
imi SiF_6	HS
dox 4-hydroxybenzoate	HCCS
dox 4-nitrobenzoate	CCS

S	Simple salt
HS	Hydrated salt
CCS	Co-crystal of a salt
HCCS	Hydrated co-crystal of a salt
HDS	Hydrated double salt

4.1 Hydrate formation

Hydrate formation is an important aspect of solid-state chemistry to consider in API formulation due to its effect on physical properties. Hydrates can be unstable in hot or low humidity conditions because the water molecules can be lost. Additionally, hydrated forms of salts are generally less water soluble than anhydrous equivalents, partly due to the strong hydrogen bonding networks within the solid-state.[1]

Hydrate formation was prevalent in the data set elucidated in this work, making up 34.5% of all structures when the three types of hydrates were combined. This was a much higher rate of hydration than is seen in general for structures of organic compounds. Infantes and Motherwell[2] found that only 6.6% of all organic structures in the Cambridge structural database[3] were hydrates, this rose to 14% when they limited the scope to only bioactive compounds. Note that one simple difference is that the new structures were all crystallised from aqueous media, but the same is not true for the database survey. A later study by Haynes et al[4] found hydration occurred for 22.5% of NH^+ containing pharmaceutical salts, this study is of particular relevance here because the APIs studied in this work fall within that scope.

4.1.1 Hydrate formation as a result of anion type

Haynes et al.[4] divided their dataset of NH^+ containing pharmaceutical salt structures by type of NH^+ group and then according to anion type. A similar treatment for distribution of hydrates within the 29 structures elucidated in this work is illustrated in Figure 23.

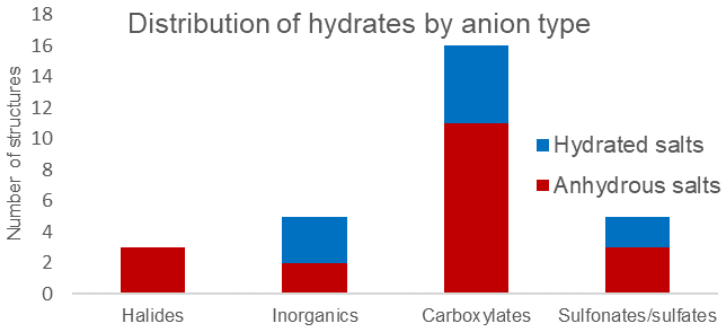

Figure 23: Distribution of hydrates by anion type.

For secondary amines, Haynes et al. determined that 16.1% of the 725 structures within the scope chosen were hydrates. When looking specifically at halide, carboxylate/carbonate, and sulfate/sulfonate anions, they found rates of hydration of 13.2%, 17.4%, and 29.3% respectively.[4] Within this work, nortriptyline was the only API with a secondary amine functional group. A rate of hydration of 15% was found for the 13 structures newly elucidated, which is an excellent fit with the Haynes data. One of the two hydrates had a carboxylate anion and the other had an inorganic counterion. (This corresponds to 20% and 50% hydration rates respectively but note the extremely small sample numbers for this limited data set). Whereas Haynes et al found that sulfonates and sulfates had the highest rate of hydration, none of the four structures containing sulfonate anions elucidated in this work formed hydrates. Again, this disparity is likely due to the small data set in this work.

For tertiary amines, Haynes et al. found a hydration rate of 14.5% of 649 structures. Thus, tertiary amine salt forms were found to have a similar, if slightly lower, rate of hydration than secondary amine salts. When looking specifically at halide, carboxylate/carbonate, and sulfate/sulfonate anions, they found rates of hydration of 18.75%, 16.7%, and 25.0% respectively.[4] In

this work, amitriptyline, imipramine and doxepin all contained a tertiary amine functional group. Here, 8 out of 16 salts were hydrated giving an extremely high rate of hydration of 50%. For the carboxylate and sulfonate anions, hydration rates of 36.4% (4/11) and 100% (2/2) were found. While a higher rate of hydration for salts with sulfonate anions followed the trend found by Haynes et al, it is difficult to draw conclusions from the limited dataset.

4.2 Hydrogen bonding

Hydrogen bonding is the intermolecular or intramolecular force which arises due to the attraction between a proton bonded to an electronegative atom such as nitrogen, oxygen, or fluorine (known as the hydrogen bond donor D) and another electronegative atom (known as the hydrogen bond acceptor A). This interaction would be denoted as D-H···A, with O-H···N being a typical example.

Amitriptyline, imipramine and doxepin cations each contain a tertiary amine with a formally charged proton which is readily available for hydrogen bonding. Nortriptyline cations contain a secondary amine with two such protons available for hydrogen bonding. The hydrogen bonds originating from the TCA cations will be investigated further.

There was a total of 86 hydrogen bonds originating from the APIs' N-H hydrogen bond donor found in the 29 new TCA salt forms studied. All elements of bifurcated hydrogen bonds were counted as 1 single hydrogen bond for this analysis. The majority was present in the 13 new nortriptyline salt forms which accounted for 46 of these hydrogen bonds (53.5%). Of the tertiary amines, the six new amitriptyline crystal structures accounted for 11 (12.8%) amine hydrogen bonds, the eight new imipramine crystal structures accounted for 26 (30.2%)

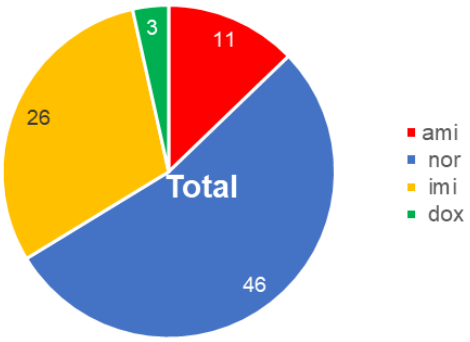

Figure 24: Distribution of hydrogen bonds within the TCA dataset.

and the two new doxepin crystal structures accounted for 3 (3.5%), see Figure 24.

4.2.1 Hydrogen bond acceptor types

There were 11 N-H hydrogen bonds within the amitriptyline dataset; 6 of these were to the water solvent molecules and 5 were to the carboxylate anion. For nortriptyline, there were a total of 46 N-H hydrogen bonds; 4 were to water molecules, 14 were to carboxylate anions, 8 were to sulfonate anions, and 20 were to halides. Imipramine had a total of 26 N-H hydrogen bonds; 4 were to water, 11 were to carboxylate anions, 2 were to sulfonate anions, and 9 were to halides. Finally, there were 3 N-H hydrogen bonds for doxepin, they were all to carboxylate anions. Again, all bifurcated hydrogen bonds were counted as 1 single hydrogen bond for this analysis. See Figure 25 for a visual breakdown of hydrogen bond acceptor type by TCA. See Table 30 and Table 31 for a breakdown of hydrogen bond acceptors per structure.

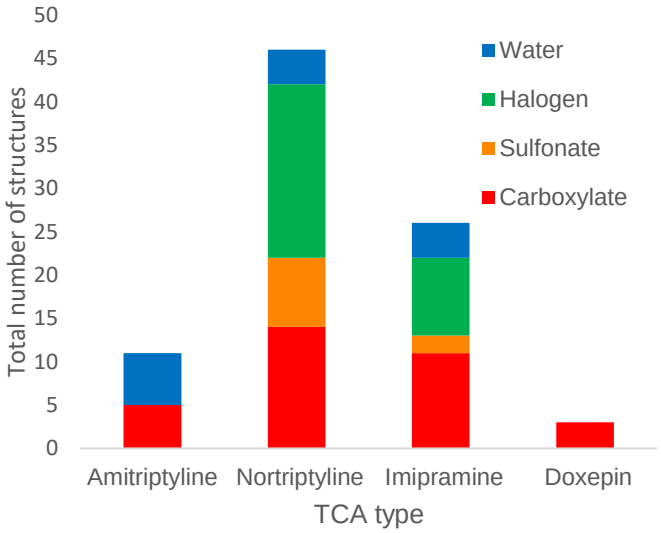

Figure 25: Distribution of hydrogen bond acceptors within the TCA dataset.

Table 30: Hydrogen bond acceptors per structure for amitriptyline (ami) and nortriptyline (nor)

Dibenzocycloheptenes			
Crystal	**Unit cell**	**H bond acceptors from TCA nitrogen H bond donor 1**	**H bond acceptors from TCA nitrogen H bond donor 2 (nortriptyline only)**
ami HBF_4	4:4:5	water O4w	N/A
		Water O3w	
		Water O1w	
		Water O5w	
ami oxalate	2:2	carboxylic O2, O3	
		carboxylic O8	
ami 4-nitrobenzoate	1:2	carboxylic O2	
ami metanilate	2:1:3:1cl	Water O1w	
		Water O2w	
ami mucate	1:1:3	carboxylic O2, mucic carbonyl O3	
ami salicylate	1:1	carboxylic O1	
nor tosylate	1:1	sulfonic O2	sulfonic O1
nor 4-hydroxyphenyl acetate	2:2	carboxylic O4	carboxylic O4
		carboxylic O1	carboxylic O1
nor besylate	1:1	sulfonic O2, O3	sulfonic O2
nor malonate	1:1	carboxylic O3	carboxylic O3
nor edisylate	2:1	sulfonic O3	sulfonic O2
		sulfonic O4	sulfonic O6
nor glutarate	2:1:1	carboxylic O4	carboxylic O1
		carboxylic O4	carboxylic O2
nor mucate	1:1	carboxylic O2	carboxylic O1
nor salicylate	1:1	carboxylic O2	carboxylic *O1, O2*
nor HBr	2:2	Br2	Br2
		Br1	Br1
nor NaBr	2:2	Br1	Br2
		Br1	Br2
nor HBF_4	2:2	F2, F6	F1, F4
		F5	*F2, F6*
Nor SiF_6	4:2:6	Water O1w	Water O2w
		F6	F3
		Water O5w	Water O4w
		F11	F7
Nor KI	2:2	I1	I1
		I2	I2

Hydrated

Table 31: Hydrogen bond acceptors per structure for imipramine (imi) and doxepin (dox)

Dibenzazepines		
Crystal	**Unit cell**	**H bond acceptors from TCA nitrogen H bond donor 1**
imi HBF_4	4:4	F6
		F3
		F11
		F15
imi 3-hydroxybenzoate	1:1	carboxylic O1
imi 4-hydroxybenzoate	8:8	carboxylic O21
		carboxylic O3
		carboxylic O23, O24
		carboxylic O6
		carboxylic O8
		carboxylic O15
		carboxylic O17
		carboxylic O11
imi oxalate	2:2:3	carboxylic O1
		water O1w
imi tosylate	2:2:2	water O1w
		water O2w
imi SiF_6	6:3:16.5	water O8w
		F1
		F7, F11
		F14, F18
		F2, F5
		F8, F12
imi salicylate	1:1	carboxylic O2
imi sulfate	2:1:8	sulfonic O2
		sulfonic O3
Dibenzoxepins		
Crystal	**Unit cell**	**H bond acceptors from TCA nitrogen H bond donor 1**
dox 4-hydroxybenzoate	2:2:1	carboxylic O10
		carboxylic O3
dox 4-nitrobenzoate	1:1:1	carboxylic O4

Hydrated

4.2.2 Contact ion pairs vs solvent-separated ion pairs

The TCA structures were further characterised as ‘contact ion pairs’ or ‘solvent separated ion pairs’. Contact ion pairs (CIP) were defined as the TCA cations having hydrogen bonds with the anion. These CIPs were further broken down by anion type, namely carboxylate, sulfonate, or halide CIPs. Solvent-separated ion pairs (SSIP) were defined as hydrated crystal structures where all hydrogen bonds originating from the cation interacted with solvent present in the solid state. In this data set, the only solvent present was water.

In the 10 hydrated structures elucidated in this work, there were 28 independent hydrogen bonds originating from the N-H hydrogen bond donor. 14 of these interacted with the water molecules present, 5 formed hydrogen bonds with the carboxylate anions and 9 with halides. Only three out of ten hydrates were characterised as SSIPs; ami HBF_4, ami metanilate, and imi tosylate. This corresponds to 30% of the dataset. Another three hydrated structures had cations with mixed hydrogen bond acceptors. The hydrogen bond acceptor water to anion ratio was 4:8, 1:6 and 1:1 for nor hexafluorosilicate, imi hexafluorosilicate, and imi oxalate respectively. Finally, nortriptyline glutarate, imi sulfate and dox 4-hydroxybenozate were hydrated salt forms with no hydrogen bonding between the TCA cation and water.

It’s interesting to note that nortriptyline hexafluorosilicate and imipramine hexafluorosilicate formed hydrates which contrasts with the anhydrous nature found for all TCA and pure halide salt forms, both within this work and those found in the literature.[9 - 15]

4.2.3 Hydrate formation as a result of available hydrogen bond donor/acceptor

Research into the effect of the presence of hydrogen bond donor and acceptor groups on hydrate formation was carried out by Infantes et al.[5] They investigated 12 different donor-acceptor parameters to correlate to hydrate formation frequency in a dataset of nearly 35000 organic crystal structures. In their study the only parameter that showed a strong correlation with the occurrence rate of hydration was the sum of the number of hydrogen bond donors and acceptors (SDA) in each structure, excluding water molecules, see Figure 26.

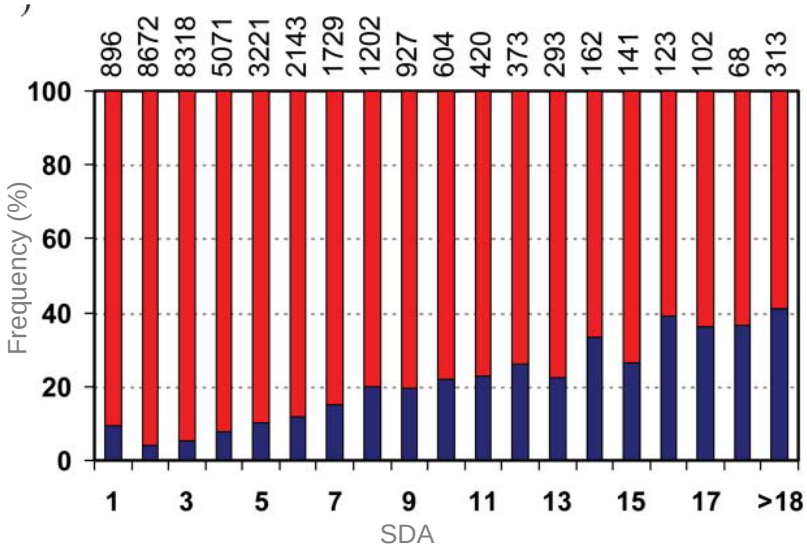

Figure 26: Hydrate (blue) and anhydrate (red) frequency for different donor + acceptor sum ranges.[5]

To generate a similar bar chart for the TCA structures from this work, the sum of donor and acceptor atoms for each structure, excluding water molecules, was divided by the Z' value. Structures were then classified as hydrate or anhydrate to determine if a similar trend would be observed, see Figure 27. Interestingly, a similar simple trend could not be observed. However, the rates of hydration above and below the average SDA, 5.7, were found to be 28% and 45% respectively. This gives some support to the idea that hydration is more likely at higher SDA, which corresponds to the results found in the study by Infantes et al.[5]

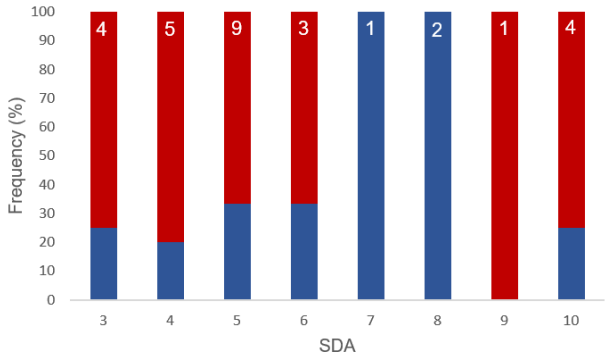

Figure 27: Hydrate (blue) and anhydrate (red) frequency for different donor + acceptor sum ranges.

Whereas Infantes et al. found no correlation between rate of hydration and the ratio of donor to acceptor atoms, Desiraju[6] had earlier reported a relationship between these factors in his 1991 paper comparing hydrate occurrence to donor/acceptor ratio excluding the water molecules from this determination. His work showed that the vast majority of hydrates within the scope occurred when there were less donor atoms than acceptors, see Figure 28. Specifically, he found that 65% of the hydrates had a donor/acceptor ratio below 0.5.

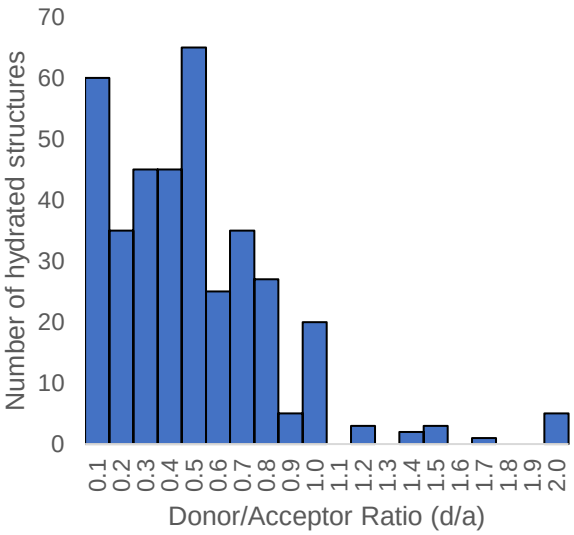

Figure 28: Histogram of donor/acceptor ratio for 411 hydrated non salt and metal-free crystal structures.[6]

Later work on structures of salt forms of the biological amine tyramine supported Desiraju's conclusion that hydrate formation was favoured by lack of donor groups.[7] These works imply that the main role of water is to supply the "missing" donor atoms to allow Etter's rule, that all good acceptors should be paired with a good donor[8], to hold.

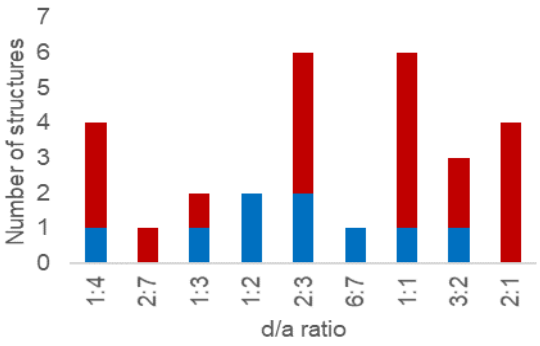

Figure 29: Number of hydrates (blue) and anhydrates (red) compared to donor/acceptor ratio.

The TCA structures were analysed using Desiraju's method to generate a similar diagram. 70% of hydrates compared to 55% of all structures had a d/a ratio below 1, see Figure 29. Therefore, for the given TCA structures hydrate formation is somewhat more likely at lower d/a ratios. Note that going to very low ratios (1:4) does not seem to increase the rate of hydrate formation.

See Table 32 for information on the number of hydrogen bond donors and acceptors, the donor/acceptor ratios and the sum for each structure in the data set. Hydrated forms were highlighted in blue bolded text.

Table 32: Hydrogen bond donor/acceptor numbers, ratios and sums for the TCA data set.

	Total excl. H_2O			Excl. H_2O / Z'				
Crystal	**Hbond donors**	**Hbond acceptors**	**Z'**	**Hbond donors**	**Hbond acceptors**	**Ratio**	**d/a**	**Sum**
ami oxalate	4	6	1	4	6	2:3	0.67	10
ami mucate	**3**	**2**	**1**	**3**	**2**	3:2	**1.50**	**5**
ami metanilate	**2**	**4**	**2**	**1**	**2**	1:2	**0.50**	**3**
ami salicylate	2	2	1	2	2	1:1	1.00	4
ami 4-nitrobenzoate	2	7	1	2	7	2:7	0.29	9
ami HBF_4	**2**	**8**	**2**	**1**	**4**	1:4	**0.25**	**5**
nor HBr	4	2	2	2	1	2:1	2.00	3
nor NaBr	4	2	2	2	1	2:1	2.00	3
nor KI	4	2	2	2	1	2:1	2.00	3
nor malonate	3	3	1	3	3	1:1	1.00	6
nor glutarate	**4**	**4**	**1**	**4**	**4**	1:1	**1.00**	**8**
nor mucate	4	2	1	4	2	2:1	2.00	6
nor salicylate	3	2	1	3	2	3:2	1.50	5
nor 4-hydroxyphenylacetate	6	4	2	3	2	3:2	1.50	5
nor edisylate	4	6	1	4	6	2:3	0.67	10
nor besylate	2	3	1	2	3	2:3	0.67	5
nor tosylate	2	3	1	2	3	2:3	0.67	5
nor HBF_4	2	8	2	1	4	1:4	0.25	5
nor SiF_6	**8**	**12**	**2**	**4**	**6**	2:3	**0.67**	**10**
imi oxalate	**4**	**6**	**2**	**2**	**3**	2:3	**0.67**	**5**
imi salicylate	2	2	1	2	2	1:1	1.00	4
imi 3-hydroxybenzoate	2	2	1	2	2	1:1	1.00	4
imi 4-hydroxybenzoate	16	16	8	2	2	1:1	1.00	4
imi sulfate	**2**	**4**	**1**	**2**	**4**	1:2	**0.50**	**6**
imi tosylate	**2**	**6**	**2**	**1**	**3**	1:3	0.33	**4**
imi HBF_4	4	16	4	1	4	1:4	0.25	5
imi SiF_6	**6**	**18**	**3**	**2**	**6**	1:3	**0.33**	**8**
dox 4-hydroxybenzoate	**6**	**7**	**2**	**3**	**3.5**	6:7	**0.86**	**6.5**
dox 4-nitrobenzoate	2	8	1	2	8	1:4	0.25	10

4.3 Unit cell Z'

The term Z' is defined as the number of times the compound formula is present in the asymmetric unit. This differs from Z, which is the number of compound formulas in the unit cell. Using the compound formula takes salt forms with a cation/anion ratio above or below one into account in determining the value of Z'. In the CSD[3], a Z' range of 1/96 to 32 was found with a massive majority of 95.3% of structures having a Z' of ½, 1 or 2. Specifically, Steiner found that only 8.8% of structures had a Z' value larger than 1 and only 0.07% of structures had a Z' larger than 4.[9] In this work, 14 structures had a Z' value of 1, 11 had a Z' of 2, two had a Z' value of 4 and one structure each was elucidated for Z' values of 3 and 8, see figure 4.7. This corresponds to 14% of structures having a Z' other than ½, 1 or 2, which is a much larger percentage than the overall CSD database. Additionally, 52% of newly elucidated TCA crystal structures have a Z'>1 compared to only 8.8% of all structures in the CSD. Furthermore, 1 of 29 structures has a Z' greater than 4 which corresponds to roughly 3% which is far greater than the 0.07% of structures found in the database with a Z' over 4. See Figure 30 for an overview of the Z' distribution. The exact percentages may be somewhat misleading as the number of samples is small, but it would appear that all four TCA bases are much more likely to form Z'>1 structures than is normal. Understanding why this might be would be fundamentally interesting.

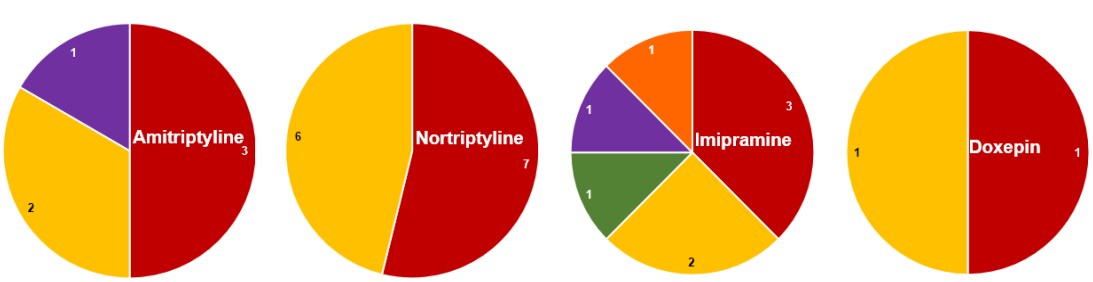

Figure 30: Distribution of Z' values in TCA crystal structures.

One explanation for the high occurrence of Z' values over 1 could be the different possible molecular conformations that can be adopted by the TCA cations.

4.3.1 Ring/chain conformation

The first set of conformations to be compared involves the direction of the chain in relation to the central ring, see Figure 31. The arrow on the ring starts at the backbone atom that is coplanar with the atom subtended by the chain. Figure 31 parts a and b show the nortriptyline cation in nor mucate in the A conformation and c and d show the nortriptyline cation in nor malonate in the B conformation.

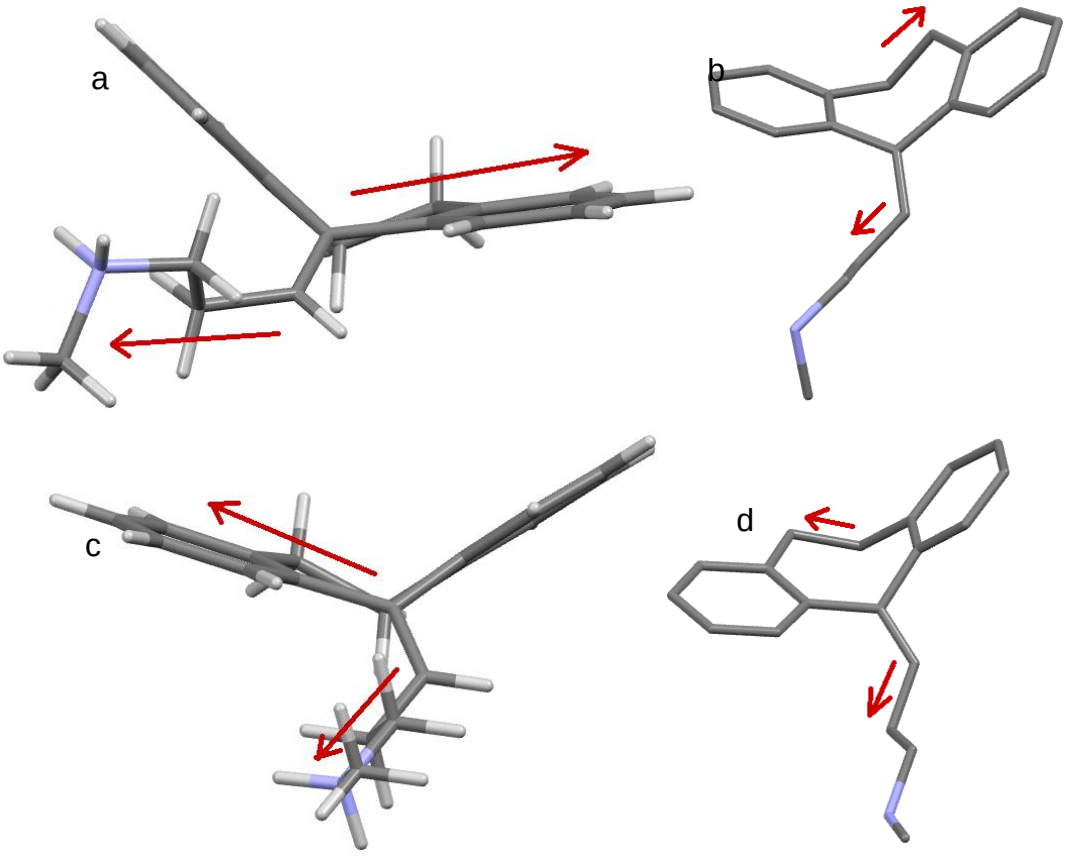

Figure 31: Examples of conformations A and B relating the chain to the tricyclic ring.

The majority of the TCA cations were found to be in the A conformation. Out of a total of 63 crystallographically independent cations, 49 (78%) were in the A conformation and only 14 (22%) were determined to be the B

conformation. 18 newly elucidated crystal structures had 2 or more independent cations in the structure. Three of these had more than one cation due to the 2:1 ratio of cation to anion, while the rest were truly Z'>1 structures. Out of these 18 structures, 11 contained only one type of conformation while the other 7 structures contained a mix of A and B conformation. Excluding the Z'=1 structures, this changes to 9 structures with one type and 6 structures with mixed conformers. This data suggests that the difference in this particular conformation cannot completely explain the high occurrence of Z'>1, because the majority of such structures only contain one of the conformations.

4.3.2 Torsion angle α

Next, two torsion angles were compared. Torsion angle α was defined as C14-C15-C16-C17 for amitriptyline and nortriptyline, C13-C14-C15-C16 for doxepin, and C14-N1-C15-C16 for imipramine. C14 was defined as being on the ring that is coplanar with the atom subtended by the chain. Conformer X was defined as having an angle range from 144.01° to 179.90° for all TCAs. The angle ranged from 0.23° to 8.29° for conformer Y for ami, nor, and dox while conformer Z had an angle range of 52.90° to 68.47° for imi. See Figure 32 for examples of conformer X, Y, and Z for torsion angle α.

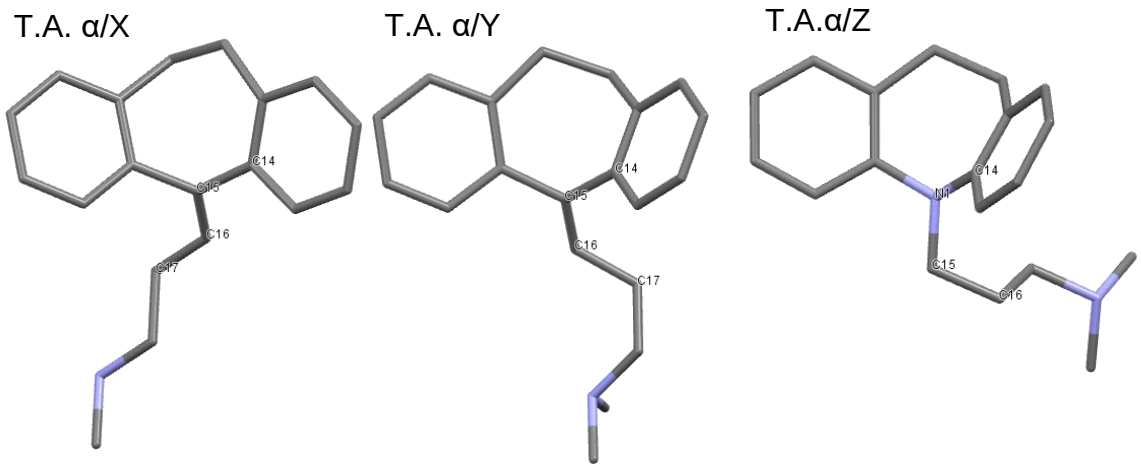

Figure 32: Examples of conformer X, Y and Z for torsion angle α.

The data set of 29 crystal structures contained a total of 63 cations. Out of 63 cations, 34 were conformer X (54%),15 were conformer Y (24%), and 14 were conformer Z (22%), see Figure 33.

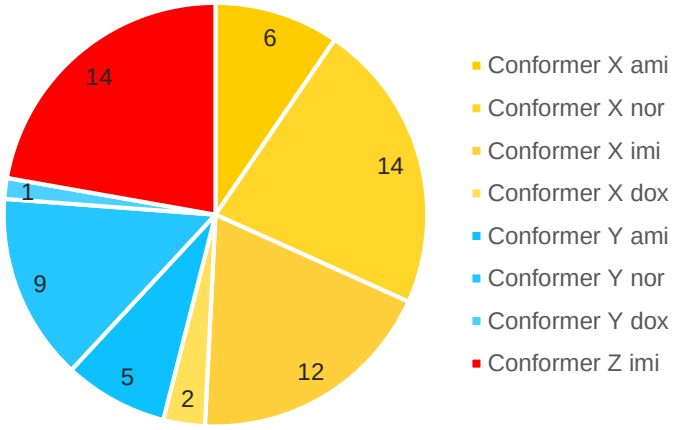

Figure 33: Distribution of conformers for angle α.

4.3.3 Torsion angle β

Torsion angle β was defined as C16-C17-C18-N1 for amitriptyline and nortriptyline, C15-C16-C17-N1 for doxepin, and C15-C16-C17-N2 for imipramine. For conformer M the torsion angle ranged from 60.24° to 79.77° and can also be described as the gauche confirmation, whereas Conformer N was defined as having an angle range from 152.42° to 179.85° and can be described as the anti confirmation. See Figure 34 for examples of conformer M and N for torsion angle β.

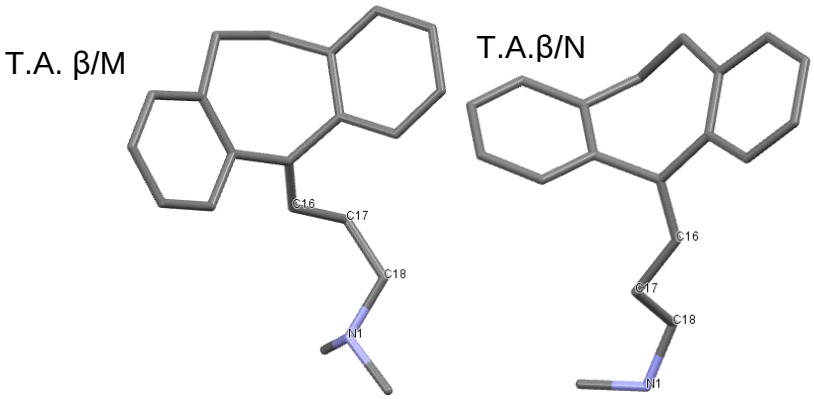

Figure 34: Examples of conformer M and N for torsion angle β.

Out of 63 cations, 13 were conformer M (21%) and 50 were conformer N (79%). See Figure 35 for the distribution of conformers by TCA. Conformer N is likely favoured due to its anti confirmation being energetically favourable due to lower steric hindrance.[10]

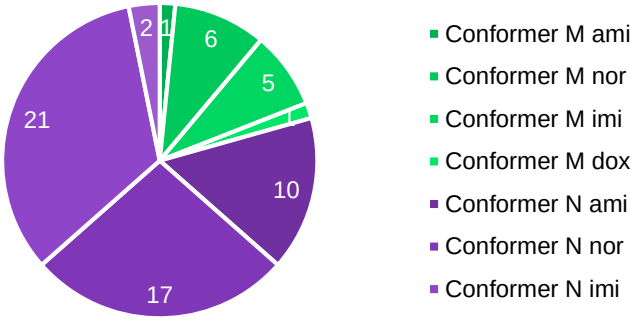

Figure 35: Distribution of conformers for angle β.

4.3.4 Conformation combinations

A combination of these different conformers is a likely explanation for the higher rate of Z' over 1 seen for these TCA cations. Out of 15 crystal structures with Z' over 1, only two were made up of multiple cations in the same conformation. Both of these had a Z' of 2. The crystal structure with the highest Z' value was imipramine 4-hydroxybenzoate with a Z' of 8. Within the 8 independent cations present in the asymmetric unit, there were 3 distinct conformations; AYN, BYM, and BXM, see Figure 36. Note that in their review Steed and Steed suggest that one factor favouring high Z' structures may be that the structure consists of small, rigid, inflexible molecules.[9] This is certainly not the case for the TCA salt structures studied here.

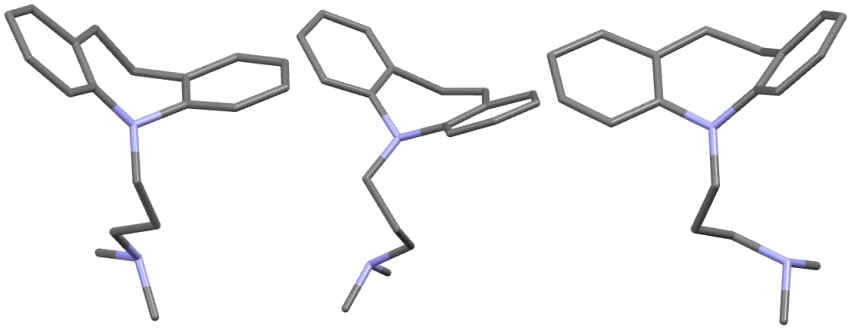

Figure 36: Imipramine cation conformations found in imipramine 4-hydroxybenzoate, from left to right AZN, BZM and BXM.

See Table 33 and Table 34 for the confirmation data analysis per structure.

Table 33: Conformation data for the amitriptyline (ami) and nortriptyline (nor) structures

Structure	Crystal	Ring/chain conformation	Torsion angle α	Torsion angle β
ami HBF_4	4:4:5	A	Y	N
		A	X	N
		A	Y	N
		A	X	N
ami oxalate	2:2	A	Y	N
		A	X	N
ami 4-nitrobenzoate	1:2	A	Y	M
ami mucate	1:1:3	A	X	N
ami metanilate	2:1:3:1Cl	A	X	N
		A	Y	N
ami salicylate	1:1	A	X	N
nor HBF_4	2:2	A	X	N
		A	X	M
nor tosylate	1:1	A	X	N
nor besylate	1:1	A	Y	N
nor malonate	1:1	B	X	N
nor edisylate	2:1	A	X	M
		A	X	M
nor glutarate	2:1:1	A	Y	N
		A	X	N
nor mucate	1:1	A	X	N
nor 4-hydroxyphenylacetate	2:2	A	Y	N
		A	Y	N
nor salicylic	1:1	A	X	N
nor HBr	2:2	B	Y	N
		A	X	M
nor NaBr	2:2	A	Y	M
		B	X	N
nor SiF_6	4:2:6	A	Y	N
		A	X	N
		A	Y	N
		A	Y	N
nor KI	2:2	A	Y	M
		B	X	N
	disorder	A	Y	M

Table 34: Conformation data for the imipramine (imi) and doxepin (dox) structures

Structure	Crystal	Ring/chain conformation	Torsion angle α	Torsion angle β
imi HBF_4	4:4	A	X	M
		A	Z	M
		B	X	N
		B	Z	N
imi oxalate	2:2:3	A	Z	N
		A	Z	N
imi sulfate	2:1:8	B	X	N
		A	X	N
imi SiF_6	6:3	B	X	N
		B	X	N
		B	X	N
		A	X	N
		A	X	N
		A	Z	N
imi salicylate	1:1	A	X	M
imi 3-hydroxybenzoate	1:1	A	Z	N
imi 4-hydroxybenzoate	8:8	B	X	M
		A	Z	N
		A	Z	N
		A	Z	N
		A	Z	N
		A	Z	N
		B	Z	M
		A	Z	N
imi tosylate	2:2:2	B	X	N
		B	Z	N
dox 4-hydroxybenzoate	2:2:1n	A	Y	N
		A	X	N
dox 4-nitrobenzoate	1:1:1n	A	X	M

4.3.5 Disorder as a cause for high Z' values

Another thing of note was the frequent full or partial cation disorder found in this data set. As a side note, this disorder is the commonest reason why several of the structures reported have higher R factors than is ideal. Five of the TCA salt structures contained a cation site where all atoms of the cation were disordered. These were amitriptyline metanilate, nortriptyline glutarate, nortriptyline tetrafluoroborate, nortriptyline iodide, and doxepin 4-nitrobenzoate. Additionally, the amitriptyline cation in ami mucate was partially disordered throughout the entire tricyclic ring system. See Figure 37 for the disorder in nortriptyline iodide. This disorder is related to the discussion above on molecular conformation and Z' values. As an example, nortriptyline iodide has a Z' of 2 and the ordered cation site has conformation combination AYM. The major conformer on the other site is the opposite BXN. But this site was fully disordered, and the minor disorder component was determined to be conformation AYM. Thus, the availability of many different cation conformations results in a structural set with a high percentage of Z'>1 structures and a high percentage of disordered structures. Here a Z'>1 structure indicates an ordered array of the different conformations. Disorder may truly be that – the structure does not successfully discriminate between the available conformations. There is however a chance that larger super cells or modulated structures have not been identified here and that these structures are ordered but with high Z' values.

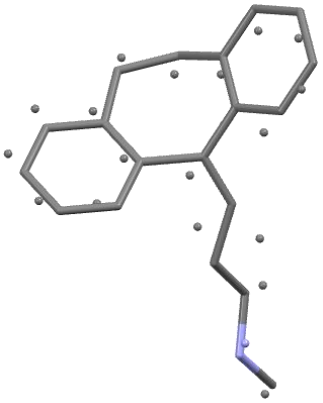

Figure 37: Disorder found in nortriptyline iodide.

4.4 Nortriptyline solubility

Salt formation is the most common option used by pharmaceutical companies to improve the aqueous solubility of ionisable APIs. Solubility is often improved by salt formation due to the inherent polarity of salts and the additional functional groups providing beneficial intermolecular interactions.

The solubility of a selection of nortriptyline salts was determined by preparing duplicate slurries of each salt in deionised water, diluting a known amount of each saturated solution, and then carrying out UV/VIS analysis, see section 3.7.3 for the full experimental procedure. The average absorbance was compared to the calibration curve prepared in section 3.7.1 to obtain the concentration. The concentration was then corrected for the dilution factor of each sample to give the approximate aqueous solubility, see Table 35.

The solids obtained from the slurry experiments were analysed by x-ray powder diffraction which determined that most of the bulk materials matched the phase identified by single crystal diffraction previously, see Figure 39 to Figure 43 for the Pawley fit of the single crystal unit cell to the XRPD data. The bromide salt is the monoclinic polymorph shown in Table 14. During this process, a new phase of nortriptyline salicylate was identified by XRPD, see Figure 44. As a full structural determination was not performed from the XRPD data, the exact chemical nature of this phase is thus unknown.

Table 35: Solubility slurry experiment results

	Absorbance	Concentration (mol/L)	Solubility corrected for dilution (mol/L)	Average (mol/L)	% difference
Nor Chloride (1.2)	0.754	4.05E-05	8.09E-02	8.71E-02	15
Nor Chloride (2.2)	0.852	4.66E-05	9.32E-02		
Nor Bromide (1)	0.862	4.72E-05	4.72E-02	4.59E-02	6
Nor Bromide (2)	0.819	4.45E-05	4.45E-02		
Nor Iodide (1.2)	0.290	1.14E-05	5.71E-03	4.30E-03	49
Nor Iodide (2.2)	0.200	5.78E-06	2.89E-03		
Nor salicylate (1.2)	0.118	6.45E-07	3.22E-04	4.01E-04	49
Nor salicylate (2.2)	0.123	9.58E-07	4.79E-04		
Nor tosylate (1)	0.148	2.52E-06	2.52E-03	2.08E-03	35
Nor tosylate (2)	0.134	1.65E-06	1.65E-03		
Nor besylate (1)	0.180	4.53E-06	4.53E-03	4.34E-03	8
Nor besylate (2)	0.174	4.15E-06	4.15E-03		
Nor free base	0.168	3.77E-06	3.77E-03	2.62E-03	61
Nor free base	0.131	1.46E-06	1.46E-03		

Usually, salt formation of an API will improve aqueous solubility.[1] However, the solubility experiments found that the nortriptyline free base showed a higher solubility than the salicylate and tosylate salts. The single crystal structure of the free base was not elucidated so it could not be directly compared to the XRPD pattern obtained from the free base slurry experiments. However, this XRPD diffractogram contained peaks matching the chloride salt diffractogram and thus indicating the presence of chloride salt, see Figure 45. To further investigate, a sample of the prepared free base material was submitted for microanalysis to determine the residual chloride content. 2.698 % of chloride was observed. It was concluded that the results were influenced by the high solubility of the small amount of chloride salt remaining in the free base material. Due to this, and the poor reproducibility shown above, the free base solubility was not accurate and shall be ignored in the discussion below.

Despite problems with precision, especially for the less soluble materials, the data is able to place the nortriptyline salts in order of solubility. The most soluble salt form of nortriptyline was clearly the chloride salt which was over 200 times more soluble than the salicylate salt, which was determined to be the least soluble, see Figure 38. The bromide salt is also orders of magnitude more soluble than the non chloride samples. The iodide and besylate are then somewhat more soluble than the tosylate which is somewhat more soluble than the salicylate i.e. Cl > Br >>I ≥ besylate > tosylate > salicylate. With the exception of the new and hence chemically unidentified salicylate salt form, all are anhydrous forms and thus hydration state is not a variable here.[1] The largest solubility differences are for the halide ions, and these follow periodic table order and the order of the ions enthalpy of hydration.[29] This might suggest that for these salts solution state properties are more important than solid state properties in determining solubility. From a commercial standpoint, typically there would be no reason from this data not to use the chloride salt as the commercial API. It has the greatest aqueous solubility and chloride is inherently safe and cheap.

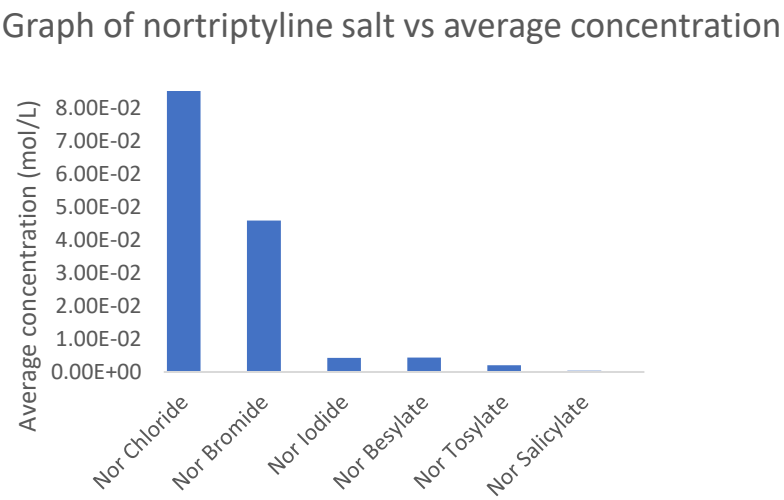

Figure 38: Graph of average concentration vs nortriptyline salt form.

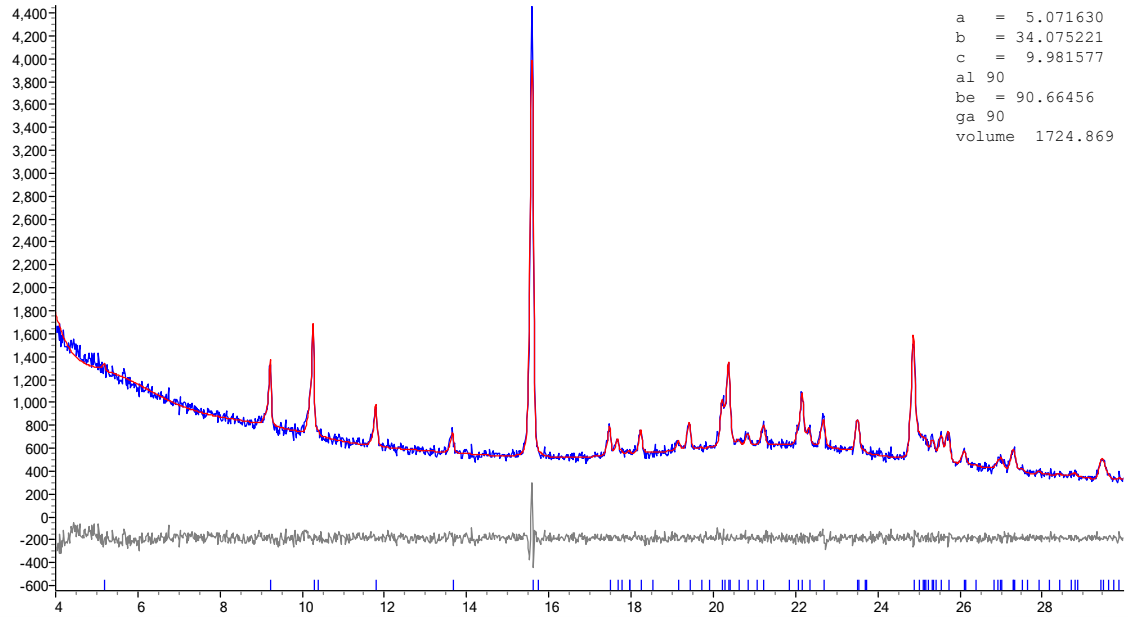

Figure 39: Pawley fit of Chloride SX cell (JINGIW) to PXRD data

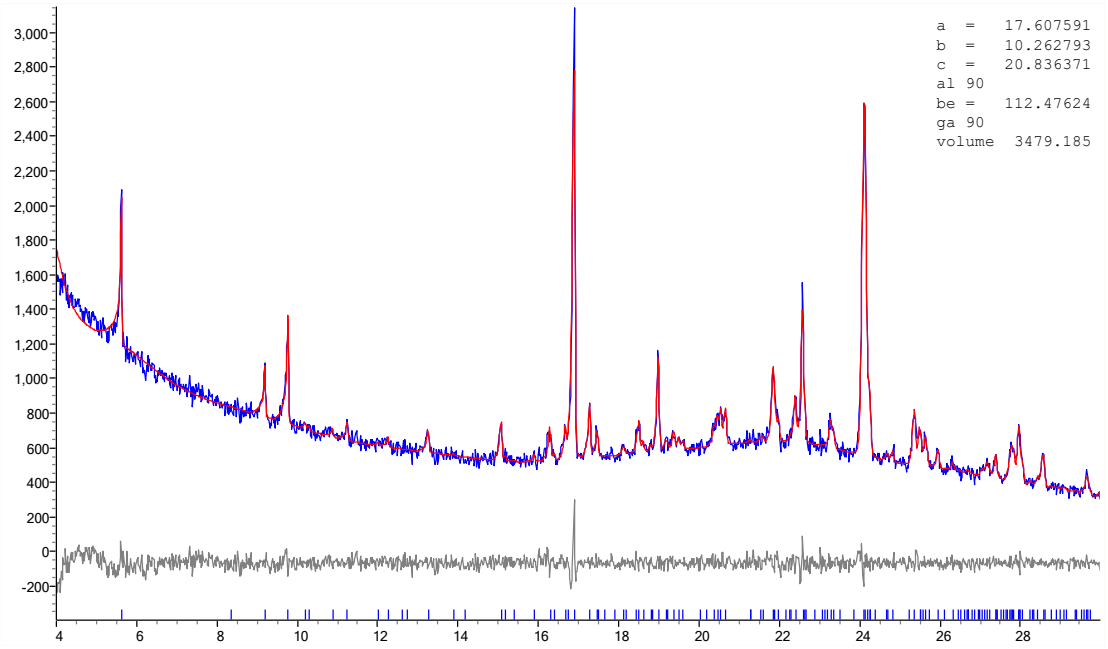

Figure 40: Pawley fit of Monoclinic Bromide SX cell (nor_nabr in Table 14) to PXRD data

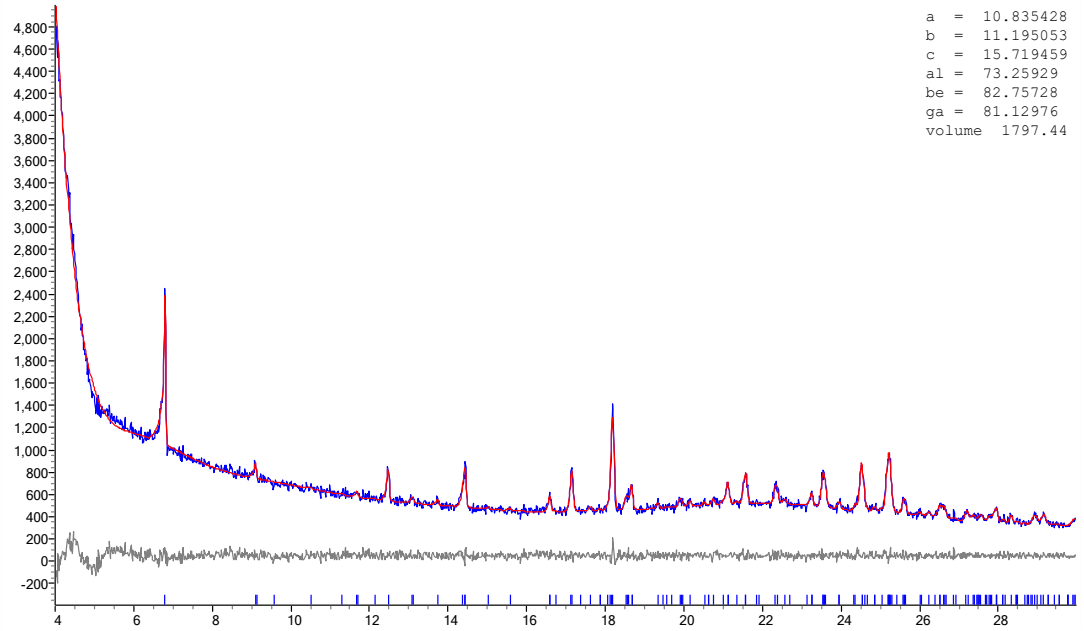

Figure 41: Pawley fit of Iodide SX cell to PXRD data

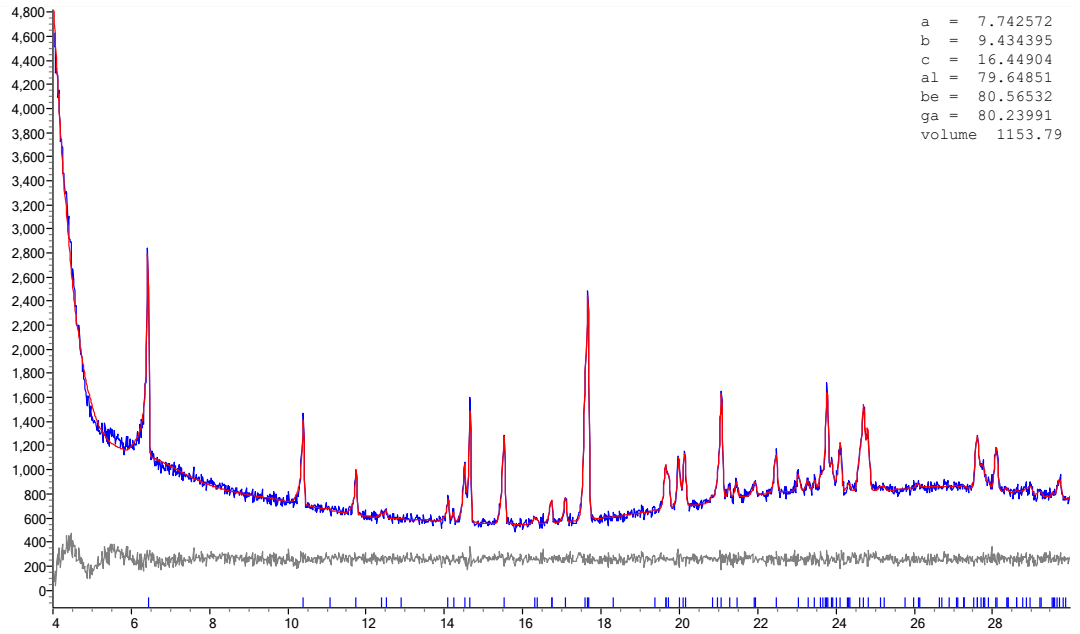

Figure 42: Pawley fit of Tosylate SX cell to PXRD data

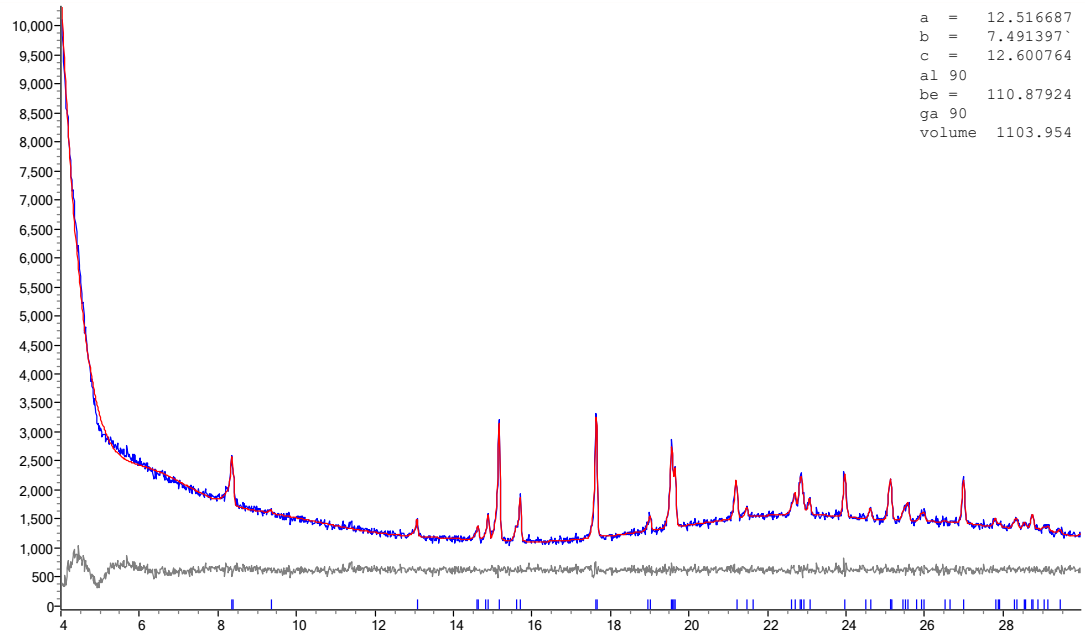

Figure 43: Pawley fit of Besylate SX cell to PXRD data

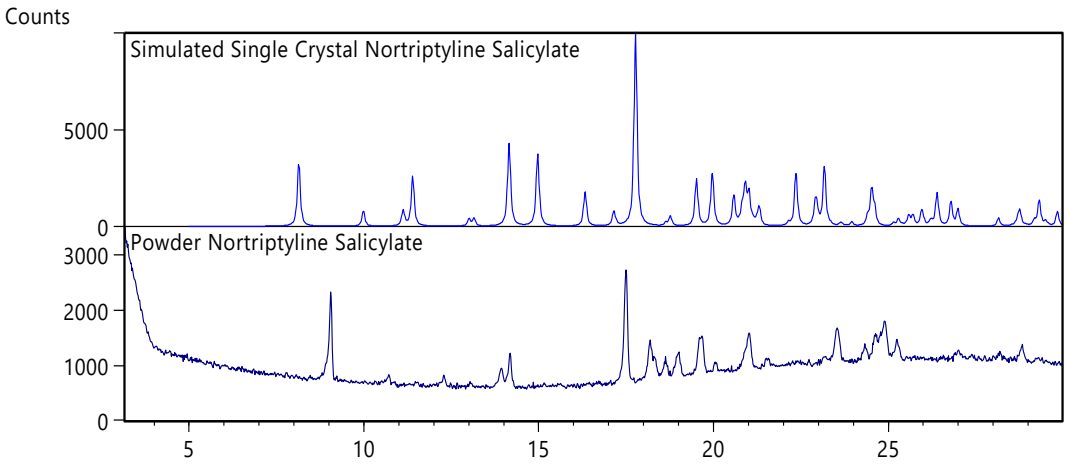

Figure 44: Simulated XRPD 2θ diffractogram of the nortriptyline salicylate single crystal (top) vs the experimental XRPD 2θ diffractogram of the bulk material used in the solubility assessment (bottom)

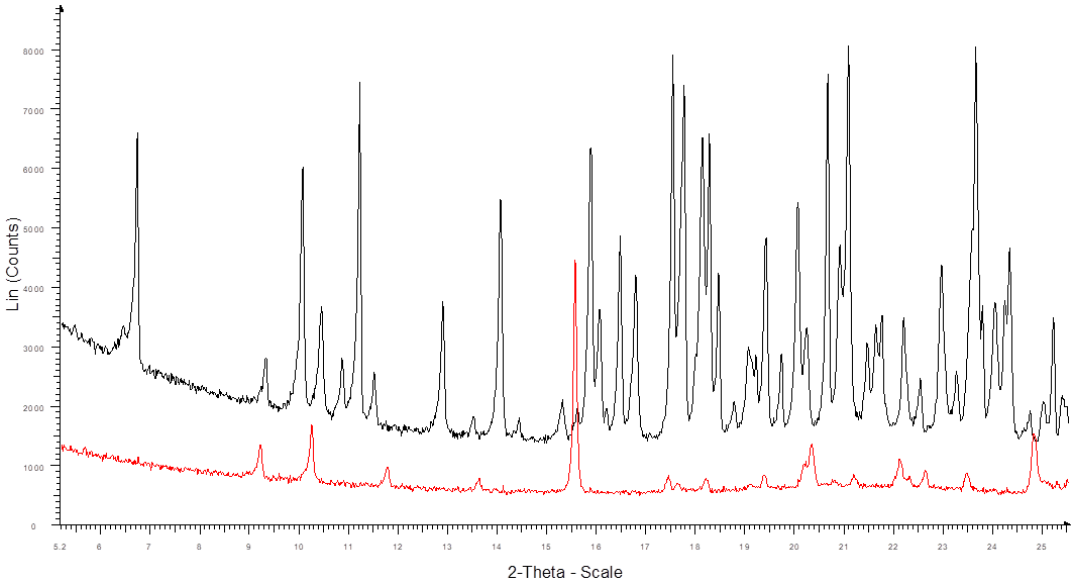

Figure 45: XRPD 2θ diffractogram overlay of the nortriptyline free base (black) and the nortriptyline chloride (red)

4.5 Structural analysis

4.5.1 ConQuest database search

The ConQuest database search of tricyclic antidepressants found 13 structures to add to the structural analysis. The 13 cif files obtained in the search were added to the cif files for the 29 structures elucidated in this work. The full data set of 42 structures is listed in Table 36.

The ConQuest database search of carbamazepine and dihydrocarbamazepine found 85 structures for the structural analysis. The full data set is listed in Table 37, where A refers to carbamazepine and form B refers to dihydrocarbamazepine.

Table 36: Full tricyclic antidepressant salt form dataset for structural analysis

CSD code or sample ID	Cation	Anion	CSD code or sample ID	Cation	Anion
YOVZEO	amitriptyline	chloride	IMIPRC	imipramine	chloride
ami_HBF4	amitriptyline	tetrafluoroborate	IMIPRB	imipramine	bromide
ami_oxalic	amitriptyline	oxalate	MIGQID	imipramine	picrate
ami_4nitro	amitriptyline	4-nitrobenzoate	imi_oxalic	imipramine	oxalate
ami_mucic	amitriptyline	mucate	imi_sulfate	imipramine	sulfate
DIKWEA	amitriptyline	picrate	imi_3hyd	imipramine	3-hydroxybenzoate
ami_meta	amitriptyline	metanilate/chloride	imi_4hyd	imipramine	4-hydroxybenzoate
ami_sal	amitriptyline	salicylate	imi_HBF4	imipramine	tetrafluoroborate
nor_sal	nortriptyline	salicylate	imi_ptolsulf	imipramine	Tosylate
JINGIW	nortriptyline	chloride	imi_SiF6	imipramine	hexafluorosilicate
nor_ptolsulf	nortriptyline	tosylate	imi_sal	imipramine	salicylate
nor_benzsulf	nortriptyline	besylate	dox_4hyd	doxepin	4-hydroxybenzoate
nor_malonic	nortriptyline	malonate	dox_4nitro	doxepin	4-nitrobenzoate
nor_edisulf	nortriptyline	edisylate	AFEVOX	desipramine	Picrate
nor_glutaric	nortriptyline	glutarate	HISHEX	desipramine	Picrate
nor_HBr	nortriptyline	bromide (HBr)	PUKGEI	desipramine	Chloride
nor_NaBr	nortriptyline	bromide (NaBr)	CIMPRA01	clomipramine	Chloride
nor_SiF6	nortriptyline	hexaflurosilicate	DUNGAV	clomipramine	Picrate
nor_KI	nortriptyline	iodide	DUNKED	trimipramine	Maleate
nor_4hydphen	nortriptyline	4-hydroxyphenylacetate	FUHGIY	lofepramine	Chloride
nor_HBF4	nortriptyline	tetrafluoroborate			
nor_mucic	nortriptyline	mucate			

Table 37: Full carbamazepine (A) and dihydrocarbamazepine (B) dataset for structural analysis

CSD code	API	Anion/solvent
ABOQUF	A	Hydroquinone
AFEVEN	B	Formamide solvate
AFEZOB	B	DMSO solvate
CBMZPN03	A	N/A
CBMZPN11	A	N/A
CBMZPN12	A	N/A
CMBZPN16	A	N/A
CBMZPN27	A	N/A
CRBMZA01	A	Acetone solvate
FAYXOV	A	4-amino-2-hydroxybenzoic acid
FAYXUB	A	4-amino-2-hydroxybenzoic acid monohydrate
FAYYAI	A	4-Amino-2-hydroxybenzoic acid methanol
FEFNOT09	A	dihydrate
FEFNOT11	A	dihydrate
FOMXAH	A	Furfural solvate
GINFOZ	A	Trifluoroacetic acid solvate
GINFOZ02	A	Trifluoroacetic acid solvate
HEMRIB	B	N/A
HUQWIB	A	Oxonium tetrafluoroborate pentahydrate
HUQWOH	A	Tetrafluoroborate hemihydrate
JORGEE	A	Hemikis(oxonium) hemikis(chloride) monohydrate
KICWOK	A	Pyrimethamine methanol solvate
KIWBEY	A	N,N-dimethyl acetamide solvate
KIWBIC	A	N-methylpyrrolidone solvate
KIWBOI	A	Nitromethane solvate
LEXPIQ	A	Anthracene-9-carboxylic acid
LEXPOW	A	Naphthalene-1-carboxylic acid monohydrate
LEXPUC	A	2,3-Dihydroxybenzoic acid methanol solvate
LEXQAJ	A	2,3-Hydroxybenzoic acid
LOFKIB	A	Isonicotinamide
MIMQIJ	A	Tetrahydrofuran solvate
MOXVAX	A	Benzoic acid
MOXVEB	A	Adipic acid
MOXVIF01	A	4-Hydroxybenzoic acid
MOXVIF02	A	4-Hydroxybenzoic acid
MOXVIF03	A	4-Hydroxybenzoic acid
MOXVOL	A	Glutaric acid
MOXVUR	A	Malonic acid
MOXWAY	A	Salicylic acid
MOXWEC	A	L-1-hydroxy-2-naphthoic acid
MOXWIG	A	DL-tartaric acid
MOXWOM	A	Maleic acid
MOXXAZ	A	(+)-Camphoric acid
OTESEM	B	Saccharin
PEYSOD	A	Monohydrate
QANQUS	A	N,N,-dimethylformamide solvate
SAPDUJ	A	2,2,2-Trifluoroethanol solvate
SEZDIL	B	Formic acid solvate
TAZRAO	A	Aspirin

CSD code	API	Anion/solvent
UNEYIV02	A	DMSO solvate
UNEYIV05	A	DMSO solvate
UNEYOB	A	Benzoquinone solvate
UNEYUH	A	Terephthalaldehyde solvate
UNEZAO	A	Saccharin
UNEZAO01	A	Saccharin
UNEZES	A	Nicotinamide
UNEZIW	A	Acetic acid solvate
UNEZOC	A	Formic acid solvate
UNEZUI	A	Butyric acid solvate
UNIBEY	A	5-Nitroisophthalic acid methanol solvate
UNIBIC	A	Hemikis(adamantane-1,3,5,7-tetracarboxylic acid)
UNIBOI	A	Formamide solvate
UWAZID	A	Thiourea
VACTAU01	B	N/A
VACTAU02	B	N/A
VACTAU03	B	N/A
VACTAU04	B	N/A
VEXLOA01	B	Acetic acid solvate
VEJZUI	A	Chlorothiazide acetone solvate hemihydrate
VIGGOI	A	Quinoxaline-N,N'-dioxide
VUBCEA	A	Ammonium bromide
VUBCEA01	A	Ammonium bromide
WEYFEN	A	Hemikis(fumaric acid)
XAQQUC	A	4,4'-bipyridine
XAQRAJ	A	4-aminobenzoic acid
XAQREN	A	4-aminobenzoic acid monohydrate
XAQRIR	A	2,6-pyridinedicarboxylic acid
XOBCEX	A	Hemikis(malonic acid)
XOBCIB	A	Hemikis(succinic acid)
XOXHEY	A	4-Aminobenzoic acid
YABHIU	A	Pterostilbene
YADZAH	A	Monohydrate
YAJGEY	A	Thiosaccharin
YAJGIC	B	Thiosaccharin
YUXDIG	A	Acridinium triiodide iodine

4.5.2 Crystal packing similarity of tricyclic antidepressant salt forms

The crystal packing similarity tool available within the Mercury software[18] was used to calculate the level of packing similarity between the structures listed in Table 36. This was used to find isostructural groups within a data set of tricyclic antidepressant structures obtained from the literature by searching the CCDC structural database[19] and structures elucidated in this work. See section 4.5.1 for further details.

A tree diagram was constructed based on the number of similar molecular fragments between the structures within the data set, see Figure 46.

The structures were listed with the number of molecular fragments in common increasing as you go down the tree diagram. Structures were named isostructural in cases where the matching molecular cluster contained at least 15 molecules.

Four isostructural groups were identified:

1. Desipramine picrate (AFEVOX), amitriptyline picrate (DIKWEA), and imipramine picrate (MIGQID)
2. Amitriptyline metanilate/chloride (ami_meta) and imipramine hexafluorosilicate (imi_SiF6)
3. Imipramine chloride (IMIPRC) and imipramine bromide (IMIPRB)
4. Nortriptyline bromide (nor_HBr) and nortriptyline iodide (nor_KI)

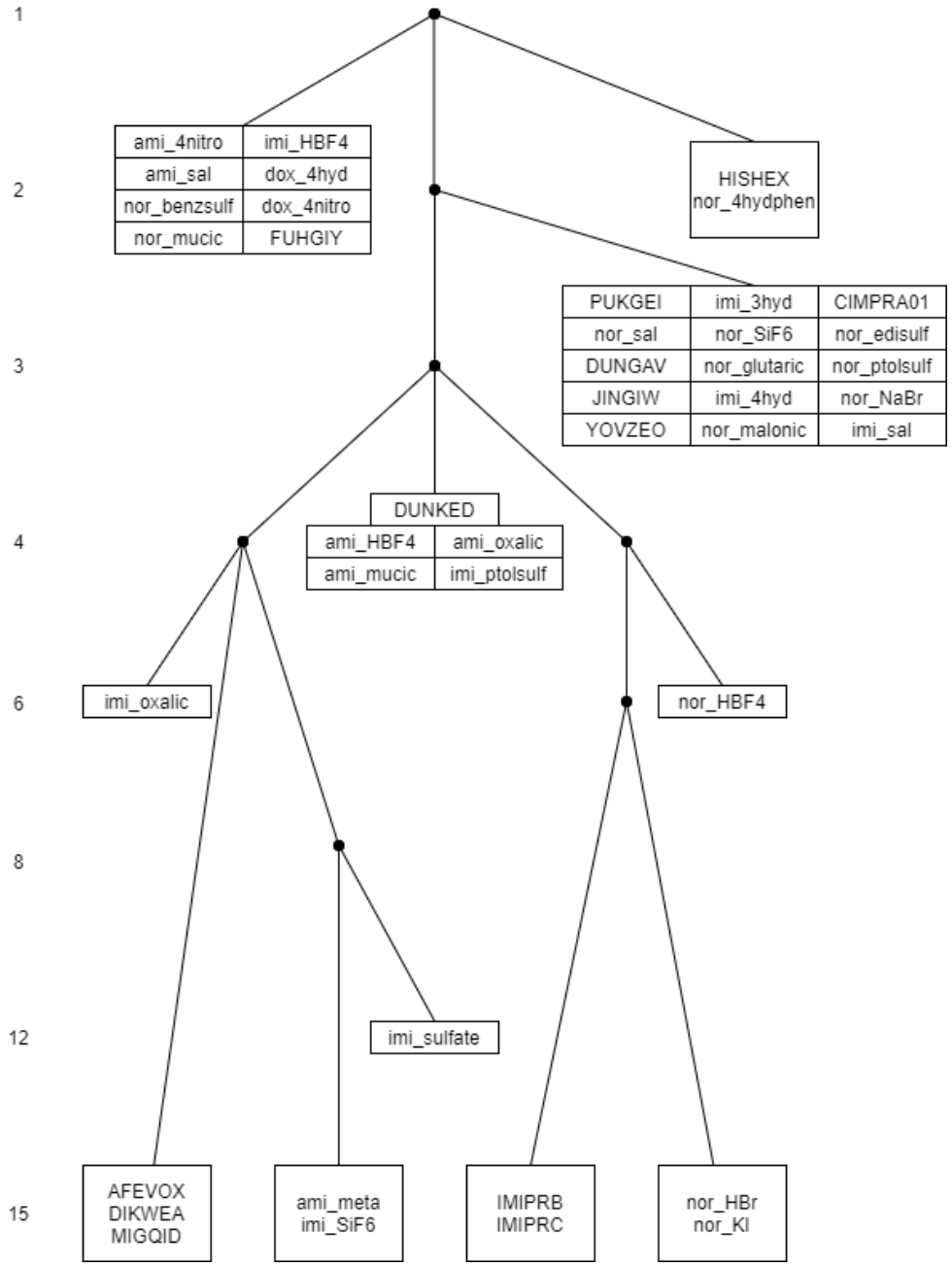

Figure 46: Tree diagram of tricyclic antidepressant salt forms

4.5.2.1 Group 1

Group 1 consists of desipramine picrate (AFEVOX), amitriptyline picrate (DIKWEA), and imipramine picrate (MIGQID), see Figure 48.

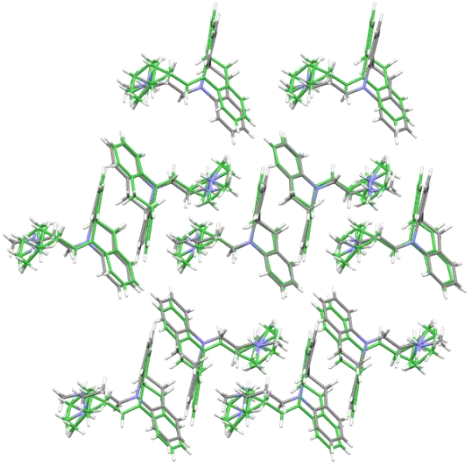

Figure 48: Overlay of desipramine picrate hydrate and amitriptyline picrate (green). Viewed along the crystallographic a axis.

The three tricyclic antidepressant salts in group 1 all contain the same counterion, picrate (see Figure 47), but different TCA cations, amitriptyline, imipramine and desipramine. This group is a nice illustration of the counterion imposing the same packing structure on different APIs. This structural group also encompassed both anhydrous forms and the hydrated desipramine form, indicating that the packing motif is robust even enough to encompass solvation changes and the associated hydrogen bonding changes. Amitriptyline picrate and imipramine picrate contain a discrete hydrogen bond between the TCA amine group and the picrate counterion. On the contrary, desipramine picrate hydrate contains a ring hydrogen bonded network involving the TCA amine group, water molecules, and the picrate counterion.

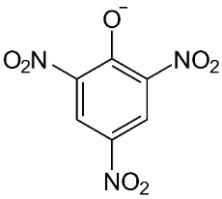

Figure 47: Picrate anion

Interestingly, there were an additional two anhydrous picrate salts in the structural analysis data set, namely an anhydrous desipramine picrate and a clomipramine picrate, that were not in group 1. Note that the anhydrous desipramine form does not from part of Group 1 whilst the monohydrate desipramine form does, despite the other members of the group being anhydrous.

The three salt forms in group 1 were refined in the P-1 space group and all have broadly similar unit cell dimensions. The anhydrous desipramine picrate was refined in the C2/c space group while the clomipramine picrate was refined in the P-1 space group like the three picrate salts in group 1, but has a very different unit cell and Z' =2 rather than Z' =1 as seen in Group 1.

Despite the different packing, the clomipramine picrate contains a discrete hydrogen bond similar to the one observed in amitriptyline and imipramine picrate.[20]

Despite featuring different APIs, the conformations as described in section 4.3 matched well for this group. The three salts contained a ring/chain conformation denoted as conformer A, torsion angle α was conformer X for the imipramine and amitriptyline picrate salts and conformer Y for the desipramine salt, and torsion angle β was found exclusively as the N conformer. Thus, although the cation packing seems here to be determined by the anion, only a limited amount of variation is allowed in the cation conformation.

The salt forms in group 1 illustrate that many factors are at play in forming isostructural groups. The three isostrucutral salts were refined in the same space group and contained the same counterion but did not share hydrogen bonding motifs, had different APIs and different hydration states. Whereas the clomipramine picrate satisfied the first two parameters and even shared the same hydrogen bonding motif as two of the three salts in group 1 but did not form part of the isostructural series.

4.5.2.2 Group 2

Group 2 consisted of amitriptyline metanilate/chloride (ami_meta) and imipramine hexafluorosilicate (imi_SiF6), see Figure 49.

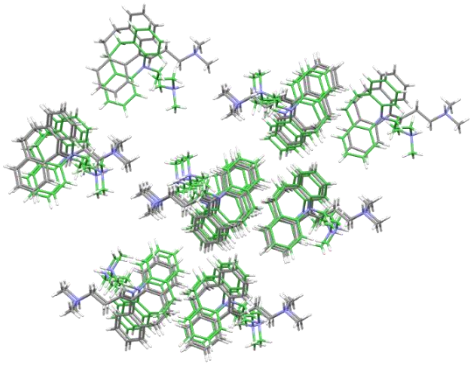

Figure 49: Overlay of amitriptyline metanilate chloride hydrate and nortriptyline hexafluorosilicate hydrate (green)

The two salt forms in group 2 do not have an obvious reason for being isostructural. Interestingly, both metanilate and chloride anions were present in the amitriptyline salt, likely due to unwanted remaining chloride in the prepared free base sample. The metanilate, chloride and hexafluorosilicate counterions are obviously unrelated in both shape and size. The metanilate counterion, $H_2NC_6H_4SO_3$, came from an aryl sulfonic acid while hexafluorosilicate is an octahedral inorganic species.

Both salt forms are hydrates and both form hydrogen bonds from the TCA amine group to water molecules. The amine in the amitriptyline metanilate salt exclusively formed discrete hydrogen bonds to water molecules, despite the presence of chloride anions and charged sulfonate groups. It is thus one of the few SSIP structures as described in Section 4.2.2. On the other hand, the nortriptyline amine group formed hydrogen bonds to water molecules in a ring motif and also to the hexafluorosilicate fluorine atoms.[20]

Both salt forms were refined in the P-1 space group. However, the unit cells are different, and the amitriptyline salt has a Z' of 2 whereas the nortriptyline salt has a Z' of 4.

As in group 1, despite featuring two different APIs, the conformations matched well for this group. Both salts contained a ring/chain conformation denoted as conformer A, torsion angle α was a mixture of conformers X and Y for the different formula units within the asymmetric unit, and torsion angle β was found exclusively as the N conformer. Like in group 1, differences were observed in torsion angle α within this isostructural group, whereas the other conformations matched.

Overall, the two salts in this group seem to be very different from each other. It is thus surprising that they adopt isostructural cation packing. Why these two un-alike structures do so whilst other more similar species do not is unclear.

4.5.2.3 Group 3

Group 3 consists of imipramine chloride (IMIPRC) and imipramine bromide (IMIPRB), see Figure 50.

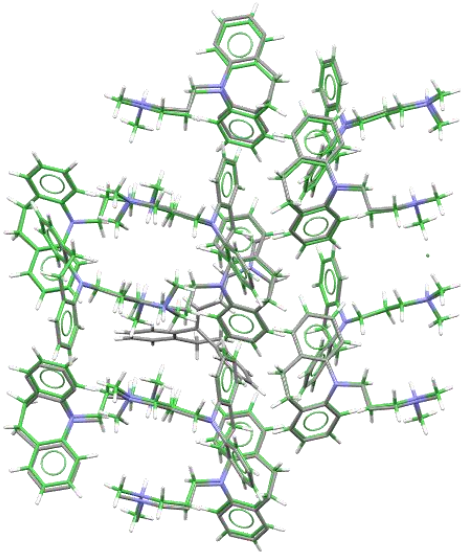

Figure 50: Overlay of imipramine bromide and imipramine chloride (green). Viewed along the crystallographic a axis.

The two structures in this group are isostructural and isomorphous in their entirety as opposed to just with respect to the cation packing. In line with this the structures and their contents are much more similar than is the case with the groups described above. Imipramine bromide and imipramine chloride have the same TCA cation, are both anhydrous, and they both have a halide counterion.

The hydrogen bonding is also identical, with the TCA amine group and the halide counterion connecting in 0D discrete hydrogen bonding networks.[20]

When considering why this pair of structures should be so similar, it may be relevant that imipramine has a more rigid structure due to the nitrogen group in the tricyclic ring. Conformationally, it was found to only form one type of torsion angle α, see section 4.3.2, as opposed to the two conformations observed in the other TCAs in the data set elucidated in this work. Thus, the imipramine halide salt forms had fewer conformational options and hydrogen bond donors associated with the cation, and this paired with the similarity in the counterion's shape and functionality likely supported the formation of isostructural compounds.

4.5.2.4 Group 4

Group 4 consists of nortriptyline bromide (nor_HBr) and nortriptyline iodide (nor_KI), see Figure 51.

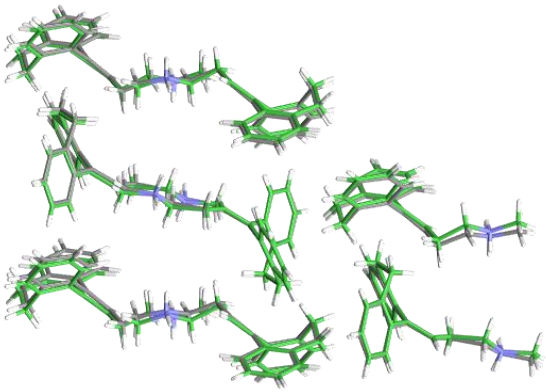

Figure 51: Overlay of nortriptyline bromide and nortriptyline iodide (green). Viewed along the crystallographic a axis.

The salt forms in group 4 follow the same observations as the ones in group 3. Both salt forms have the same TCA free base, nortriptyline, and they both have halide counterions. The counterions were bromide and iodide in this case. Notably, the nortriptyline chloride was included in the structural analysis dataset but was not found to be isostructural with these salt forms. Unfortunately, from the point of view of analysing the solubility values found for these salts, the bromide polymorph that is isostructural with the iodide is not the polymorph that was recovered from the aqueous solubility study.

Nortriptyline bromide and iodide were both anhydrous salt forms that formed hydrogen bonds between the TCA amine and the halide counterion in a 0D ring hydrogen bonding network where the hydrogen bonding did not propagate along any axes. Nortriptyline chloride was also anhydrous, but contrary to the salts in group 4, formed 0D (i.e. not propagating along any unit cell axis) discrete hydrogen between the amine group and the chloride counterions.[20]

Both salt forms in group 4 were refined in the P-1 space group whereas nortriptyline chloride was refined in $P2_1/c$. Additionally, both nortriptyline bromide and iodide had Z' values of 2, whereas nortriptyline chloride had a Z' of 1.

In the case of group 4, the Z' value and the hydrogen bonding motif seem to be defining similarities between the salt forms.

In summary, the four cation packing isostructural groups fall into two types. Groups 1 and 2 are very diverse and illustrate that cation packing can be isostructural even where the structures that make up the groups involve different cations, different anions and different solvation states. Group 1 seems to be a group where identical cation packing is caused by the presence of the picrate anion. In contrast groups 3 and 4 contain pairs of closely related structures which differ only in the detail of the halide anion. Here isostructural packing of the cation is simply a subset of a larger structural similarity.

4.5.3 Crystal packing similarity of carbamazepine and dihydrocarbamazepine forms

The crystal packing similarity tool available within the Mercury software[18] was used to calculate the level of packing similarity between the structures listed in Table 37. This was used to find isostructural groups within a data set of carbamazepine and dihydrocarbamazepine structures obtained from the literature by searching the CCDC structural database[19]. See section 3.8.3 for further details.

A tree diagram was constructed based on the number of similar molecular fragments between the structures within the data set, see Figure 46.

The structures were listed with the number of molecular fragments in common increasing as you go down the tree diagram. Structures were named isostructural in cases where the matching molecular cluster contained at least 15 fragments.

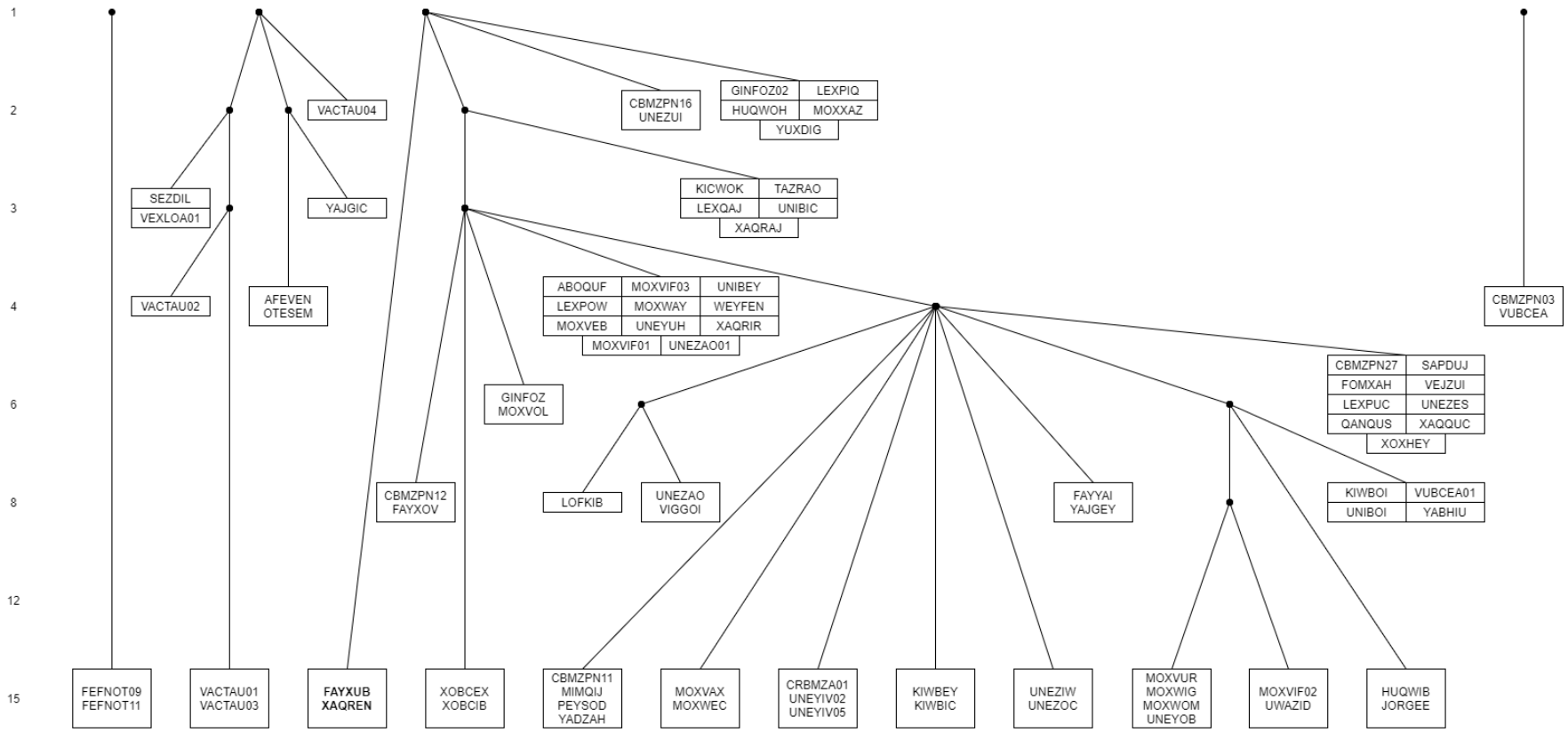

Figure 52: Tree diagram of carbamazepine and dihydrocarbamazepine forms

Twelve isostructural groups were identified:

1. Carbamazepine dihydrate (FEFNOT09 and FEFNOT11)
2. Dihydrocarbamazepine (VACTAU01 and VACTAU03)
3. 4-Amino-2-hydroxybenzoic acid bis(carbamazepine) monohydrate (FAYXUB and XAQREN)
4. Carbamazepine hemikis(malonic acid) (XOBCEX) and carbamazepine hemikis(succinic acid) (XOBCIB)
5. Carbamazepine (CBMZPN11), carbamazepine tetrahydrofuran solvate (MIMQIJ), carbamazepine monohydrate (PEYSOD and YADZAH)
6. Carbamazepine benzoic acid (MOXVAX) and carbamazepine L-1-hydroxy-2-naphthoic acid (MOXWEC)
7. Carbamazepine acetone solvate (CRBMZA01) and carbamazepine DMSO solvate (UNEYIV02, and UNEYIV05)
8. Carbamazepine N,N-dimethyl acetamide solvate (KIWBEY) and carbamazepine N-methylpyrrolidone solvate (KIWBIC)
9. Carbamazepine acetic acid solvate (UNEZIW) and carbamazepine formic acid solvate (UNEZOC)
10. Carbamazepine malonic acid (MOXVUR), carbamazepine DL-tartaric acid (MOXWIG), carbamazepine maleic acid (MOXWOM), and carbamazepine benzoquinone solvate (UNEYOB)
11. Carbamazepine 4-hydroxybenzoic acid (MOXVIF02) and bis(carbamazepine) thiourea (UWAZID)
12. Tetrakis(carbamazepine) oxonium tetrafluoroborate pentahydrate (HUQWIB) and hemikis(oxonium) hemikis(chloride) carbamazepine monohydrate (JORGEE)

4.5.3.1 Group 1

At first glance, it appears as though FEFNOT09 and FEFNOT11 are identical, since they are isostructural carbamazepine dihydrates. See Figure 53 for an overlay of the two forms.

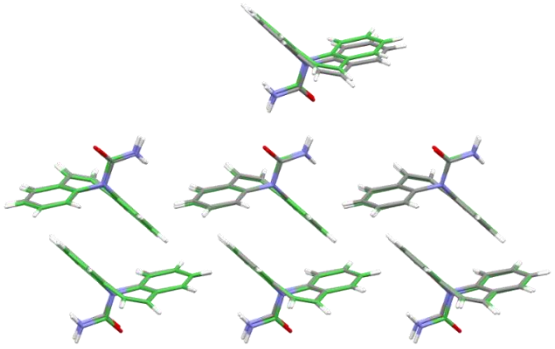

Figure 53: Comparison of FEFNOT09 and FEFNOT11 (green).

However, the two structures were solved in different space groups. FEFNOT11 was solved in the higher symmetry orthorhombic space group Cmca whereas FEFNOT09 was solved in the monoclinic space group $P2_1/c$. Both structures had a Z' of 1. As centred and primitive versions of the same cell, the unit cell parameters differed for the *a* axis length and the β angle. The *a* axis was 10.144(4) Å and the β angle was 103.763(12)° for FEFNOT09 whereas the *a* axis length was 19.705(8) Å and the β angle was 90° for FEFNOT11.

Both structures form 2D hydrogen bonding networks between the API and the water molecules propagating along the *a* and *b* axes.

It seems likely that these structures are the same form but erroneously solved in different crystal systems. This is the most likely explanation according to the most detailed reanalysis of the two potential structures, a neutron diffraction study that favours the orthorhombic structure.[21] However, the disorder implicit in this model blurs the situation, and it may be that the lower symmetry structure is also correct and that the two potential structures actually differ, perhaps due to small changes in the amount of water present in the crystal.[22]

4.5.3.2 Group 2

The case of group 2 is similar to group 1. Both structures that make up this group, VACTAU01 and VACTAU03, are anhydrous dihydrocarbamazepine forms. The only difference between these structures is in the space group and unit cell parameters. See Figure 54 for an overlay of the two forms.

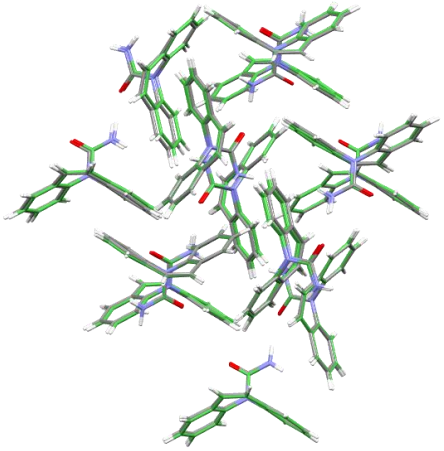

Figure 54: Comparison of VACTAU01 and VACTAU03 (green).

VACTAU01 was solved in the monoclinic space group $P2_1/c$, with a Z' of 1 and unit cell parameters of *ca.* 5.5 x 9.3 x 24.3 Å and angles of 90°, *ca.* 96°, and 90°.

Whereas VACTAU03 was solved in the lower symmetry triclinic space group P-1, with a Z' of 2 and unit cell parameters of a: 5.4 x 9.2 x 24.2 Å and angles of *ca.* 88°, 84°, and 89°.

Both structures had the same 1D chain hydrogen bonding network between the amine hydrogen bond donor and the carbonyl hydrogen bond acceptor which propagated along the b axis.

From packing analysis alone, as in group 1, it seems possible that the material for these structures were the same form but erroneously solved in different crystal systems. However, in the original report of the lower symmetry triclinic structure such an interpretation was rejected due to reported small but significant differences in the two structures' powder diffraction patterns.[23] Thus the current consensus seems to be that these are two closely related but different polymorphs.[24]

4.5.3.3 Group 3

Group 3 was made up of two 4-amino-benzoic acid derivatives of bis(carbamazepine) monohydrate co-crystals (FAYXUB and XAQREN), see Figure 55 for an overlay of the two carbamazepine molecules. The difference between them is that FAYXUB also bears a hydroxyl group on the acid ring and XAQREN does not.

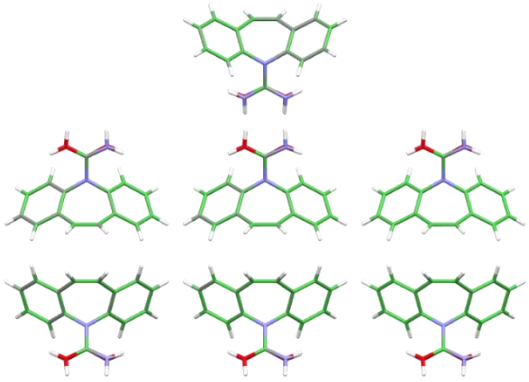

Figure 55: Comparison of FAYXUB and XAQREN (green).

Both FAYXUB and XAQREN were solved in the monoclinic space group $P2_1/n$ with a Z' of 1. The unit cell parameters were also very similar.

Both structures had the same 0D hydrogen bonding network between two 4-amino-benzoic acid molecules, four carbamazepine molecules, and two water molecules.

Group 3 is thus an example of an isostructural packing group which includes structures with only a small chemical difference between them.

4.5.3.4 Group 4

Group 4 is made up of carbamazepine hemikis(malonic acid) (XOBCEX) and carbamazepine hemikis(succinic acid) (XOBCIB), see Figure 56.

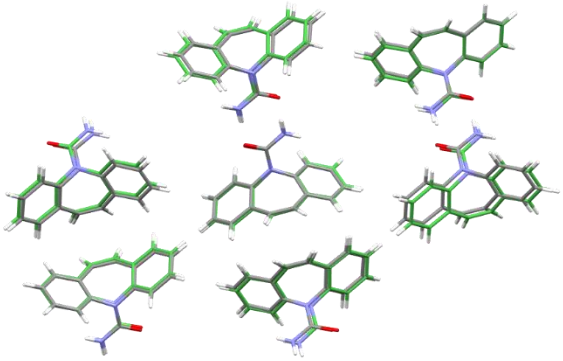

Figure 56: Comparison of XOBCEX and XOBCIB (green).

Both structures were solved in the monoclinic space group P2/n, with Z' of 1 (one CBZ molecule and half of the dicarboxylate dianion per asymmetric unit) and had very similar unit cell parameters.

Malonic and succinic acid form very similar counterions, they are both dicarboxylic acids. The only difference is that succinic acid has an additional methylene group. In the salt forms in group 4, both acid molecules were sited on the 2-fold symmetry axis.

Both co-crystals have 1D hydrogen bonding networks. The hydrogen bonding network in XOBCEX consisted of a single ring graph set with four hydrogen bond donors and four hydrogen bond acceptors. Whereas, the hydrogen bonding network in XOBCIB formed two different ring graph sets, one with hydrogen bonds between the carbamazepine amine hydrogen bond donors and the carboxylic acid acceptors, and a second from the carbamazepine amine donor to the carboxylic acid acceptor then from the carboxylic acid donor to the carbamazepine carbonyl acceptor. See Figure 57 for an image of the different hydrogen bonding motifs. The distance between N2 and O2 in XOBCEX is 3.419 Å, generally considered too long for a hydrogen bond, causing the difference in hydrogen bonding. Comparatively, the distance between N1 and O2 in XOBCIB is 2.984 Å.

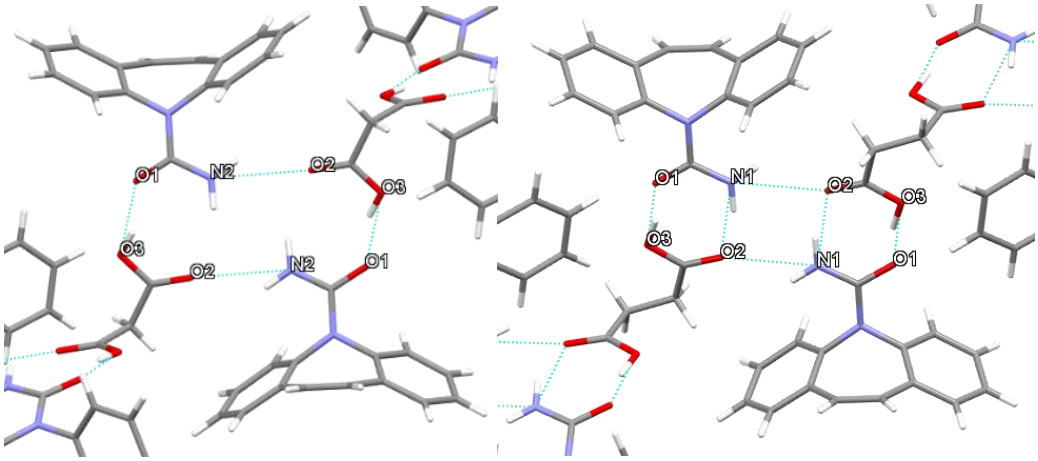

Figure 57: Hydrogen bonding in XOBCEX (left) and XOBCIB (right)

A third salt form from the data set has a similar counterion, fumaric acid. This structure formed an anhydrous hemikis salt form with the counterion present on the symmetry axis like the two salt forms in group 4. Fumaric acid is a dicarboxylic acid like malonic and succinic acid but has an ethylene group in the carbon chain. Unlike the co-crystals in group 4, the fumaric acid co-crystal structure was solved in the monoclinic space group $P2_1/c$ and formed

a discreet 0D hydrogen bonding network between two carbamazepine molecules and a fumaric acid molecule. The planarity of the fumaric acid molecule could explain why this co-crystal was not isostructural with the non-planar malonic and succinic forms.

In group 4, the co-former selection appears to be the main driving force for the isostructural nature of the two co-crystals. They were also both anhydrous with comparable hydrogen bonding motifs. Additionally, the unit cells were of a similar size, both structures were solved in the P 2/n space group and had a Z' of 1. There are thus many similarities with Group 3 (isostructural groups formed by similar anions) but here the hydrogen bonding of the two structures differs whereas in Group 3 the two structures have similar hydrogen bonding as well as similar cation packing,

4.5.3.5 Group 5

Group 5 consists of a CBZ polymorph and 3 structures containing small amounts of solvent. Four structures were found in group 5: an anhydrous carbamazepine (CBMZPN11), carbamazepine 0.1 tetrahydrofuran solvate (MIMQIJ), and two carbamazepine hydrates (PEYSOD and YADZAH with 1/3 and 1/6 of a water per CBZ respectively). See Figure 58 for an overlay of two of the forms.

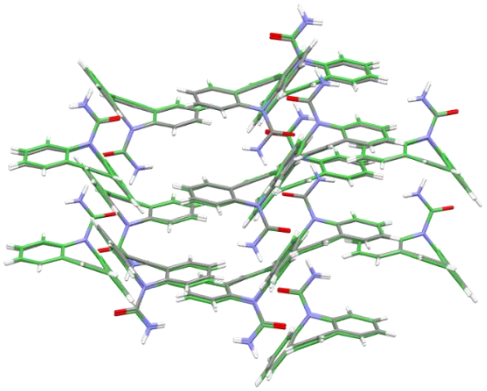

Figure 58: Comparison of CBMZPN11 and MIMQIJ (green).

CBMZPN11 was solved in the triclinic space group P-1 and had a Z' of 4. MIMQIJ, PEYSOD, and YADZAH were solved in the much higher symmetry trigonal space group R-3 and had a Z' of 1. These three latter structures also had very similar unit cell dimensions of *ca.* 35 x 35 x 5 Å and angles of 90°, 90° and 120°. Comparatively, CBMZPN11 seems quite different with unit cell dimensions of *ca.* 5 x 21 x 22 Å and angles of *ca.* 84°, 88°, and 85°,

however, these latter dimensions are close to those of the primitive reduced cell of the trigonal solvates.

In all four structures, discreet 0D hydrogen bonding networks were present between two carbamazepine molecules. Any solvent that was present was not involved in hydrogen bonding with the API. All solvates are channel solvates with channels of solvent running parallel to the crystallographic *a* axis.

Interestingly, an anhydrous carbamazepine polymorph (CBMZPN03) was solved in the R-3 space group like three of the structures in group 5 with a Z' of 1 and matching hydrogen bonding but this form was not isostructural with group 5.

In group 5, the packing of the dimeric carbamazepine hydrogen bonding motif seems to be the main driving force. While, the group contained a mix of anhydrous, solvated and hydrated forms, the solvents did not form hydrogen bonds with the carbamazepine molecules. Whilst the similarity between an anhydrous form and two fractional channel hydrates is unexceptional, it is interesting that the much larger THF solvent can also be incorporated into the channels of this structural type.

4.5.3.6 Group 6

Group 6 consisted of carbamazepine salts with benzoic acid (MOXVAX) and carbamazepine L-1-hydroxy-2-naphthoic acid (MOXWEC). See Figure 59 for an overlay.

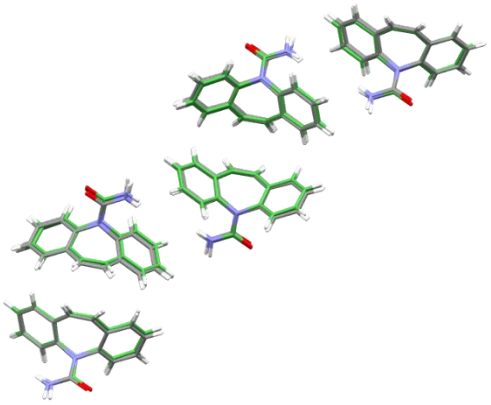

Figure 59: Comparison of MOXVAX and MOXWEC (green).

MOXVAX was solved in the monoclinic space group C2/c whereas MOXWEC was solved in the monoclinic space group $P2_1/c$. Both co-crystals had a Z' of 1. The structures had different unit cell dimensions; however, axes b

and c were similar; *ca.* 29 x 5 x 25 Å for MOXVAX compared to *ca.* 17 x 5 x 24 Å for MOXWEC.

Benzoic acid and 1-hydroxy-2-naphthoic acid are comparable co-formers. Both contain a carboxylic acid group and have aromatic character. This likely helped form isostructural forms despite the large size difference between them.

Both co-crystals formed 0D discreet hydrogen bonds between the carbamazepine amide group and the co-former carboxylic acid group giving heterodimers.

There was a number of other structures in the data set containing co-formers with aromatic character and carboxylic acid groups, these were not isostructural with the structures in group 6. An example is carbamazepine 4-aminobenzoic acid (XOXHEY), a clear difference here is that the hydrogen bonding network was very different from the structures in group 6. XOXHEY contained a 1D hydrogen bonding network between two carbamazepine amide groups and between two 4-aminobenzoic acid carboxylic acid groups, additionally there was a hydrogen bond between the amine group of the acid and the carbamazepine carbonyl. A similar hydrogen bond motif was observed for carbamazepine 4-hydroxybenzoic acid (MOXVIF01).

A combination of co-former similarities and hydrogen bonding motif supported the formation of isostructural compounds.

4.5.3.7 Group 7

Group 7 consists of a carbamazepine acetone solvate (CRBMZA01) and two carbamazepine DMSO solvates (UNEYIV02 and UNEYIV05), see Figure 60 for an overlay.

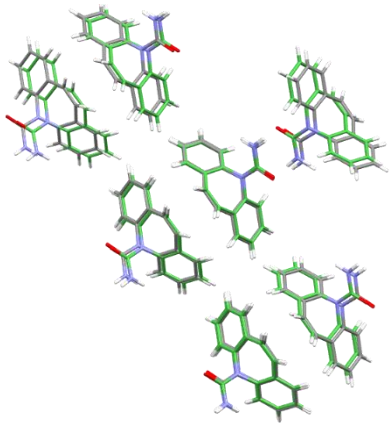

Figure 60: Comparison of CRBMZA01 and UNEYIV02 (green).

All three structures in group 7 were solved in the triclinic space group P-1. CRBMZA01 and UNEYIV02 had a Z' of 1 whereas UNEYIV05 had a Z' of 2. The main difference between UNEYIV02 and UNEYIV05 was in the unit cell dimensions, with unit cell axes of *ca.* 7 x 9 x 12 and 9 x 12 x 15 Å respectively and angles of *ca.* 95 x 95 x 100 ° for both. CRBMZA01 matched the unit cell dimensions of the Z' = 1 DMSO solvate very well with dimensions of *ca.* 7 x 9 x 12 and angles of *ca.* 96 x 93 x 101.

All three structures are solvates. Acetone and DMSO are structurally very similar with the only difference being that the sulphur in DMSO is a carbon in acetone.

CRBMZA01 formed 0D hydrogen bonding networks where two carbamazepine amide groups formed homodimeric pairs with two acetone molecules hydrogen bonded to these in a pendant fashion. UNEYIV02 and UNEYIV05 formed the same 0D hydrogen bonding network. This motif is well known for solvates of amides.[25] Interestingly, the same hydrogen bonding motif was observed in a dihydrocarbamazepine DMSO solvate (AFEZOB) in the data set. However, this structure was not isostructural with group 7, likely due to the small structural difference within the API.

The similarity of the solvents in these solvates appeared to be the feature that allows formation of isostructural packing series here. There were limited hydrogen bonding options due to there being only one hydrogen bond acceptor in the solvent co-former, which seemed to result in similar packing.

4.5.3.8 Group 8

Group 8 consisted of carbamazepine N,N-dimethyl acetamide solvate (KIWBEY) and carbamazepine N-methylpyrrolidone solvate (KIWBIC), see Figure 61 for an overlay.

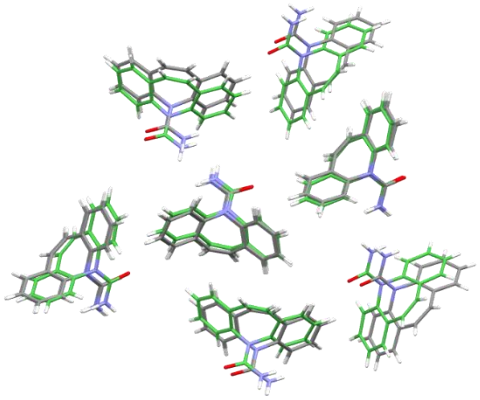

Figure 61: Comparison of KIWBEY and KIWBIC (green).

KIWBEY and KIWBIC were both solved in the monoclinic $P2_1/c$ space group and had a Z' of 1. Both structures had very similar unit cell dimensions. The dimensions were *ca.* 7.5 x 19.5 x 11.8 Å for KIWBEY and *ca.* 7.5 x 19.5 x 11.9 Å for KIWBIC. Angle β was *ca.* 96.6 ° for KIWBEY and *ca.* 98.0° for KIWBIC.

Both structures were solvates, a N,N-dimethyl acetamide and an N-methylpyrrolidone solvate for KIWBEY and KIWBIC respectively. Both solvents have tertiary amide functionality, which indicates that they will have the same hydrogen bonding capabilities. A further similarity is that in both structures the solvent is highly disordered.

As with Group 7 above, both KIWBEY and KIWBIC form 0D hydrogen bonding networks where two carbamazepine amide groups form a homodimer with two pendant solvate molecules. This is the same hydrogen bonding motif seen in group 7 and elsewhere.

As observed in group 7, the similarity of the solvents and their structural roles in these structures appeared to be the driving force in forming isostructural structures. Despite similar hydrogen bonding motifs, groups 7 and 8 were not mutually isostructural. This indicates that co-former size can have a distinct effect in addition to hydrogen bonding motif.

4.5.3.9 Group 9

Group 9 consisted of carbamazepine acetic acid solvate (UNEZIW) and carbamazepine formic acid solvate (UNEZOC), see Figure 62 for an overlay of the two structures.

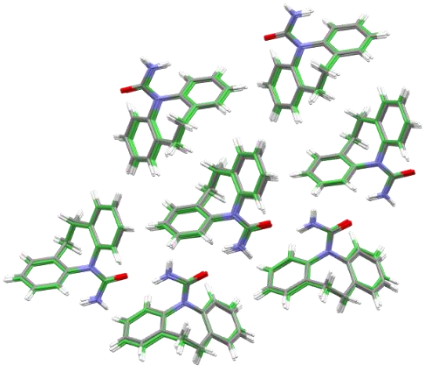

Figure 62: Comparison of UNEZIW and UNEZOC (green).

Both UNEZIW and UNEZOC were solved in the monoclinic space group $P2_1/c$ and had a Z' of 1. Both structures had very similar unit cell dimensions. The dimensions were *ca.* 5.1 x 15.7 x 18.5 Å for UNEZIW and *ca.* 5.2 x 14.7 x 17.9 Å for UNEZOC. Angle β was *ca.* 96.5° for UNEZIW and *ca.* 98.1° for UNEZOC.

The structures were both solvates, acetic acid and formic acid solvates for UNEZIW and UNEZOC respectively. Both solvents are very simple carboxylic acids, the only difference is that acetic acid has a methyl group where formic acid has a proton. The hydrogen bonding capabilities of the solvents are identical with a hydrogen bond donor and acceptor each.

Both structures formed 0D hydrogen bonding motifs with three rings in a ladder-like orientation containing two solvent molecules and two carbamazepine molecules. The first and third rings contained hydrogen bonds between the carbamazepine amine and the carboxylic acid carbonyl, and between the carbamazepine carbonyl and the carboxylic acid OH. The centre ring contained hydrogen bonds between two carbamazepine amine groups and two carboxylic acid carbonyls. An alternative description of this motif is that it consists of two acid/amide heterodimers that are bonded together into a tetramer by N-H···O interactions.

The similarity of the solvents in both size, functional group, and hydrogen bonding capability seem to be the driving force in creating the isostructural structures in group 9.

4.5.3.10 Group 10

Group 10 consists of carbamazepine malonic acid (MOXVUR), carbamazepine DL-tartaric acid (MOXWIG), carbamazepine maleic acid (MOXWOM), and carbamazepine benzoquinone solvate (UNEYOB)

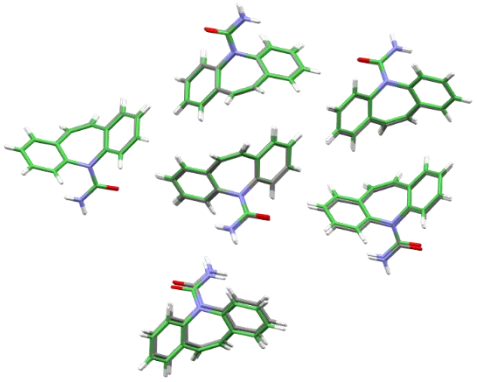

Figure 63: Comparison of MOXVUR and MOXWIG (green).

All four structures were solved in monoclinic space group $P2_1/c$ and had a Z' of 1. The unit cells were very similar with dimensions of *ca.* 10 x 27 x 5 Å and angles of 90, *ca.* 104, and 90°.

Interestingly, MOXVUR, MOXWIG, and MOXWOM were all dicarboxylic acids, whereas UNEYOB was a benzoquinone solvate. Benzoquinone is similar to dicarboxylic acids in that it contains two carbonyl groups, but it lacks any hydrogen bond donors. The co-formers range in molecular weight from 104 g/mol (malonic acid) to 150 g/mol (DL-tartaric acid) this shows they are similar in size.

The three dicarboxylic acids had different hydrogen bonding capabilities, as opposed to previously discussed isostructural groups where the co-formers contained the same hydrogen bonding. Malonic acid (MOXVUR) and maleic acid (MOXWOM) contain two carboxylic acid groups and therefore two hydrogen bond donors and two hydrogen bond acceptors. They contain no other functional groups with hydrogen bonding capabilities. DL-tartaric acid (MOXWIG) contains two secondary alcohol groups in addition to the two carboxylic acid groups, these add two hydrogen bond donors. Benzoquinone (UNEYOB) has two carbonyl functional groups which provide two hydrogen bond acceptors. The hydrogen bonding motifs could not be determined for this isostructural group because the co-formers for MOXVUR, MOXWIG, and MOXWOM were removed from the .cif files by the authors using the SQUEEZE program due to disorder[26]. Examination shows that all structures

can be described as channel solvates with the solvent (or co-former) channels running parallel to the c axis.

Even though the co-formers in group 10 had similar functional groups, they were not the same and did not provide the same hydrogen bonding capabilities. The co-former size could be the reason the structures were isostructural, but this is unclear.

4.5.3.11 Group 11

Group 11 consisted of carbamazepine 4-hydroxybenzoic acid (MOXVIF02) and bis(carbamazepine) thiourea (UWAZID), see Figure 64.

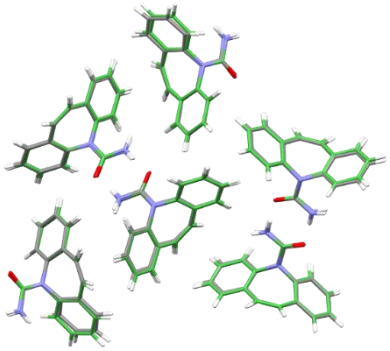

Figure 64: Comparison of MOXVIF02 and UWAZID (green).

MOXVIF02 was solved in the C2/c and UWAZID in the Cc monoclinic space groups. Interestingly, UWAZID was described as containing two carbamazepine molecules and one thiourea co-former in the asymmetric unit. MOXVIF02 was described in a higher symmetry space group with one carbamazepine molecule and one solvent per asymmetric unit. The unit cell dimensions were very well matched with axes of *ca.* 20 x 5 x 26 Å for both structures while angle β was slightly more different with an angle of *ca.* 95° for MOXVIF02 and *ca.* 90.9° for UWAZID. The solvent of the higher symmetry MOXVIF02 was so disordered that it was not included in the final structure. It would be interesting to know if a lower symmetry model akin to that of UWAZID was ever attempted.

4-hydroxybenzoic acid and thiourea and are very different co-formers. Thiourea is an organosulfur compound with amine groups whereas 4-hydroxybenzoic acid has carboxylic acid and hydroxy functional groups. Additionally, the intermolecular interactions these compounds are capable of are very different. 4-hydroxybenzoic acid has a benzene ring capable of π-π stacking, a carboxylic acid group that will act as both a hydrogen bond donor

and acceptor, and a hydroxy group that will act as a hydrogen bond donor. Dissimilarly, thiourea has two primary amine groups with four hydrogen bond donors and a sulphur which could (and here does) act as a weak hydrogen bond acceptor.

As in group 10, the co-former in MOXVIF02 was removed due to disorder and thus the hydrogen bonding motif could not be determined and compared to UWAZID.[21] UWAZID had a 2D hydrogen bonding network propagating along and down the *a* axis. Two carbamazepine molecules formed a ring-like hydrogen bonding motif between two amine groups and two carbonyl groups. The carbonyl group also acted as a hydrogen bond acceptor for a thiourea amine group. Additionally, the thiourea molecules formed a chain-like hydrogen bonding motif where the amine hydrogen bond donors hydrogen bonded to the sulphur hydrogen bond acceptors. Again, as in group 10, the two compounds of group 11 can be described as channel solvates, here with the channels running parallel to the *b* axis.

Overall, the two co-crystals in this group seem to be very different from each other. It is thus surprising that they adopt isostructural cation packing. Why these two un-alike structures do so whilst other more similar species do not is unclear.

4.5.3.12 Group 12

Group 12 consisted of two inorganic co-crystal forms, tetrakis(carbamazepine) oxonium tetrafluoroborate pentahydrate (HUQWIB) and hemikis(oxonium) hemikis(chloride) carbamazepine monohydrate (JORGEE), see Figure 65 for an overlay.

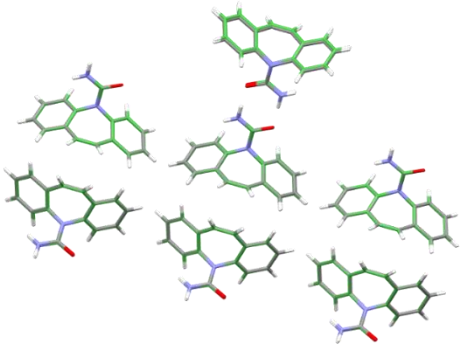

Figure 65: Comparison of HUQWIB and JORGEE (green).

Both HUQWIB and JORGEE were solved in the monoclinic C2/c space group and had a Z' of 1. As in previous isostructural groups, the unit cell dimensions match very well with cell axes lengths of *ca.* 30 x 5 x 21 Å. The same was true for the angles, where angle β was *ca.* 120° for both structures.

Both structures contain the oxonium cation H_3O^+, an ion with three hydrogen bond donors, and both structures are further hydrated. Additionally, the structures have counterions to the oxonium that contain halogens, chloride in JORGEE and tetrafluoroborate in HUQWIB.

Hydrogen bonding in HUQWIB appeared to take the form of a 0D motif where two carbamazepine molecules form a ring motif as per the typical amide homodimer, and each carbonyl additionally acts as a hydrogen bond acceptor from a water molecule. The tetrafluoroborate and oxonium ions were disordered in the same location, and therefore the hydrogen bonding could not be determined uniquely. JORGEE formed a complex 3D hydrogen bonding system based on a similar smaller unit akin to that described above for HUQWIB. Additionally, the carbamazepine molecules hydrogen bond to an oxonium molecule and to either a water molecule or chloride ion. The oxonium and the water/chloride were further involved in a 6 membered hydrogen bonding ring motif with two water molecules, two oxonium ions and two chloride ions. Due to the high level of disorder and partial occupation of the non-carbamazepine compounds, it is possible that the HUQWIB hydrogen bonding matches the motif seen in the JORGEE structure.

Once again, it appears the similarities in the counterions/co-formers seem to be what lead to this isostructural group.

In summary, the 12 carbamazepine isostructural groups seem to require similarity of components and fall into three types.

Groups 1 and 2 appear to be made up of polymorphs, if indeed there is any difference between the two forms in group 1, otherwise these may be the same form solved in different crystal symmetries.

Of the remaining ten isostructural groups, seven consisted of groups where the co-formers were geometrically and functionally similar to each other. These were groups 3, 4, 6, 7, 8, 9, and 12. For example, the co-formers in group 3 were both 4-aminobenzoic acid derivatives, the co-formers in group 4 were closely related dicarboxylic acids, and the structures in groups 7, 8, and 9 were all solvates with solvent co-formers of roughly the same size and that shared similar hydrogen bonding capabilities. Group 6 has the largest difference between the co-formers. While both co-formers contained a carboxylic acid functional group and had aromatic character, there was a large size discrepancy.

The three remaining groups, groups 5, 10, and 11, had more variation in co-former and solvation state. For example, groups 5 and 10 contained mixtures of anhydrous free API, solvated structures and co-crystals. Group 11 contained seemingly unrelated co-formers, with one being thiourea, an organosulfur compound, and the other 4-hydroxybenzoic acid which is an organic carboxylic acid with aromatic character. The driving force of isostructural packing here seemed to be the hydrogen bonding motif. Indeed, all three groups were made up of channel solvate type structures. It is to be expected that a channel within a crystal structure can accommodate larger differences in the co-formers.

No isostructural groups were found that contained a mixture of carbamazepine and dihydrocarbamazepine. The hope was that despite the small differences in composition, these structures could have matching

packing motifs. This contradicts a paper by Arlin et al. that described an isostructural relationship between dihydrocarbamazepine form II and carbamazepine form V.[27]

Overall, in most cases in groups 4 through 12, the unit cell dimensions were very similar. This could be further studied as a tool to predict isostructural forms where there are other factors that suggest it is likely, due to co-former or counterion similarities and hydrogen bonding capabilities.

The investigation of isostructural relationships within the carbamazepine data set was carried out due to the structural similarities to the tricyclic antidepressants studied in this work. The hope was that the TCAs would adopt similar cation packing motifs and would therefore be isostructural with the well-studied carbamazepine and dihydrocarbamazepine. The TCA packing study above produced isostructural groups that included different APIs in the same group, raising hopes that other similar molecules cold also be included. A crystal packing similarity study using a combined data set of the carbamazepine and TCA structures was carried out, unfortunately, no overlap was observed. This is similar to the above packing similarity study on carbamazepine and dihydrocarbamazepine where none of the isostructural groups contained more than one type of API. Three distinct packing motifs were discussed in the carbamazepine structural analysis by Childs et al., these were named ‘Translation Stack’, ‘Inversion Cup’, and ‘Coformer Pairing’.[28] It would be interesting to compare these to the packing motifs of the TCA data set, perhaps in combination with a Hirshfeld surface type analysis.[30] However, time restraints rule thus out at this time and so this is suggested here merely as further work.

4.6 References

1) Grant, D. J. W.; Higuchi, T. *Solubility Behaviour of Organic Compounds*; Wiley: New York, **1990**.

2) Infantes, L.; Motherwell, W. D. S. *CrystEngComm*, **2002**, *4*, 454–461.

3) Groom, C. R.; Allen, F. H. *Angew. Chem. Int. Ed.*, **2014**. *53*, 662-671.

4) Haynes, D. A.; Jones, W.; Motherwell, W. D. S. *CrystEngComm*, **2005**, *7*, 342-345.

5) Infantes, L.; Fabian, L.; Motherwell, W. D. S. *CrystEngComm*, **2007**, *9*, 65–71.

6) Desiraju, G. R. *J. Chem. Soc. Chem. Commun.* **1991**, *6*, 426–428.

7) Briggs, N.E.B.; Kennedy, A.R.; Morrison, C.A. *Acta Cryst B*, **2012**, *68*, 453-464.

8) Etter, M. C. *Acc. Chem. Res.*, **1990**, *23*, 120–126.

9) Klein, C.L.; Lear, J.; O'Rourke, S.; Williams, S.; Liang, L. *J. Pharm. Sci.*, **1994**, *83*, 1253-1256.

10) Klein, C.L.; Banks, T.A.; Rouselle, D. *Acta Cryst. C*, **1991**, *47*, 1478-1480.

11) Post, M.L.; Kennard, O.; Horn, A.S. *Acta Cryst. B*, **1975**, *31*, 1008-1013.

12) Paulus, E.F. *Acta Cryst. B*, **1978**, *34*, 1942-1947.

13) Jasinski, J.P.; Butcher, R.J.; Hakim Al-Arique, Q.N.M.; Yathirajan, H.S.; Ramesha, A.R. *Acta Cryst. E*, **2010**, *66*, 674-675.

14) Reck, G. *CSD Communication*, **2006**.

15) Bandoli, G.; Nicolini, M.; Casellato, U. *J. Chem. Crystallogr.*, **1987**, *17*, 281-293.

16) Steed, K.M.; Steed, J.W., *Chem. Rev.* **2015**, *115*, 2895−2933.

17) McMurray, J.E. *Organic Chemistry 6th ed.*; Brooks Cole: Belmont, **2003**.

18) Macrae, C.F.; Sovago, I.; Cottrell, S.J.; Galek, P. T. A.; McCabe, P.; Pidcock, E.; Platings, M.; Shields, G. P.; Stevens, J. S.; Towler, M.; Wood, P. A., *J. Appl. Cryst.*, **2020**, *53*, 226-235.

19) Groom, C.R.; Bruno, I. J.; Lightfoot, M. P.; Ward, S. C., *Acta Cryst.*, **2016,** *72*, 171-179.

20) Etter, M. C.; MacDonald, J. C.; Bernstein, J., *Acta Cryst. B,* **1990**, *46, 2*56–262.

21) Sovago, I.; Gutmann, M. J.; Senn, H. M.; Thomas, L. H.; Wilson, C. C.; and Farrugia, L. J., *Acta Cryst. B*, **2016**, *72*, 39-50.

22) Harris, R. K.; Ghi, P. Y.; Puschmann, H.; Apperley, D. C.; Griesser, U. J.; Hammond, R. B.; Ma, C.; Roberts, K. J.; Pearce, G. J.; Yates, J. R.; and Pickard, C. J., *Org. Process Res. Dev.*, **2005**, *9*, 902-910.

23) Leech, C. K.; Florence, A. J.; Shankland, K.; Shankland, N.; and Johnston, A., *Acta Cryst. E*, **2007**, *63*, 0675-0677.

24) Arlin, J-B.; Johnston, A.; Miller, G. J.; Kennedy, A. R.; Price, S. L.; and Florence, A. J.; *CrystEngComm*, **2010**, *12*, 64-66.

25) Buist, A. R.; Kennedy, A. R.; Shankland, K.; Shankland, N.; and Spillman, M. J., *Cryst. Growth Des.*, **2013**, *13*, 5121-5127.

26) Childs, S.L.; Wood, A.P.; Rodríguez-Hornedo, N.; Sreenivas Reddy, L.; and Hardcastle, K.I., *Cryst. Growth Des.*, **2009**, *9*, 1869–1888.

27) Arlin, J-B.; Price, S. L.; and Florence, A. J., *Chem. Commun.*, **2011**, *47*, 7074-7076.

28) Childs, S.L.; Wood, A.P.; Rodríguez-Hornedo, N.; Sreenivas Reddy, L.; and Hardcastle, K.I., *Cryst. Growth Des.*, **2009**, *9*, 1869–1888.

29) Atkins, P.W.; and DePaula, J., *Physical Chemistry*, 8th edition; Oxford University Press: New York, **2006**.

30) McKinnin, J.J.; Spackman, M.A.; and Mitchell, M.S., *Acta Cryst B*, **2004**, *60*, 627-668.

5 Conclusion

The active pharmaceutical ingredient, also known as the API, is the biologically active molecule present in medication. The solid state of APIs is the preferred state due to the stability and advantageous material properties generally demonstrated. These properties strongly depend on the number, type and strength of intermolecular interactions in the solid and are therefore properties that can be controlled and altered by changing the solid-state structure without having to alter the API molecule.

There are four main ways to alter the solid-state structure and change material properties without altering the API molecule. Altering the solid-state structure affects the number, type and strength of intermolecular interactions. There are several ways to alter these interactions and thereby changing material properties. The options include the choice between amorphous and crystalline material, investigating the polymorphic landscape of the API, and co-crystal or salt formation. Salt formation was the route that was focussed on in this work.

A salt screen was carried out on four closely related tricyclic antidepressants: amitriptyline, nortriptyline, imipramine, and doxepin. All salt formation experiments were carried out exclusively in water in order to reduce the number of variables when comparing the resulting salt forms. Slow cooling followed by slow evaporation was the chosen method of crystallisation with the aim to grow single crystals suitable for single crystal x-ray diffraction. A dataset of 29 newly elucidated salt forms was generated.

From this data set a selection of nine nortriptyline salt forms was made for an apparent aqueous solubility study. The salt forms were selected due to the counterions being ‘Generally Regarded as Safe’ (GRAS) for use in pharmaceutical industry. The salt forms used were bromide, iodide, salicylate, mucate, methane sulfonate, tosylate, besylate and oxalate. Unfortunately, the reactions between the nortriptyline free base and mucic acid and methane sulfonic acid were unsuccessful. A solubility assessment

was carried out on the other salt forms and a clear trend was observed, where the salt forms with halogen counterions showed a higher solubility than organic counterions. The most soluble salt form of nortriptyline was the chloride salt which was over 200 times more soluble than the salicylate salt, which was determined to be the least soluble.

Structural analysis was carried out on the data set which found that it would appear that all four TCA bases were much more likely to form Z' > 1 structures than is normal. Only 8.8% of structures in the CSD were found to have a Z' value larger than 1, compared to 52% of newly elucidated TCA crystal structures from this work. Three conformational motifs were investigated as possible causes for this increased likelihood of anomalous Z' values. Three ring/chain conformations were identified, as well as three torsion angle α, and two torsion angle β options. Indeed, in structures with higher Z' values, API molecules with mixtures of these conformations were observed. In addition to structures with Z'>1, full or partial cation disorder was found in this data set. Particularly, five of the TCA salt structures contained a cation site where all atoms of the cation were disordered. There is a chance that larger super cells or modulated structures have not been identified here and that these structures could be ordered with higher Z' values.

The structures were further analysed as part of a larger data set of tricyclic antidepressants obtained from the CSD by the crystal packing similarity tool in Mercury. Four isostructural groups were identified. It appeared that the four cation packing isostructural groups could be divided into two types. Groups 1 and 2 contained different API molecules and/or very diverse counterions, and different hydration states. This illustrated that cation packing can be isostructural even where the structures that make up the groups involve different cations, different anions, and different solvation states. Group 1 seems to be a group where identical cation packing is caused by the presence of the picrate anion. In contrast groups 3 and 4 contain pairs of closely related structures which differ only in the detail of the halide anion.

Here isostructural packing of the cation is simply a subset of a larger structural similarity.

The crystal packing similarity analysis was repeated with a dataset of 85 carbamazepine and dihydrocarbamazepine structures found in the CSD. Here, 12 isostructural groups were identified, that could be split into three types. Type 1, groups 1 and 2, consisted of polymorphic forms. In group 1, it may be possible that the structures were not isostructural, but indeed the same form, but solved in different crystals systems. For type 2, it appeared the groups were made up of structures where the co-formers were geometrically and functionally similar to each other. Here, isostructural packing of the cation is simply a subset of a larger structural similarity, as in the second type of TCA isostructural groups. Type 3 had less in common, the structures in each group contained either dissimilar co-formers or different solvation states. The driving force of isostructural packing here seemed to be the hydrogen bonding motif and the link between this and the structures in the type 3 groups being channel solvates. Overall, in most cases in groups 3 through 12, the unit cell dimensions were very similar. This could be further studied as a tool to predict isostructural forms.